Modeling and Simulation of a Downer-Type Fluid Catalytic Cracking Unit

by

Eid Musaad H. Al-Mutairi

A Thesis Presented to the

FACULTY OF THE COLLEGE OF GRADUATE STUDIES

KING FAHD UNIVERSITY OF PETROLEUM & MINERALS

DHAHRAN, SAUDI ARABIA

In Partial Fulfillment of the
Requirements for the Degree of

MASTER OF SCIENCE

In

CHEMICAL ENGINEERING

October, 1999

INFORMATION TO USERS

This manuscript has been reproduced from the microfilm master. UMI films the text directly from the original or copy submitted. Thus, some thesis and dissertation copies are in typewriter face, while others may be from any type of computer printer.

The quality of this reproduction is dependent upon the quality of the copy submitted. Broken or indistinct print, colored or poor quality illustrations and photographs, print bleedthrough, substandard margins, and improper alignment can adversely affect reproduction.

In the unlikely event that the author did not send UMI a complete manuscript and there are missing pages, these will be noted. Also, if unauthorized copyright material had to be removed, a note will indicate the deletion.

Oversize materials (e.g., maps, drawings, charts) are reproduced by sectioning the original, beginning at the upper left-hand corner and continuing from left to right in equal sections with small overlaps.

Photographs included in the original manuscript have been reproduced xerographically in this copy. Higher quality 6" x 9" black and white photographic prints are available for any photographs or illustrations appearing in this copy for an additional charge. Contact UMI directly to order.

Bell & Howell Information and Learning
300 North Zeeb Road, Ann Arbor, MI 48106-1346 USA
800-521-0600

UMI®

MODELING AND SIMULATION OF A DOWNER-TYPE FLUID CATALYTIC CRACKING UNIT

BY

EID MUSAAD H. AL-MUTAIRI

A Thesis Presented to the
DEANSHIP OF GRADUATE STUDIES

KING FAHD UNIVERSITY OF PETROLEUM & MINERALS
DHAHRAN, SAUDI ARABIA

In Partial Fulfillment of the
Requirements for the Degree of

MASTER OF SCIENCE
In

CHEMICAL ENGINEERING

OCTOBER, 1999

UMI Number: 1398757

UMI®

UMI Microform 1398757
Copyright 2000 by Bell & Howell Information and Learning Company.
All rights reserved. This microform edition is protected against
unauthorized copying under Title 17, United States Code.

Bell & Howell Information and Learning Company
300 North Zeeb Road
P.O. Box 1346
Ann Arbor, MI 48106-1346

KING FAHD UNIVERSITY OF PETROLEUM & MINERALS
Dhahran 31261, Saudi Arabia

DEANSHIP OF GRADUATE STUDIES

This thesis is written by

EID MUSAAD H. AL-MUTAIRI

under the direction of his Thesis Advisor and approved by his Thesis Committee, has been presented to and accepted by the Deanship of Graduate Studies, in partial fulfillment of the requirements for the degree of

MASTER OF SCIENCE IN CHEMICAL ENGINEERING.

Thesis Committee

Dr. Abdullah A. Shaikh
(Chairman)

Dr. Jorge N. Beltramini
(Member)

Dr. Dulaihan K. Al-Harbi
(Member)

井野隆
Dr. Takashi Ino
(Member)

Dr. Abdullah A. Shaikh
(Department Chairman)

Dr. Abdullah M. Al-Shehri
(Dean of Graduate Studies)

Date: 23-10-99

ACKNOWLEDGMENT

Praise and gratitude to ALLAH Almighty, with whose gracious help it was possible to accomplish this work.

I am sincerely grateful to Dr. Abdullah A. Shaikh for his guidance and encouragement. The training and experience I got from him were wonderful.

I am also thankful to the other member of the committee, Dr. Takashi Ino, for his cooperation, help and valuable suggestions during the course of research work. I thank also other members of the committee Dr. Dulaihan K. Al-Harbi and Dr. Jorge N. Beltramini for their comments and constructive criticisms.

I would like to thank HS-FCC project team at RI-KFUPM for their cooperation and help ,namely, Mr. Abdul-Bari, Dr. Ikeda, Mr. Rahat Saeed & Dr. Faizurrahman.

TABLE OF CONTENTS

LIST OF TABLES vi

LIST OF FIGURES vii

ABSTRACT (Arabic) xi

ABSTRACT (English) xii

1. INTRODUCTION 1

1.1 Fluid catalytic cracking 1

1.2 The FCC downer reactor 2

1.3 Objectives of the research 3

2. LITERATURE REVIEW 5

2.1 General overview 5

2.2 Kinetics of FCC reaction 7

2.3 Hydrodynamics of the downer in FCC process 10

2.4 Modeling downer reactors 16

3. DEVELOPMENT OF FCC-DOWNER UNIT MODEL 19

3.1 Downer-regenerator model development 19

3.2 The downer model 20

3.3 The regenerator model 28

4. SIMULATION RESULTS & DISCUSSION 49

4.1 Introduction 49

4.2 Parameters used in simulation 50

4.3 Numerical procedure 57

4.4 Model results and comparison with P.P. data 57
4.5 Parametric study for some operational parameters 64
4.6 Parametric sensitivity of the FCC-downer 106

5. CONCLUSIONS AND RECOMMENDATIONS........................ 117

NOMENCLATURE.. 120

LITERATURE CITED.. 125

APPENDIX A: DETAILED DERIVATION OF THE DOWNER MODEL EQUATIONS.. 133

APPENDIX B : DETAILED DERIVATION OF REGENERATOR MODEL EQUATIONS.. 138

APPENDIX C: COMPUTER CODES DEVELOPED TO ACHIEVE THE SIMULATION.. 150

APPENDIX D: FCC-DOWNER UNIT OUTPUT SAMPLE.............. 163

LIST OF TABLES

Table		Page
2.1	Review of reaction kinetics schemes proposed for FCC reaction	13
2.2	Summary of hydrodynamics studies on downer in literature	17
2.3	Reactor models presented for the downer in the literature	18
3.1	Kinetic parameters for reaction in downer and regenerator	22
4.1	Operational parameters used to the FCC-Downer unit simulation	51
4.2	Physical and thermal properties used in the simulation of the FCC-downer unit	53
4.3	Kinetic and deactivation parameters for reactions in the downer and the regenerator used in the simulation of the FCC-downer	54
4.4	Heats of reactions used in the simulation of the FCC-downer unit	55
4.5	Other simulation parameters	56
4.6	Model results vs. pilot plant data	59
4.7	Optimum A_D to produce gasoline at different DOT and L_D	82
4.8	Optimum L_D at fixed A_D to produce gasoline at different DOT's	94

LIST OF FIGURES

Figure		Page
1.1	A proposed FCC design with downer reactor	4
2.1	Schematic diagram for the FCC-downer pilot plant	6
2.2	Ten-lumped model	9
2.3	Six-lumped model	9
2.4	Four-lumped model	11
2.5	Five-lumped model	11
2.6	Seven-lumped model	12
2.7	Axial gas-solids flow structure in the downer	15
3.1	Mass balance around the downer	26
3.2	Representation of energy balance at the downer entrance	29
3.3	General flow regime diagram	32
3.4	Emulsion voidage	34
3.5	Experimental value for bubble-emulsion transfer coefficient	36
3.6	Energy balance in the regenerator emulsion phase	47
4.1	Comparison of model predictions and pilot plant data for conversion and yields in the downer. (Run # 39)	60
4.2	Comparison of model predictions and pilot plant data for temperature in the downer (Run # 39)	61
4.3	Comparison of emulsion and bubble phase temperatures with P.P. data for regenerator (Run # 39)	62
4.4	Comparison of coke on regenerated catalyst with P.P. data for regenerator (Run # 39)	63
4.5	Comparison of model predictions and pilot plant data for conversion and yields in the downer (Run # 62)	65

Figure		Page
4.6	Comparison of model predictions and pilot plant data for temperature in the downer (Run # 62)	66
4.7	Comparison of emulsion and bubble phase temperature with P.P. data for regenerator (Run # 62)	67
4.8	Comparison of coke on regenerated catalyst with P.P. data for regenerator (Run # 62)	68
4.9	Effect of changing catalyst to oil ratio on conversion of gas oil	69
4.10	Effect of changing catalyst to oil ratio on gasoline yield	71
4.11	Effect of changing catalyst to oil ratio on gases yield	73
4.12	Effect of changing catalyst to oil ratio on coke yield	74
4.13	Effect of changing catalyst to oil ratio on coke on regenerated catalyst	75
4.14	Effect of changing catalyst to oil ratio on the emulsion phase temperature (regenerator temperature)	76
4.15	Effect of changing downer cross-section area on conversion of gas oil, $L_D = 1$ m	78
4.16	Effect of changing downer cross-section area on conversion of gas oil, $L_D = 2$ m	79
4.17	Effect of changing downer cross-section area on gasoline yield, $L_D = 1$ m	80
4.18	Effect of changing downer cross-section area on gasoline yield, $L_D = 2$ m	81
4.19	Effect of changing downer cross-section area on coke yield, $L_D = 1$ m	83
4.20	Effect of changing downer cross-section area on coke yield, $L_D = 2$ m	84
4.21	Effect of changing downer cross-section area on gases yield, $L_D = 1$ m	86

Figure		Page
4.22	Effect of changing downer cross-section area on gases yield, $L_D = 2$ m	87
4.23	Effect of changing downer cross-section area on coke on regenerated catalyst; $L_D = 1$ m	88
4.24	Effect of changing downer cross-section area on coke on regenerated catalyst, $L_D = 2$ m	89
4.25	Effect of changing downer cross-section area on emulsion phase temperature (regenerator temperature), $L_D = 1$ m	90
4.26	Effect of changing downer cross-section area on emulsion phase temperature (regenerator temperature), $L_D = 2$ m	91
4.27	Effect of changing length of the downer on conversion of gas oil	92
4.28	Effect of changing length of the downer on gasoline yield	93
4.29	Effect of changing length of the downer on coke yield	95
4.30	Effect of changing length of the downer on gases yield	96
4.31	Effect of changing length of the downer on coke on regenerated catalyst	98
4.32	Effect of changing length of the downer on emulsion phase temperature (regenerator temperature)	99
4.33	Effect of changing the air flow on conversion of gas oil	100
4.34	Effect of changing the air flow on gasoline yield	101
4.35	Effect of changing the air flow on coke yield	102
4.36	Effect of changing the air flow on gases yield	103
4.37	Effect of changing the air flow on coke on regenerated catalyst	104
4.38	Effect of changing the air flow on emulsion phase temperature (regenerator temperature)	105

Figure		Page
4.39	Sensitivity of the conversion of gas oil and product yields to k_g	107
4.40	Sensitivity of the downer outlet temperature and emulsion phase temperature (regenerator temperature) k_g	108
4.41	Sensitivity of the coke on regenerated catalyst to k_g	109
4.42	Sensitivity of conversion of gas oil and product yields to h	110
4.43	Sensitivity of the downer temperature and emulsion phase temperature (regenerator temperature) to h	111
4.44	Sensitivity of coke on regenerated catalyst to h	113
4.45	Sensitivity of conversion of gas oil and product yield to a_v	114
4.46	Sensitivity of the downer outlet temperature and emulsion phase temperature (regenerator temperature) to a_v	115
4.47	Sensitivity of coke on regenerated catalyst to a_v	116

خلاصة الرسالة

اسم الطالب: عيد مساعد هجّاج المطيري
عنوان الدراسة: نمذجة ومحاكاة وحدة معامل تكسير حفزي
حقل التخصص: هندسة كيميائية
تاريخ الدرجة: رجب، ١٤٢٠ هـ

بالإضافة إلى ما تحتله عملية التكسير الحفزي للزيت الثقيل من مكانة في الصناعة البتروليّة هذه الأيام. فإن أهميتها في ازدياد خصوصاً مع الأفكار الجديدة لتطوير هذه العمليّة والهادفة إلى استثمار العمليّة لتكون منتجاً للأوليفينات إضافة إلى ما تنتجه من منتجات بتروليّة. إن هذا التوجّه يربط بين الصناعة البتروليّة والبتر وكيماوية في آن واحد ويتم تحقيق ذلك عن طريق تغيير المفاعل الحفزي ليكون ذو إتجاه سفلي بدل العلوي التقليدي. المفاعل الجديد (السفلي) يتغلّب على الجوانب السلبيّة في المفاعل القدم (العلوي)، فالدراسات النظريّة الأوليّة تشير إلى أن المفاعل السفلي يقلّل الخلط الرجعي يشكل كبير كما أنه يمكن تشغيله عند درجات حرارة عالية تمكن من زيادة إنتاج الأوليفنات بنسبة واضحة.

في هذه الرسالة تم تطوير نموذج رياضي متكامل لوحدة تكسير حفزي ذات تقنيّة المفاعل السفلي حيث شمل النموذج مفاعل التكسير وكذلك مفاعل تنشيط الحفازات. حيث طوّر النموذج باستخدام الكينيتيكيّة الرباعيّة لتفاعل التكسير الحفزي وافتراض الإحتراق الكلّي في المفاعل التنشيطي. كما تم مقارنة نتائج النموذج مع نتائج المصينع الذي يستخدم نفس التقنية حيث أثبتت المقارنة توافقاً كبيراً أعطى الثقة بالنموذج المطوّر. كما تم دراسة تأثير متغيرات تشغيليّة وتصميميّة ومتغيّرات من نفس النموذج على أداء الوحدة ككل حيث تم التوصل إلى خلاصات مذكورة في طيّات الرسالة.

درجة الماجستير في العلوم
جامعة الملك فهد للبترول والمعادن
الظهران، المملكة العربية السعودية
رجب، ١٤٢٠ هـ

THESIS ABSTRACT

NAME OF STUDENT ***: Eid Musaad H. Al-Mutairi***
TITLE OF STUDY ***: Modeling and Simulation of a Downer-Type Fluid Catalytic Cracking Unit***
MAJOR FIELD ***: Chemical Engineering***
DATE OF DEGREE ***: October, 1999***

In addition to the traditional role that the FCC process plays in heavy oil cracking, nowadays this process is becoming increasingly important as a potentially flexible means to respond to changes in petrochemical product demand. It is expected that the FCC process will play a major role not merely as producer of gasoline but of light olefins as well, thus integrating refining and petrochemical industries. Great interest in this direction has been spurred by the relatively novel FCC process configuration, in which a down-flow cracking reactor (or downer) replaces the conventional riser reactor.

Preliminary theoretical studies in the literature have shown the downers could have advantages over risers. As solids back mixing is significantly reduced in the new configuration, higher temperatures are allowable to optimize production of light olefins and gasoline. In this thesis, mathematical models for downer-type FCC unit have been developed, in which conservation equations for nonisothermal downer and regenerator reactors are linked with applicable hydrodynamic findings, 4-lump cracking kinetics in the downer, and complete combustion kinetics in the regenerator. Furthermore, the mathematical models have been validated against experimental data collected in a pilot plant in which the downer and regenerator are 1 m and 1.037 m in length, respectively; and operating temperatures of around 923K can be achieved. Detailed parametric sensitivity studies including key design, operating, and model parameters, have also been carried out using different catalysts. Optimization findings are reported.

MASTER OF SCIENCE DEGREE
KING FAHD UNIVERSITY OF PETROLEUM & MINERALS
Dhahran, Saudi Arabia
October, 1999

CHAPTER 1

INTRODUCTION

1.1 Fluid Catalytic Cracking Process

Fluid Catalytic Cracking (FCC) is an industrial process that converts heavy hydrocarbons (namely gas oil), coming from primary refining, to lower molecular weight products. In the Kingdom of Saudi Arabia, there are two refineries in which FCC processes exist. These are Jeddah refinery and Samref refinery in Yanbu. Their capacity is 13,000 b/d and 90,600 b/d , respectively.

The FCC process is at the heart of a modern refinery oriented toward maximum gasoline production. As a result, a tremendous number of technological developments have been made since the installment of the first unit in 1942 (Reichle, 1992). Typical FCC units are composed of two reactors: the cracking reactor where almost all the endothermic cracking reactions and coke deposition on the catalyst occur; and the regeneration reactor, where air is used to burn off the coke on the catalyst. The catalyst that loses its activity in the reactor due to coke deposition is reactivated in the regenerator by burning off the coke utilizing air. The catalyst serves the dual purpose of catalyzing the reactants and supplying the necessary heat to the reaction.

In the 1950's, the old catalyst (i.e. amorphous silica alumina) was changed to zeolite powders, which are more active and have a higher surface area. The new catalyst (zeolites) led the researchers in the fluidization area to develop a reactor with less residence time to avoid overcracking of feed. The new improved reactor was called a riser where the flow of the feed in the reactor is much higher than the minimum fluidization velocity (u_{mf}). The riser's contact time is few seconds (i.e. very instantaneous reaction). So the flow in the riser can be approximated to a flow in a plug flow reactor (Murphy, 1992).

The riser is a very efficient catalytic cracker, therefore all FCC units were upgraded to operate with a riser reactor. In the last two decades, some drawbacks of risers appeared. Thereafter, many researches tried to analyze the main problems of the risers. The major disadvantage they documented was backmixing of catalyst particles inside the riser. Actually, a significant amount of catalyst is not used properly because of the backmixing phenomenon.

1.2 The FCC Downer Reactor

Many researchers tried to suggest a remedy that could save the catalyst and to increase the efficiency of catalytic cracking reactor. As a result of that, Gross & Ramage (1983) presented the idea of a downer reactor for catalytic cracking of gas oil instead of the riser reactor, where both the catalyst and the feedstock flow downwards inside the reactor. They claimed this would lead to uniform distribution of catalyst, decreased contact time of catalyst with the feed, and reduced coke formation.

In 1992, Murphy proposed a FCC/heavy oil cracker unit, which incorporates a downflow reactor and a riser regenerator as illustrated in Fig. 1.1. Catalyst flows from a hopper in a partially settled state, free of gas and bubbles, into a number of parallel smaller diameter downflow reactors. The catalyst is first separated by a simple inertia separator before the product vapours are passed through high efficiency cyclones for final cleaning.

Two years later, Pontier et al. (1994) patented a small apparatus utilizing downflow FCC process to justify that the downer is more efficient than the upflow pattern. After that, many researches and projects focused on studying different aspects in downer reactors and compared them with the risers to investigate the claimed advantages of downers. For example lately, Fei et al. (1997) presented that the higher the overcracking rate, as a result of backmixing in risers, the lower the gasoline yield, which is the desired product. In fact this conclusion supports the downflow reactor advantages strongly and makes it the future process of FCC.

1.3 Objectives of the Research

The objectives of this research work are as follows:

1. To review the literature related to FCC downer, on both the kinetics, hydrodynamics, and reactor models proposed for the FCC-downer process.
2. To develop a reactor model that links both the kinetics and hydrodynamics in the downer.
3. To develop a regenerator model that represents the behavior of the regeneration process.
4. To develop a comprehensive model for the whole unit linking the regenerator to the downer.
5. To test the model developed for the FCC-downer process against the experimental data obtained from a pilot plant.
6. To carry out sensitivity studies of FCC-downer using operational, design, and model parameters.

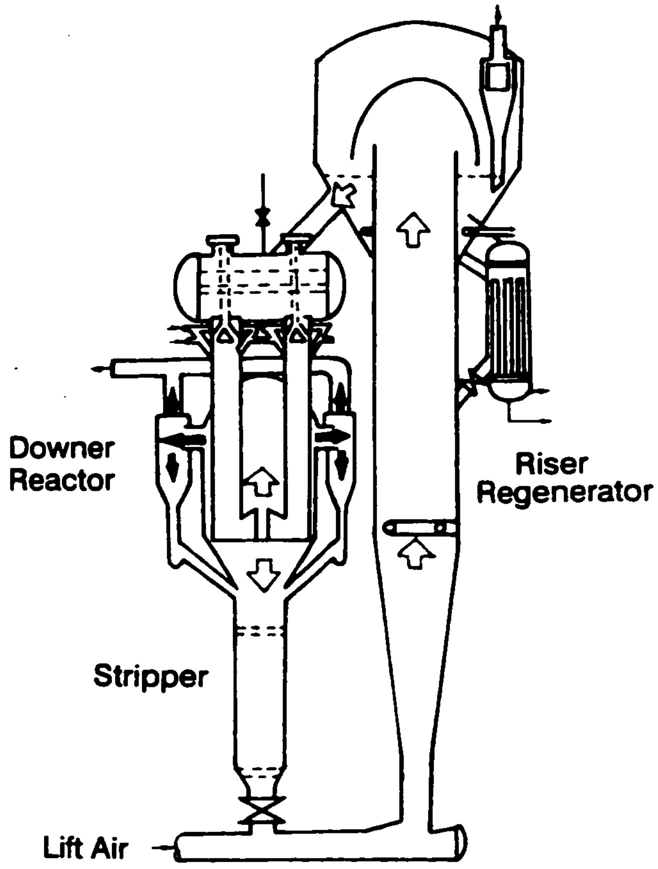
Downer Reactor
Riser Regenerator
Stripper
Lift Air

Fig. 1.1 A proposed FCC design with downer reactor (Murphy, 1992).

CHAPTER 2

LITERATURE REVIEW

2.1 General Overview

In the last five years, some researches studied the downflow reactor (i.e. the downer) extensively. They either analyzed the downer theoretically or obtained experimental results utilizing a laboratory scale apparatus (Bolkan-Kenny et al., 1994; Pontier et al. 1994). But no pilot plant data has been obtained for the downer. In fact, the High-Severity FCC (HS-FCC) project shared between KFUPM and Petroleum Energy Center-Japan (PEC) aims to construct a pilot plant as shown in Fig. 2.1, which will give valuable information to prove whether the downer is better than the riser or not. Moreover, Nippon Oil Company, Japan, is also installing a cold flow model as a demonstration unit for FCC downer process in Japan.

The HS-FCC project aims to increase the gasoline yield and that of olefins, in the product gases, which are used as feed for many petrochemical industries. Thus the project integrates the refining with the petrochemical industries in one process which is considered as a new trend in the chemical industries.

Generally, current drawbacks of risers may be overcome in downflow circulating fluidized beds systems in which the gas and the catalyst flow in the direction of gravity. Expected advantages of downers over risers by reviewing the literature are:

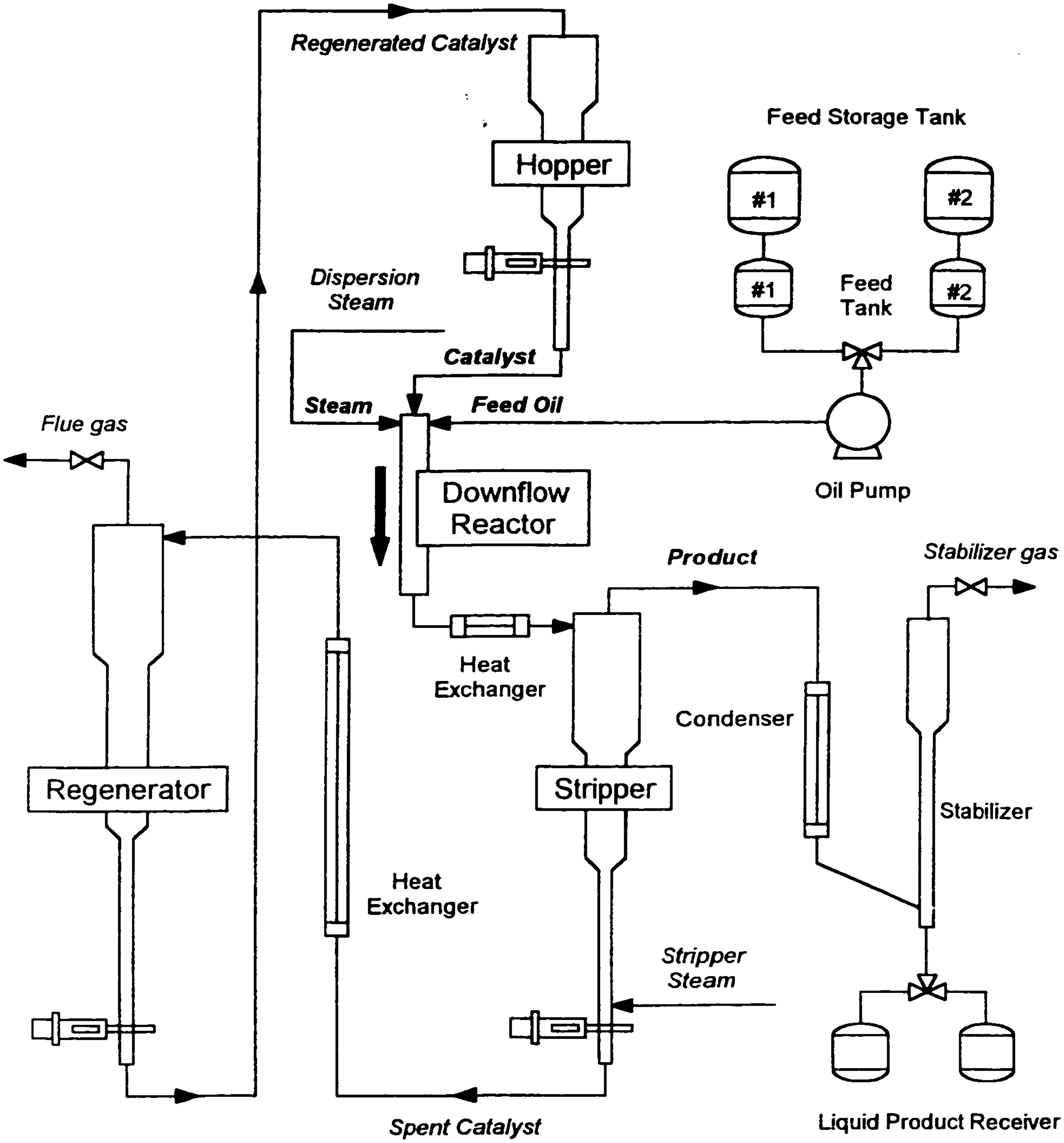
Regenerated Catalyst
Hopper
Feed Storage Tank
#1
#2
#1
Feed Tank
#2
Dispersion Steam
Catalyst
Steam
Feed Oil
Flue gas
Oil Pump
Downflow Reactor
Product
Stabilizer gas
Heat Exchanger
Condenser
Regenerator
Stripper
Stabilizer
Heat Exchanger
Stripper Steam
Spent Catalyst
Liquid Product Receiver

Fig. 2.1 Schematic diagram for the FCC-downer pilot plant

1. Backmixing is avoided so that more uniform flow and narrower residence time distribution (RTD) can be achieved, leading to better reaction control.
2. Shorter residence times can be achieved since slip velocities are small relative to the risers. That means elimination of the overcracking problem.
3. The downer can also operate at higher catalyst/oil ratios, giving improved conversions.
4. In the downer, the catalyst particles can reach a velocity higher than that of the gas allowing "forward mixing", so the gas contacts relatively fresher catalyst at all locations (i.e. enhancing the gasoline yield)

However, these features make the downer reactor a candidate for (Zhu and Wei, 1994):

1) Very fast reactions with intermediate desired products.
2) Reactions where high catalyst to gas feed ratio is required.
3) Catalytic reactions with rapid decaying catalysts

2.2 Kinetics of FCC Cracking Reaction

Gas oil, which is the feed to the FCC process, is a heavy petroleum fraction containing many of different compounds. The cracking of gas oil gives alot of products. Therefore the study of the FCC reaction kinetics presents restrictions, which should be considered in modeling the reaction scheme.

The simplest approach in studying the FCC reaction is to "lump" the reactants and products and deal with a number of components as one. Weekman & Nace (1970) analyzed the kinetics of catalytic cracking and proposed a three- lumps scheme describing the reactions carried out during the process as:

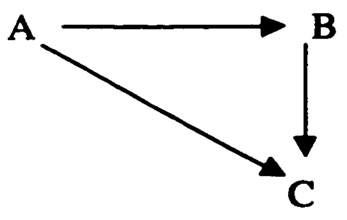

where lump A represents the feedstock (gas oil), lump B is the gasoline range hydrocarbons, and lump C is the coke and light gases.

Six years later, Jacob et al (1976) suggested a network consisting of ten lumps as shown in Fig. 2.2. This model is based upon the molecular structure and restricted to lumps that could be measured. The major advantage of such a model is that the conversion of gas oil to the different products can be determined easily. However, the model offers complicated mathematics and it also lumps the coke and light gases as one component as the three-lumped model (Ali and Rohani, 1996).

The key of this lumping scheme is as follows; the feed is lumped into paraffins (P_h,P_l), naphthenes (N_h ,N_l), aromatic rings (A_h,A_l) and aromatic groups in both the heavy (C_{Ah}) and light fractions (C_{Al}) of the charge stock. The products are divided into two lumps. One is gasoline range (G_{10}) and the other is coke and C_1---C_4 gases (C_{10}).

Takatsuka et al. (1987) observed that the catalytic cracking of residual oil (i.e. gas oil) is strongly influenced by the nature and prior treatment of the feedstock. So they included the feed stock in the cracking kinetics to give a six-lump model as shown in Fig. 2.3. In this figure, VR/CSO refers to vacuum resid and VGO/HCO refers to vacuum gas oil.

Lee et al. (1989) proposed four-lump kinetics for cracking of gas oil as illustrated in Fig. 2.4. In this model, the light gases and coke are separated from each other to form two lumps instead of one compared to the three and ten lump schemes. In fact, many researchers prefer to work with the four-lump model because of its moderate mathematical simplicity and good results obtained through modeling (Bolkan-Kenny et al., 1994).

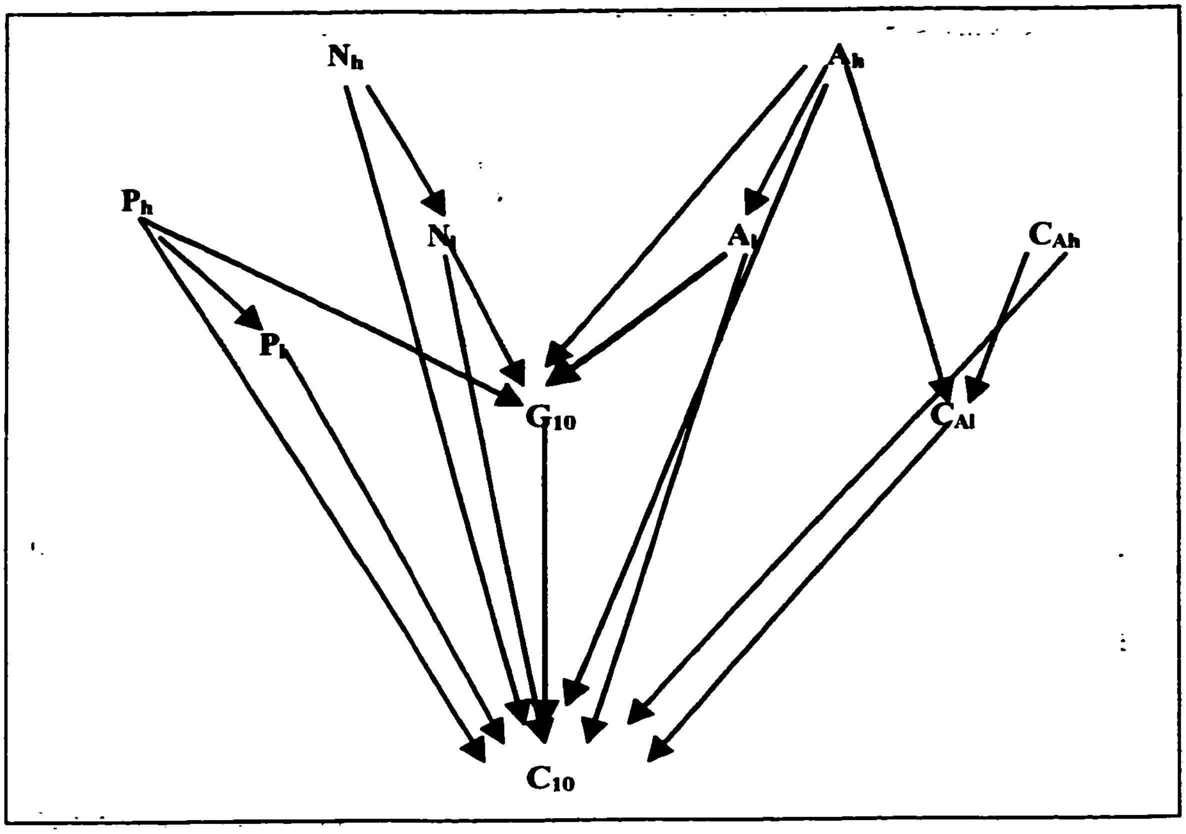
Nh
Ah
Ph
Nl
Al
CAh
Pl
G10
CAl
C10

Fig.2.2 Ten-lumped model (Jacob et al., 1976)

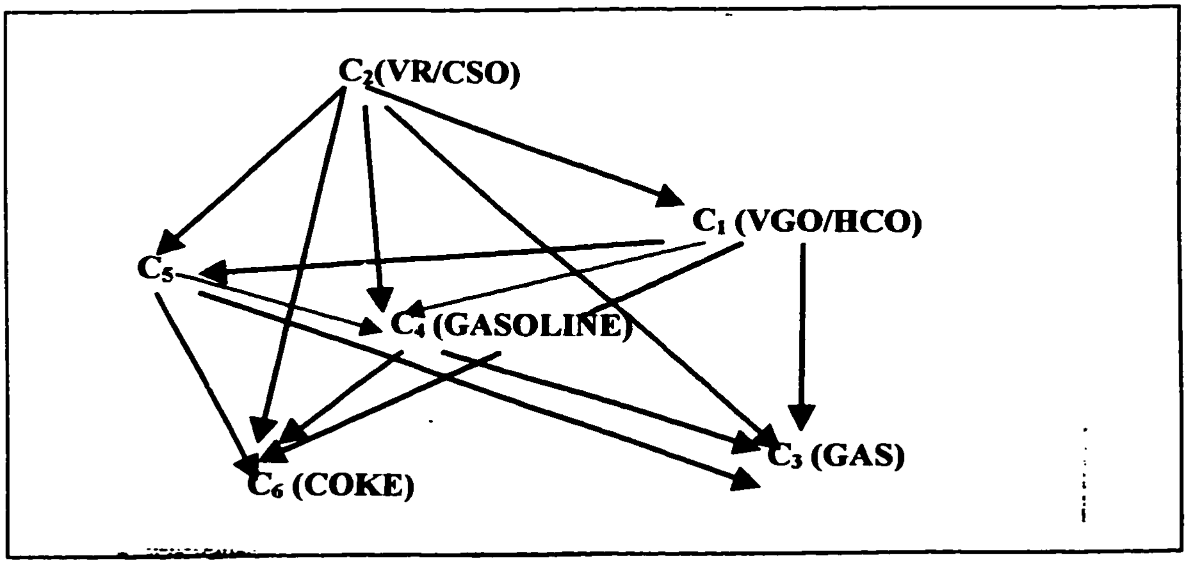
C2(VR/CSO)
C1 (VGO/HCO)
C5
C4 (GASOLINE)
C3 (GAS)
C6 (COKE)

Fig. 2.3 Six- lumped model (Takatsuka et al 1987)

Corella and Frances (1990) introduced one more lump to give a five-lumped model as shown in Fig. 2.5. The five groups are: Feed stock (A), Gas oil (O), Gasoline (E), Light gases (G) and coke (C). These lumps are interconnected with seven different kinetic cracking constants. Most recently, Al-Khattaf and de Lasa (1999) suggested a seven-lumped scheme as shown in Fig. 2.6. The seven lumps are: Gas oil, Olefins, Napthenes Paraffins, Aromatic, Methane and Coke. A tabulated comparison between the various schemes suggested is presented in Table 2.1.

2.3 Hydrodynamics of the Downer in FCC Process

Many studies on the hydrodynamics of the downer were presented in the literature. They discussed the type of the flow in the downer and compared it with the conventional riser reactors (e.g., Yang et al. (1991); Zhu and Wei (1995)).

Yang et al. (1991) and Wang et a al. (1992) suggested that in the downer, the section from the top to the position where particle velocities are equal to the gas velocity is called the"first acceleration section". Then particle velocity increases further until the slip velocity between the particles and gas, U_{slip} , defined as the particle velocity minus the gas velocity, reaches a value where the drag force counter-balances the gravitational force. This section has been referred to as the "second acceleration section". When the gravitational force is in balance with the drag, both particles and gas velocities remain constant downstream, and the remainder of the downer may be named the constant velocity section as shown in Fig. 2.7. Yang et al (1991) measured radial solids concentrations for both the riser and the downer under similar operating conditions. They concluded that the radial profiles of solids is more uniform in the riser than the downers.

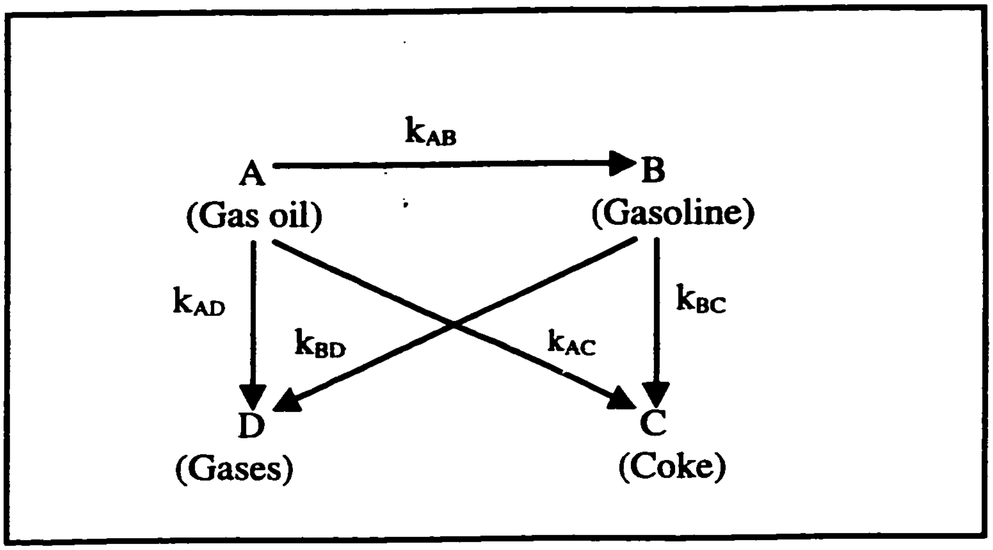
k_{AB}
A
(Gas oil)
B
(Gasoline)
k_{AD}
k_{BD}
k_{AC}
k_{BC}
D
(Gases)
C
(Coke)

Fig. 2.4 Four-lumped model (Lee et al. 1989)

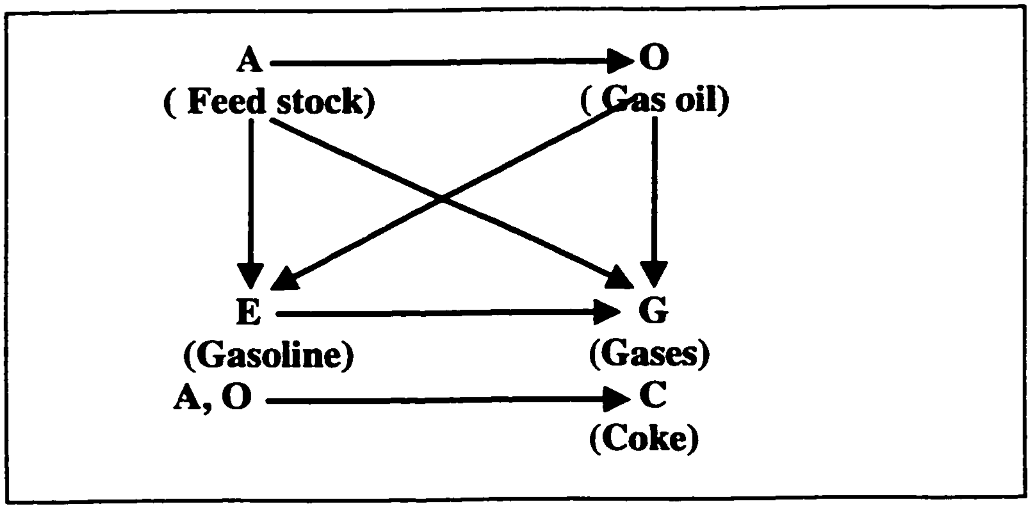
A
(Feed stock)
O
(Gas oil)
E
(Gasoline)
G
(Gases)
A, O
C
(Coke)

Fig. 2.5: Five-lump model (Corella & Frances 1990)

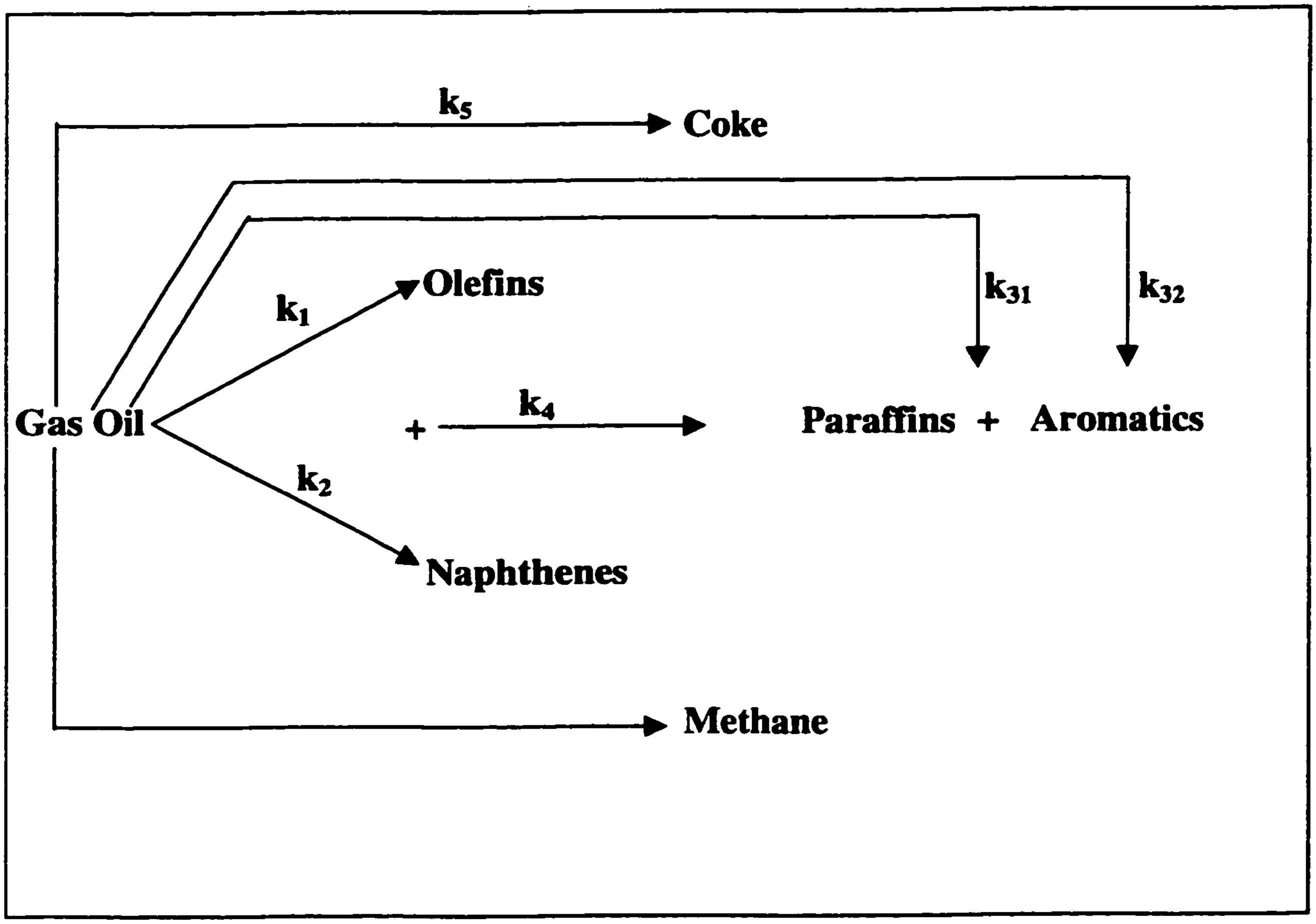
k5
Coke
k31
k32
k1
Olefins
Gas Oil
+
k4
Paraffins + Aromatics
k2
Naphthenes
Methane

Fig. 2.6: Seven-lump model (Al-Khattaf and de Lasa, 1999)

Table 2.1 Review of reaction kinetics schemes proposed for FCC reaction

TYPE OF SCHEME	SUGGESTED BY	LUMPS	KINETIC CONSTANTS	ADVANTAGES	DRAWBACKS
Three-lumped	Weekman & Nace (1970)	1- Gas oil 2- Gasoline 3- Light gases & coke	3 reaction constants	• simple mathematically • can determine gas oil conversion and gasoline yield simultaneously	• it lumps coke and light gases into one component
Ten-lumped	Jacob et al. (1976)	1,2- Paraffins 3,4- Naphthenes 5,6- Aromatic rings 7,8- Aromatic groups 9- Gasoline 10- Gases & coke	17 reaction constants	• gas oil conversion can be estimated and the production rate of some particular products can be calculated	• complicated mathematically • experimentally tedious • lumping of gases and coke as one component
Six-lumped	Takatsuka et al. (1987)	1- Gas oil 2- VR 3- Light gases 4- Gasoline 5- LCO 6- Coke	6 reaction constants	• separates gases from coke	• applicable for the case studied
Four-lumped	Lee et al. (1989)	1- Gas oil 2- Gasoline 3- Coke 4- Light gases	5 reaction constants	• simple mathematically • separates gases from coke • agreement between theory and experiment	• does not predict olefins yields
Five-lumped	Corella & Frances (1990)	1- Feedstock 2- Gas oil 3- Gasoline 4- Coke 5- Light gases	7 reaction constants	• gases and coke are as two lumps	• more applicable for hydrocracking units (suggests that feedstock cracks to gas oil)
Seven-lumped	Al-Khattaf & de Lasa (1999)	1- Gas Oil 2- Olefins 3- Naphthenes 4- Paraffins 5- Aromatics 6- Mathane 7- Coke	7 reaction constants	• Olefins in separate lump • Coke in separate lump	• needs to be established more

Moreover, the radial gas velocity profiles along the downer differ significantly from those observed in the risers (Zhu et al. 1995). Muldowney (1995) stated that the main difference between the hydrodynamics of the downer and the riser in few words: "If a tiny observer were standing on a catalyst particle in a riser, he would see oil passing upward around him. In a downer, he would see oil vapour approximately stagnant around him".

Bolkan-Kenny et al. (1994) presented a hydrodynamic model based upon a one-dimensional model. On the other hand, Kimm et al (1996) developed a hydrodynamic model for laboratory scale down flow reactors, incorporating the solids circulation rate and superficial gas velocity. Then, the gas and particle velocity profiles were calculated.

Compared with the riser reactors, downers have a much more uniform radial gas – solids flow pattern. This is likely due to change of the direction of the gas and soiids flow from opposing gravity to following it (Zhu et al., 1995).

In both the downer and the riser, higher local solids concentration results in the reduction of drag coefficient. In the riser, where the drag is the driving force for the particle flow, reduction of drag decreases the upward particle velocity, which in turn increases the tendency for particle aggregation. It is noted that increased local gas and particle velocities in the downer tend to reduce the extent of particle aggregation. Therfore, the system stabilizes by itself and a more uniform radial flow structure is present in the downer (Zhu & Wei, 1994). Table 2.2 summarizes the work done in the downer hydrodynamics area.

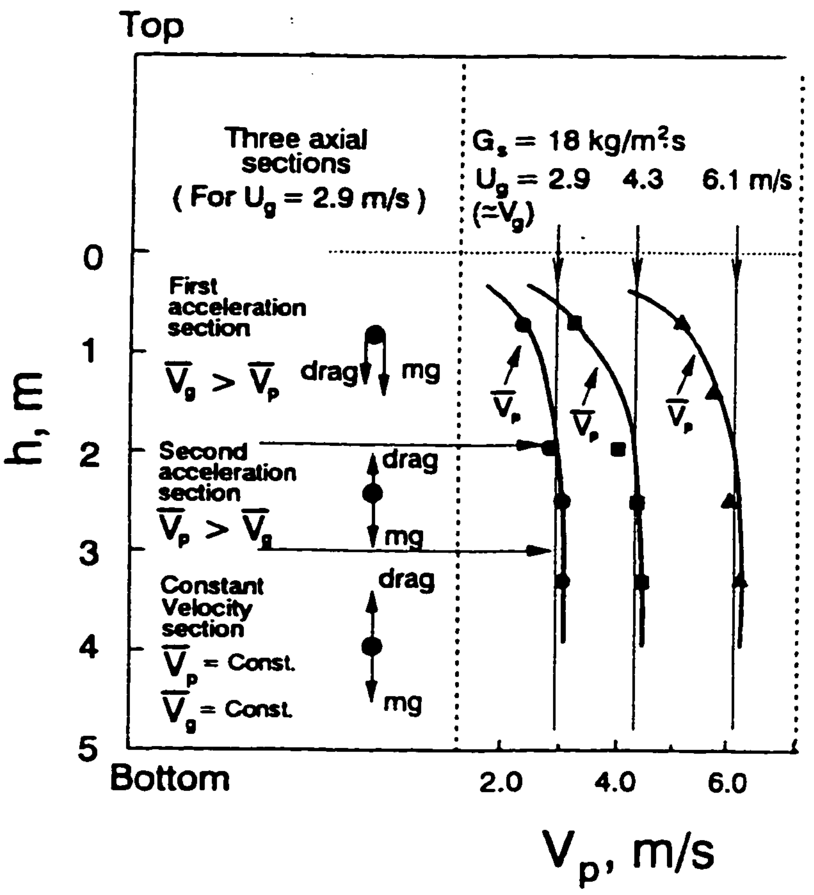

Fig. 2.7 Axial gas-solids flow structure in the downer (Zhu et al, 1995)

2.4 Modeling Downer Reactors

A general model of the downer reactor is obtained by combining the hydrodynamics, reaction kinetics of the FCC reaction, and conservation equations on a differential control volume. There are only two papers in the open literature reporting models for the downer reactor.

Bolkan-Kenny et al., (1994), developed a model that relates the hydrodynamics with kinetics to give regerious reactor modeling for downers. In a given control volume, first the hydrodynamic parameters and the reaction rates were solved for using separate modules. Then, the information gathered from these modules was coupled in the material balance equation and the molar flow rates of all components were computed. Finally, the gas velocity was corrected for volumetric expansion. The values at the exit of a given control volume were used as the input values to the adjacent control volume. This illustrates a feature of their simulator in that as more complex and newly developed kinetics become available, they can be readily accommodated in the proposed simulation since the reaction kinetics is described as a separate module. They used four-lump kinetics and one-dimensional hydrodynamic model with plug flow assumption.

Recently, Fei et al. (1997), claim that the plug flow derivation in risers is oversimplified. So they introduced a dispersion model (one-dimensional hydrodynamics and four-lump kinetics) to give a rigorous comparison between the risers and downers. They utilized this model to show the advantages of newly developed process. Table 2.3 summarizes briefly the papers on reactor models for the downer.

TABLE 2.2 Summary of Hydrodynamic Studies on Downer in the Literature

Done by	Methodology	Type of apparatus and catalyst used	Operating conditions	Some important conclusions
Yang et al. (1991)	Experimental work with cocurrent flow	-Cocurrent downflow bed(downer) made of plexiglass of 140mm ID and 5.8 m in height using fiber optical probes to measure the different variables -FCC catalyst (d_p=59μm,ρ_p=1474 kg/m3)	-Room Temp. -Gas velocity(15-7m/s) -Solid circulation rate(8-40kg/m^2.s)	-Flow structure in the downer is divided into 3 regions: 1-first acceleration section 2-Second acceleration section 3-Constant velocity section -Both the paticle flow and radial profiles of particle velocity are more uniform than the riser.
Wang et al. (1992)	Experimental Work	-Downflow tube of 140 mm ID and 5.8m in length from plexiglass Micrometer to measure the d_p Local particle conc. In the bed was measured using probes FCC catalyst with ρ_p=1545 kg/m3 and d_p=59μm	Gas velocity=2-8m/s Solid cir. Rate=30-80 kg/m^2.s	-Flow structure presentation -Illustrating of the radial profiles of solid conc. In the Downer. -Fitted correlation to find the radial profiles of paticle velocity. -Aggregation of particles occur in both risers and downers.Suggesting a formula to get the radial voidage distribution
Bolkan-Kenny et al. (1994)	Theoretically based analysis to get a simulated behaviour inside the downer Assumptions made are: 1- the system operate at steady state 2- High heat and mass transfer rates 3- radial profiles are flat and one-dimensional model.	Octacat catalyst and Zeolite II	Tenp= 550 °C Reactor height=35m Reactor diam.=1m Solid circulation rate=200 kg/(m^2.s)	-Simulated results are with good agreement with those obtained by Aubert et al(1993) & Wang et al(1992) -Disagreement between simulated and experimental results for the pressure profiles.
Kimm et al. (1996)	Theoretical approaches based upon: 1- The system operates at steady state condition. 2- Pseudo-homogeneous assumption.	---	---	-Fitting an equation for finding the hold-up in the reactor -Max hold-up at r/R=.94 -Fitting the radial gas velocity by an empirical equation. -Study the effect of increasing the downer diameter. -The wall effects only extend from the wall to a radial distance.

Table 2.3 Reactor models presented for the DOWNER in the literature

Work done by:	Hydrodynamic model used and assumptions made	Kinetic model used	Reactor model	Remarks
Bolkan-Kenny et al.(1994)	-Plug flow model. -One dimensional. -Steady state. -Isothermal.	-Both three-lump and four -lump schemes. -Deactivation as a function of residence time.	-The reactor model was obtained by coupling the hydrodynamics model with the reaction kinetics for the FCC process. -Plug flow assumption in the downer.	-The uniform temprature assumption ignores the heat effects inside the FCC reactor.
Fei et al. (1997)	-Dispersion mixing model. -One dimensional. -Steady state. -Isothermal.	-Four-lump scheme. -Deactivation as a function of coke content in the catalyst.	-Dispersion model is used in conjuction with four-lump kinetics. -Study on effect of Peclet no.	- Heat effects in the downer are neglected.

CHAPTER 3

DEVELOPMENT OF FCC-DOWNER UNIT MODEL

3.1 Downer-Regenerator Model Development

The schematic diagram of the whole unit was shown in Figure 2.1. This unit is composed of two reactors:

1. The downer reactor where the gas oil and catalyst are fed from the top of the downer causing the endothermic cracking reactions to occur.
2. The regenerator reactor where coke on the spent catalyst is burned by air through exothermic reactions in order to reactivate the catalyst. The heat released from the reactions inside the regenerator plays a major role in keeping the unit heat balanced.

In the proposed model, the stripper role is not considered because it does not change the heat or the mass of the spent catalyst stripped from the products of the downer. Thus, it can be assumed that the temperature of the spent catalyst leaving the downer is the same as that entering the regenerator. Moreover, the model is derived based on complete combustion mode to model correctly the behavior of the pilot plant where the air is fed in excess leading to complete combustion. However, most commercial conventional FCC-riser units are operated with partial combustion mode not to exceed the temperature rating of the regenerator internals, since the oxidation of CO to CO_2 generates 2.5 times more heat than combustion of C to CO (Sadeghbeigi, 1995).

As shown in Chapter 2, the downer reactor hydrodynamics can be approximated by a plug flow reactor. It is a justifiable assumption because the downer reactor exhibits uniform radial and axial gas-solids flow pattern (Zhu, 1995).

3.2 Downer model development

Modeling of the downer reactor requires understanding of both the hydrodynamic aspects of the downer and the FCC-reaction carried out in the downer.

3.2.1 Hydrodynamics of the downer

The hydrodynamics study of downer reactors presented in Chapter 2 revealed that the radial solids fraction profile in the downer is flat and uniform which results in a large reduction of gas and solid backmixing. Therefore it can be inferred from gas-solids flow patterns that the downer is a plug-flow reactor with two-phase flow.

3.2.2 Cracking-reaction kinetics in the downer

There are many schemes proposed for FCC-reaction. The extensive study shown in Chapter 2 involved different schemes. We have selected the four-lump scheme for our model. It is fairly simple and deals with coke and gases as separate lumps. In this scheme, the cracking reactions are assumed to be second order. The reaction rates for the four lumps are:

$$(-r_A) = \phi_D \, (k_{AB} + k_{AC} + k_{AD}) y_A^2 \tag{3.1}$$

$$(-r_B) = \phi_D \left[(k_{BD} + k_{BC}) y_B - k_{AB} y_A^2\right] \tag{3.2}$$

$$(+r_C) = \phi_D \left(k_{AC}\, y_A^2 + k_{BC}\, y_B\right) \tag{3.3}$$

$$(+r_D) = \phi_D \left(k_{AD}\, y_A^2 + k_{BD}\, y_B\right) \tag{3.4}$$

where y_j is dimensionless weight percent of hydrocarbons and ϕ_D is the deactivation function.

The reaction kinetic constants are related to temperature by Arrhenuis law. They are obtained from data supplied by the team of HS-FCC project. The deactivation of the catalyst due to coke deposition has been the subject of many research works. In the present work, the deactivation kinetic model of Weekman (1979) is chosen because of its simplicity, popularity in FCC modeling, and the abundance of data available in the literature. In the four-lumped scheme, the decay of the catalyst activity due to coke deposition is represented by a function, ϕ_D, which depends on the temperature of the downer and the catalyst residence time, τ_C:

$$\phi_D = \exp\left(-\alpha\, \tau_C\right) \tag{3.5}$$

where α is the catalyst decay coefficient related to the downer by an Arrhenius equation. The deactivation function has been investigated in the MAT unit by HS-FCC project team. The data obtained are generally in good agreement with literature values. Both the FCC-reaction kinetic constants and the deactivation parameter are shown in Table 3.1.

Table 3.1 Kinetic parameters for reactions in downer and regenerator

Reaction	**Pre-exponential constant** $\left[s^{-1}\right]$	**Activation Energy** $\left[kJ/mol\right]$
k_{AB}*	620.0	47.626
k_{AC} *	88.0	60.275
k_{AD}*	60.0	39.781
k_{BC}	0.0	0.0
k_{BD}	3400.0	76.366
Coke burning , k_c	1.4×10^8 $m^3/(kmol.s)$	125
CO catalytic combustion, $k_{CO,c}$	247.75 $(m^3)^{1.5}/(kmol^{.5}.s)$	7.74
α (coking)	2.4	32.728

* *k_{AB} , k_{AC} , k_{AD} values given are multiplied by ρ_b*

3.2.3 Assumption made to derive the downer model

1. Instantaneous vaporization of the gas oil feed by the hot catalyst. It is a justifiable assumption because it takes about 0.1 s to fully vaporize the gas oil.
2. A detailed three-dimensional two-phase modeling study of the flow pattern and heat transfer in FCC riser reactors was performed by Theologos and Markots (1993). They concluded that the overall performance of the riser can be predicted using simple one dimensional mass, energy, and chemical species balances. Similarly, this assumption can be relaxed to include downer reactors since the behavior and function of both reactor types are alike.
3. Plug flow behavior is assumed for the downer according to the survey of hydrodynamics studies presented in Chapter 2.
4. The changes due to molar expansion were not accounted for in our model. Thus, the molar volume of hydrocarbons is constant along the downer. This assumption simplifies the derivations of the equations by a justifiable idea as proved by Thelogos and Markatos (1997).
5. All cracking reactions are considered to take place in the downer. This assumption is reasonable since the zeolite catalysts and the multi-function catalyst additives highly activate the cracking reaction rate. Furthermore, the coke formation sharply decreases the catalyst activity towards the exit of the downer.
6. Our model uses the four-lumped scheme to represent the different reaction rates of gas oil, gasoline, coke and gases. Use of this scheme was discussed before in section 3.2.2.
7. Catalyst deactivation follows the Weekman Model (1979). Detailed discussion was presented in section 3.2.2.

8. The downer bed has a high combined stream velocity and a very short residence time. Thus, it can be assumed that the dynamic terms due to vapor phase concentrations, coke formation and downer temperature are negligible in comparison with the corresponding terms of the coke burning and temperature in the regenerator. Therefore, the mass and energy balance equations are considered at steady state.
9. The role of steam used to disperse the feed at the entrance of the downer is neglected due to its low amount compared with the feed. Its percentage in the feed is about 2%.
10. The heat losses from the downer, H_{lD}, is an emperical parameter. Usually this is taken to be 2 - 3% in the heat balance. This value is in general the heat loss used in literature (Pierce, 1983; Sadegbiege, 1995).
11. Vapour phase and solid mass flow rates are constant and independent of position. Likewise, the gases void fraction is assumed constant and independent of position.
12. Heats of reaction are assumed constant. Other thermal and physical properties are aslo assumed constant (i.e. C_{Ps} , C_{Pg},, ρ_g).

3.2.4 The downer model equations

Based on the above discussion, the downer model equations using the four-lumped scheme are derived.

The gas oil mass balance equation is derived by taking an increment with cross sectional area A_D and a very small width ΔZ, the mass conservation principle when applied to this increment results in :

$$\frac{F_{gD}\left[y_A \Big|_{Z_D} - y_A \Big|_{Z_D + \Delta Z_D} \right]}{\Delta Z_D} = A_D \; F_{gD} \; \rho_{gD} \; \phi_D \left(-r_A\right) \tag{3.6}$$

take the limit when ΔZ_D goes to zero, equation (3.8) becomes:

$$-F_{gD} \; \frac{dy_A}{dZ_D} = A_D \, \varepsilon_{gD} \, \rho_{gD} \phi_D \left(-r_A\right) \tag{3.7}$$

rearranging equation (3.7) and substituting for the reaction term, the mass balance of gas oil becomes:

$$\frac{dy_A}{dZ_D} = \frac{-A_D \; \varepsilon_{gD} \; \rho_{gD} \phi_D}{F_{gD}} \left(k_{AB} + k_{AC} + k_{AD}\right) y_A^2 \tag{3.8}$$

Equation (3.8) is normalized by dividing the axial length inside the downer by the total length of the downer. The final gas oil mass balance equation is :

$$\frac{dy_A}{dZ} = \frac{-\phi_D \varepsilon_{gD} A_D L_D \rho_{gD}}{F_{gD}} \left[k_{AB} + k_{AC} + k_{AD}\right] y_A^2 \tag{3.9}$$

Applying the same procedure to the gasoline, coke, and light gases results in the following dimensionless equations. The detailed derivation of these equation is presented in Appendix A.

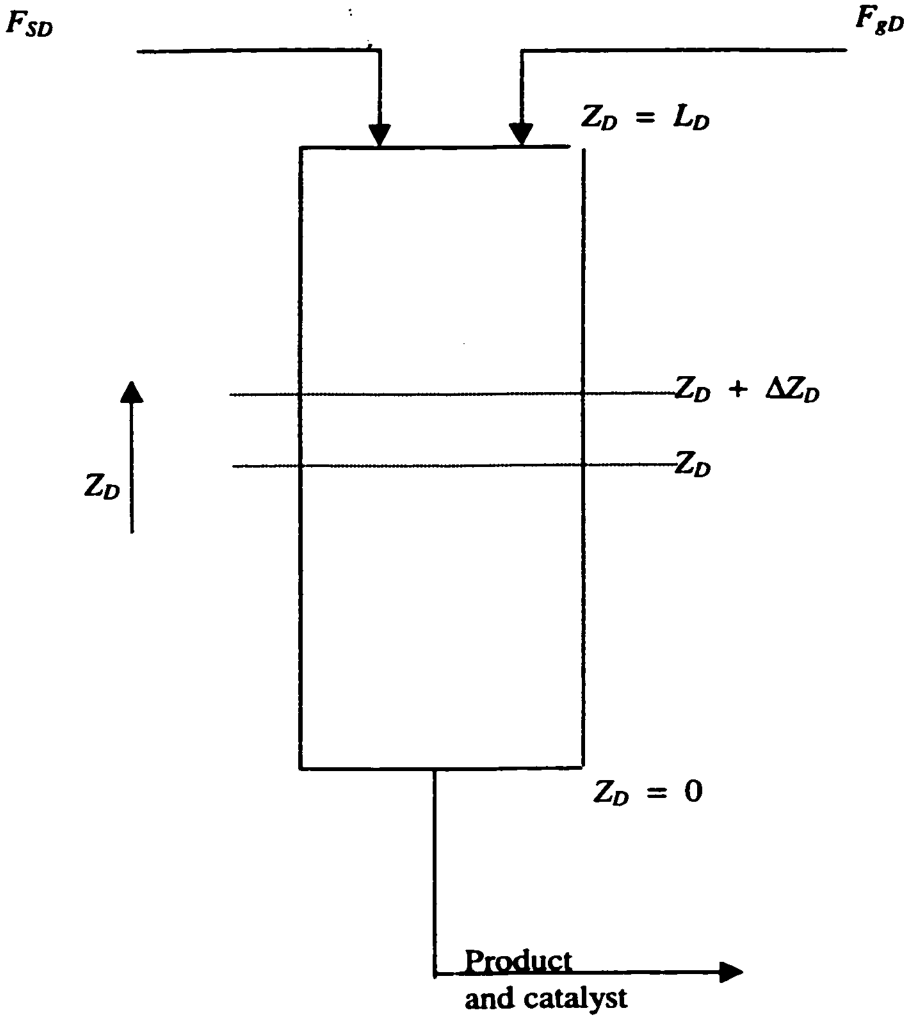
F_{SD}
F_{gD}
$Z_D = L_D$
$Z_D + \Delta Z_D$
Z_D
Z_D
$Z_D = 0$
Product
and catalyst

Fig. 3.1 Mass balance around the downer

Mass Balance of Gasoline (B):

$$\frac{dy_B}{dZ} = \frac{-\phi_D \varepsilon_{gD} A_D L_D \rho_{gD}}{F_{gD}} \left[(k_{BC} + k_{BD}) y_B - k_{AB} y_A^2 \right] \tag{3.10}$$

Mass Balance of Coke (C):

$$\frac{dy_C}{dZ} = \frac{+\phi_D \varepsilon_{gD} A_D L_D \rho_{gD}}{F_{gD}} \left[k_{AC} \ y_A^2 + k_{BC} \ y_B \right] \tag{3.11}$$

Mass Balance of Gases (D):

$$\frac{dy_D}{dZ} = \frac{+\phi_D \varepsilon_{gD} A_D L_D \rho_{gD}}{F_{gD}} \left[k_{AD} \ y_A^2 + k_{BD} \ y_B \right] \tag{3.12}$$

Energy Balance on Downer:

The energy balance of a plug flow reactor is applied for the FCC reaction to give

$$\left(F_{gD} \, C_{P_{gD}} + F_{sD} \, C_{P_s} \right) \frac{d\bar{T}}{d Z_D} = -\sum \phi_D (\Delta H_i)(-r_i) A_D \, \varepsilon_{gD} \rho_{gD} - H_{lD} \tag{3.13}$$

Then, T is normalized by T_{refD} and Z by L_D. And the term $\Sigma \ \Delta H_i \ (-ri)$ is substituted to give the final form of the energy balance on the downer.

$$\frac{dT_D}{dZ} = \frac{-\phi_D A_D L_D \, \varepsilon_{gD} \rho_{gD}}{\left(F_{gD} C_{P_{gD}} + F_{sD} C_{P_s} \right) T_{refD}} \begin{bmatrix} (\Delta H_{AB} k_{AB} + \Delta H_{AC} k_{AC} + \Delta H_{AD} k_{AD}) y_A^2 \\ + (\Delta H_{BC} k_{BC} + \Delta H_{BD} k_{BD}) y_B \end{bmatrix} + H_{lD} \tag{3.14}$$

with the boundary conditions, at Z = 1

$y_A \, (1) \ = \ 1$

$y_i \ (1) \ = \ 0 \ ; \quad i = \ B, C, \ and \ D$

$T_D \ (1) \ = \ T_{DF}$

Energy Balance at Downer Entrance:

In order to specify T_{DF}, it is necessary to write an energy balance equation at contact point between the regenerated catalyst and the "fresh" liquid gas oil. Therefore, Feed the energy balance equation at the downer entrance and according to Fig. 3.2:

$$F_{SD}\,C_{p_S}\left(T_e - T_{DF}\right) = F_{gD}\left[C_{pl}\left(T_b - T_F\right) + \frac{\Delta H_{vap}}{T_{refD}} + C_{p_{gD}}\left(T_{DF} - T_b\right)\right] \tag{3.15}$$

where T_b the dimensionless boiling temperature of gas oil and T_F is the dimensionless temperature of gas oil feed. Noting that the concentration of various hydrocarbon gases in the downer are normalized with respect to the gas oil feed concentration, and the downer temperature is normalized with respect to the gas oil feed temperature (T_{refD}).

3.3 Regenerator model development

If one wants to model the regenerator mathematically, the different physical and chemical aspects inside the regenerator should be understood. In other words, the hydrodynamics should be understood closely and the coke burning reactions of coke burning should be investigated, in order to obtain a model which could be used to predict the yields and temperatures in the regenerator. The following two sections give a background to begin modeling the regenerator.

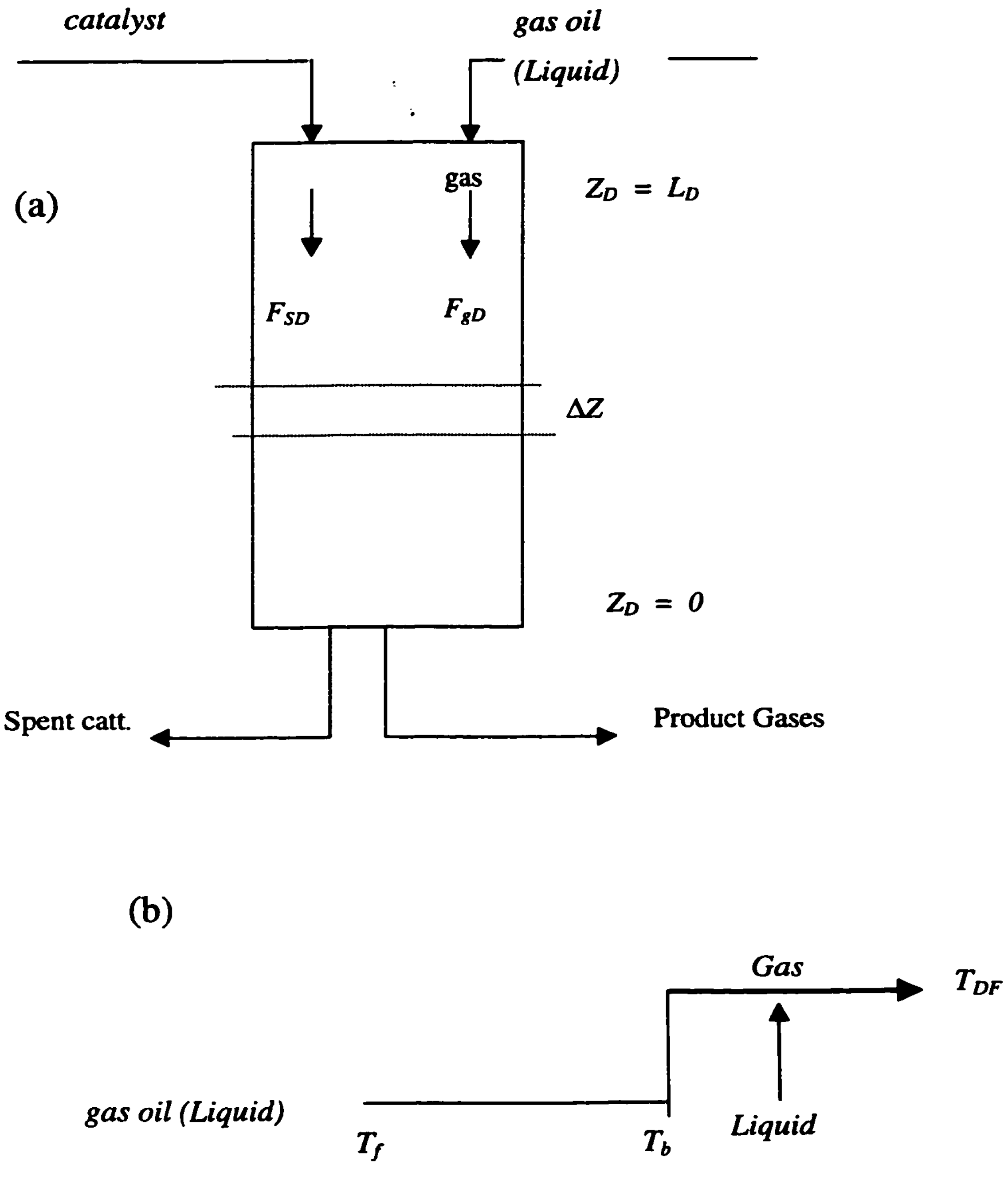
catalyst
gas oil
(Liquid)
(a)
gas
$Z_D = L_D$
F_{SD}
F_{gD}
ΔZ
$Z_D = 0$
Spent catt.
Product Gases
(b)
Gas
T_{DF}
gas oil (Liquid)
T_f
T_b
Liquid

Fig. 3.2 (a,b) : Representation of energy balance fort the downer.

3.3.1 Hydrodynamics of the regenerator

The regenerator reactor consists of two regions, the dense region and the freeboard dilute region. The freeboard zone is the section of vessel between the top surface of the dense region and the exit of the regenerator vessel. In this section, the gas stream carries some catalyst particles. The rate of solids entrainment is usually very small compared to the total amount of catalyst retained in the regenerator vessel. Most of coke on the catalyst has already been burned in the dense zone. That means, negligible combustion can be considered in this region. Thus, the effect of the freeboard region on the overall performance of the regenerator can be ignored. The dense region is further divided into two phases: a bubble phase and an emulsion phase. The bubbles move in plug flow and exchange mass and heat with the emulsion phase. In the emulsion phase the air distributors and the spent catalyst, produce enough turbulence to justify a continuous stirred tank reactor behavior.

The regenerator conditions are located under bubbling fluidized beds region. Fig 3.3 maps different fluidization regimes (Kunii and Levenspiel, 1991).

For the Pilot Plant operational conditions:

$$d_p^* = d_p \left[\frac{\rho_g (\rho_s - \rho_g) g}{\mu^2} \right] = 1.139 \qquad (3.16a)$$

and

$$u^* = U_a \left[\frac{\rho_g^2}{\mu (\rho_s - \rho_g) g} \right]^{1/3} = 0.562 \qquad (3.16b)$$

From Figure 16(b) in Kunii and Levenspiel (1991), the regenerator operation is located in *"bubbling fluidized beds"* region. The regenerator is divided into two regions the dense region where the main regeneration process takes place and the dilute region (the freeboard region at the top of the regenerator) to allow the entertainment of catalyst particles (Sadegbeigi, 1995). In our model, the effect of dilute region is ignored due to its low concentration of catalyst, as stated earlier.

It was shown from previous discussion that the regenerator operates as bubbling fluidized bed. So the dense region can be divided further into two phases: the bubble phase which is composed of the gas going through the dense bed, and the emulsion phase holding the hot solid particles (Kunii and Levenspiel, 1991).

The bubbles in the regenerator play a complex role. They produce good mixing of the solid catalyst, and affect the emulsion phase temperature through heat transfer between bubble and emulsion phases. Heat transferred to bubbles is lost from the system. Another drawback is the by-passing of a certain percentage of air without diffusion into the emulsion phase. The bubbles act as a plug rising through the bed. In the emulsion phase, the air distribution and the spent catalyst will produce enough turbulence that continuous stirred tank reactor behavior can be assumed.

The minimum fluidization velocity, U_{mf} , of the emulsion phase can be calculated from the following correlation proposed by Bueyens and Geldart (Wilson, 1997)

$$U_{mf} = \frac{9\,x\,10^{-4}\left(\rho_P - \rho_g\right)^{0.934} g^{0.934}\, d_p^{1.8}}{\mu_g^{0.087} \qquad \rho_g^{0.066}} \tag{3.17}$$

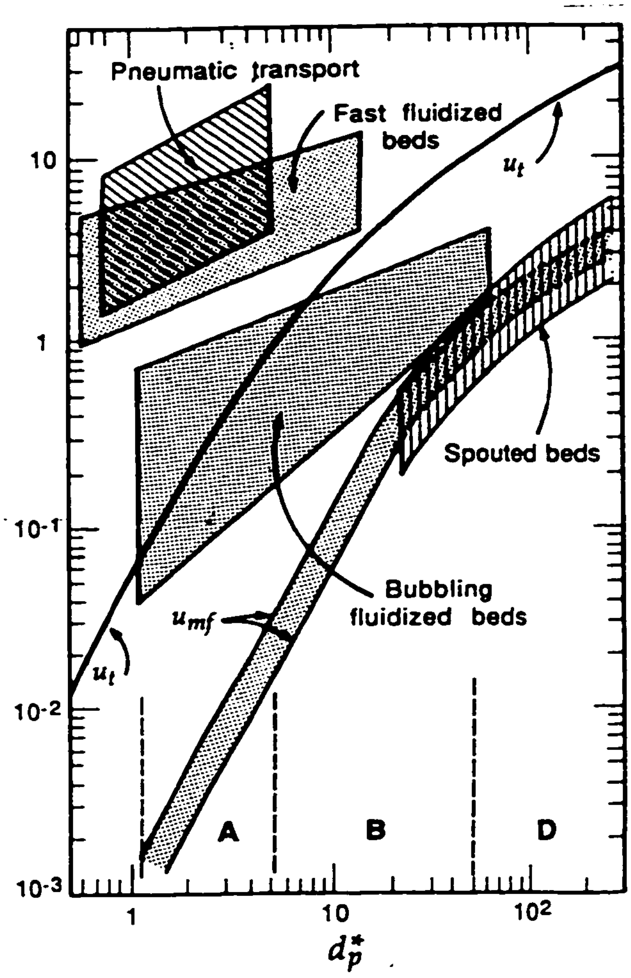

Fig. 3.3. General flow regime diagram (Fig. 3-16b in Kunii and Levenspiel, 1991).

The volumetric flow rates in the emulsion phase, G_{IG} , and in the bubble phase, G_{CG}, are :

$$G_{IG} = U_{mf} \cdot A_G \tag{3.18}$$

$$G_{CG} = (U_a - U_{mf}) A_G \tag{3.19}$$

where U_a is the velocity of air and the volume fraction of bubbles is :

$$\varepsilon_{bG} = \frac{G_{CG}\, t_a}{A_G\, L_G} = \left(U_a - U_{mf}\right) t_a \tag{3.20}$$

where t_a is the air space time in the regenerator. The void fraction or the gaseous contents in the emulsion phase, ε_{eG}, is obtained from Figure 6-5a in Kunii & Levenspiel (1991), see Fig. 3.4. There are exchanges of mass and heat between the two phases. The mass and heat transfer coefficients should be obtained.

3.3.1.1 Mass transfer coefficient between bubble and emulsion phases:

The bubble diameter should be calculated first by the following correlation (Kunii and Levenspiel, 1991).

$$d_b = 0.65 \left[\frac{\pi}{4} d_t^2 \left(U_a - U_{mf}\right)\right]^{0.4} \tag{3.21}$$

then the bubble rise velocity with respect to emulsion phase is calculated as:

$$U_{br} = 0.711 \left(g\, d_b\right)^{1/2} \tag{3.22}$$

and

$$U_b = 1.55 \left[\left(U_o - U_{mf}\right) + 14.1 \left(d_b + 0.05\right)\right] d_t^{3.2} + U_{br} \tag{3.23}$$

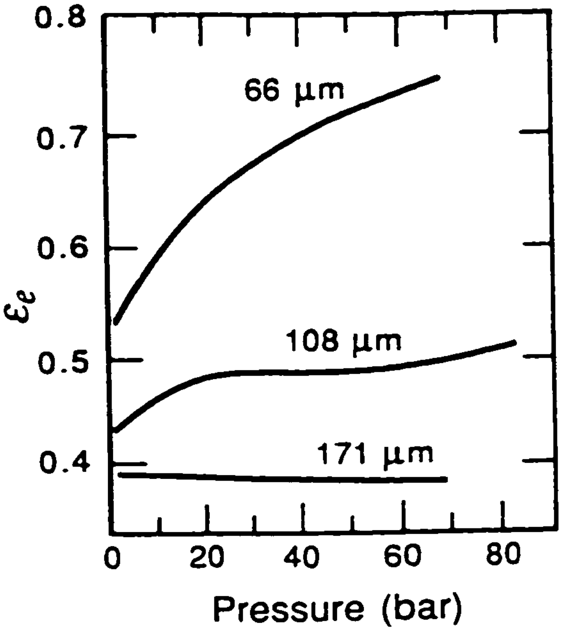

Fig. 3.4 Emulsion voidage (Fig 6-5a in Kunii and Levenspiel, 1991).

where U_o is the superficial gas velocity. Therefore, the bubble fraction, δ, is given by:

So, $$\delta = \frac{U_o}{U_b} \tag{3.24}$$

Note that the bubble emulsion interfacial area per unit volume be can obtained using the following equation (Kunii and Levenspiel, 1991):.

$$a_b = \frac{6\delta}{d_b} \tag{3.25}$$

where a_b is the same as the area of heat transfer between bubble and emulsion phases, a_v, in our model. Figure (10 – 13a) in Kunii and Levenspiel (1991) (see Fig. 3.5) gives the value of k_{be} which can be substituted in :

$$K_{be} \cong k_{be}\, a_b \frac{U_b}{U_o} \tag{3.26}$$

where K_{be} is the bubble emulsion mass transfer coefficient, k_g in our model.

3.3.1.2 Heat transfer coefficient between bubble and emulsion phase

The following Nusselt number correlation is used (Kunii and Levenspiel, 1991):

$$Nu_p = 2 + 0.6\, Re_p^{1/2}\, P_r^{1/3} \tag{3.27}$$

where $$R_{ep} = \frac{d_p U_o \rho_g}{\mu} \tag{3.28}$$

and $$P_r = \frac{C_p \mu}{k_{gas}} \tag{3.29}$$

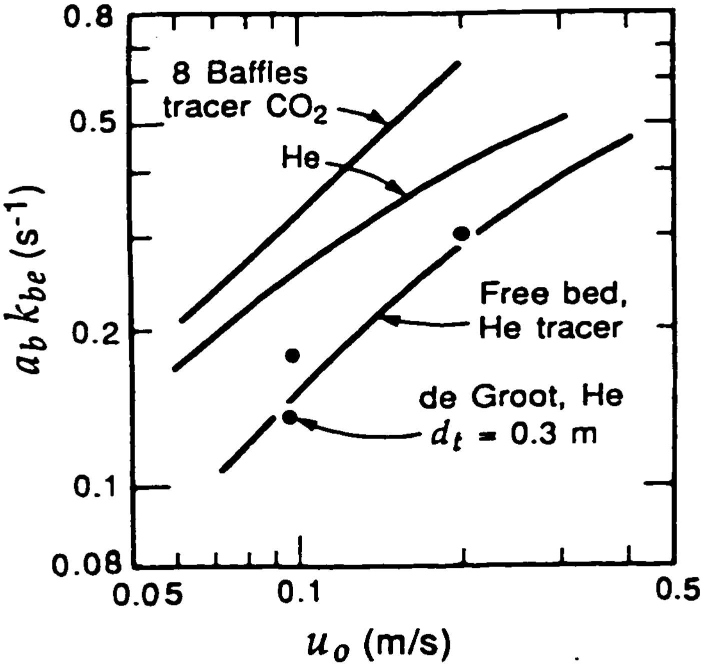

Fig. 3.5 Experimental values for bubble-emulsion transfer coefficient (Fig 10-13a in Kunii and Levenspiel, 1991).

For low R_{ep} values

$$h_{bed} = h = \frac{h_p}{3} \tag{3.30}$$

3.3.2 Coke burning kinetics in the regenerator

The mechanism and kinetics of the regeneration of coke deposits on cracking catalysts are thoroughly investigated in the literature. Moorley and de Lasa (1987, 1988) carried out investigations to determine the kinetic parameters for the regeneration of cracking catalysts. They also studied the effect of the CO post combustion reaction on the overall performance of the regenerator.

The kinetics of coke burning in this work are simulated based on the work done by Moorley and de Lasa (1987, 1988). It is assumed that the overall rate of combustion is controlled by the intrinsic kinetics of combustion.

Thus, the reactions carried out in the regenerator for the case of complete combustion are:

1. Coke combustion reaction

$$C + \frac{2\sigma+1}{2\sigma+2} O_2 \longrightarrow \frac{\sigma}{\sigma+1} CO_2 + \frac{1}{1+\sigma} CO$$

where σ is CO_2 to CO molar ratio and it is obtained by the following correlation suggested by Lee & Groves (1985):

$\sigma = 0.000953 \, exp\left(5585/T\right),$ $\quad T < 803K$

$\sigma = 1 + (T - 803)(0.00142),$ $\quad 803 \le T \le 873\ K$

$\sigma = 1.1 + (T - 873)(0.0061),$ $\quad T > 873\ K.$

2. *CO catalytic conversion to CO_2*

$$CO + \frac{1}{2} O_2 \longrightarrow CO_2$$

The reaction rate terms for both reactions are;

$$r_c \quad = \quad \frac{k_C \, W_{CG} \, C_{O_2e}}{MW_C} \tag{3.31}$$

$$r_{COe} = k_{COe} C_{COe} C_{O_2e}^{0.5} \tag{3.32}$$

The heat released by the catalytic *CO* combustion is given by Lee & Groves (1985) as follows:

$$\Delta H_{RCO_e} = -2284375 - 1.653\,T + 29.51 \times 10^{-4}\,T^2 + 425588.2/T$$

3.3.3 Assumptions made to derive the regenerator model equations

1. The regenerator dense bed is assumed to be a bubbling fluidized bed. This assumption was verified in section 3.3.1.
2. The regenerator dense bed is divided into two phases (i.e. bubble and emulsion) according to the two phase theory (Kunii and Levenspiel, 1991). The assumption of two phased was discussed in detail in the introductory part of this chapter.
3. The presence of excess air in the regenerator bed favors the complete combustion reaction. So all *CO* resulting from the coke combustion is converted to CO_2 by the excess air condition in the regenerator.

4. In the freeboard or dilute region, the concentration of the catalyst is small. Thus, the effect of the freeboard region on the overall performance of the regenerator can be assumed negligible in comparison with the dense bed effect.
5. The air distributors and bubbles produce enough turbulence to make the assumption of a continuous stirred tank reactor behavior in the emulsion phase justifiable.
6. The bubbles rise through the bed in plug flow mode. That means the bubble phase can be modeled as a plug flow reactor.
7. The homogeneous CO combustion reaction taking place in the bubble phase is assumed to be negligible comparing with the catalytic CO combustion in the emulsion phase.
8. The heat losses from the regenerator, H_{lG}, is an empirical parameter and it is taken to be 5% as in the literature (Sadegbeigi, 1995).

3.3.4 The regenerator model equations

The concentrations of various gaseous species in the regenerator are normalized with respect to the oxygen feed concentration, $\left(C_{O_2,f}\right)$ and the bubble phase and the emulsion phase temperatures are normalized with rspect to the air feed temperature ($T_{\text{air, f}}$).

The amount of coke on the spent catalyst is determined by :

$$W_{CD} = \frac{y_{CD}(0)}{C/O} \qquad (3.33)$$

where C/O is the catalyst to oil ratio.

Based on the assumptions listed in section 3.3.3 and assuming steady state conditions, the bubble emulsion phase equations are derived applying the conservation principles

3.3.4.1 Bubble phase equations

CO Mass Balance:

The carbon monoxide mass balance is:

$$L_G\left(U_a - U_{mf}\right)A_G \frac{d\,C_{CO,b}}{dz_G} = V_{gas}\ k_g\ \left(C_{CO,e} - C_{CO,b}\right) \tag{3.34}$$

Normalizing length by total length of the regenerator and concentrations by the oxygen feed concentration, we get:

$$\left(U_a - U_{mf}\right)A_G \frac{d\,y_{O_2,b}}{dz} = V_{gas}\ k_g\ \left(y_{CO,e} - y_{CO,b}\right) \tag{3.35}$$

Noting that

$$\left(U_a - U_{mf}\right)A_G = G_{CG}$$

and $V_{gas} = \varepsilon_{bG}\ A_G\ L_G$

Equation (3.35) becomes :

$$\frac{y_{CO,b}}{dz} = \frac{A_G\ L_G\ \varepsilon_{eg}\ \left(1 - \varepsilon_{bG}\right)}{G_{CG}}\, k_g\ \left(y_{CO,e} - y_{CO,b}\right) \tag{3.36}$$

Integrating

$$\int_{y_{CO,f}}^{y_{CO,b}} \frac{y_{CO,b}}{\left(y_{CO,e} - y_{CO,b}\right)} = \frac{A_G L_G \varepsilon_{eG} (1-\varepsilon_{eG}) k_g}{G_{CG}} \int_0^1 dZ \qquad (3.37)$$

Equation (3.37) will be

$$-\ell n \left(y_{CO,b} - y_{CO,e}\right) \Big|_{y_{CO,f}}^{y_{CO,b}} = \alpha_1 z \qquad (3.38)$$

Finally, the *CO* material balance in the bubble phase is:

$$y_{CO,b} = y_{CO,e} + \overline{e}^{\alpha_1 z} \left(y_{CO,f} - y_{CO,e}\right) \qquad (3.39)$$

with $y_{CO,b}(0) = y_{CO,f}$

***O_2 Mass Balance*:**

Similarly as *CO* balance, the equation of O_2 mass balance in the bubble phase will be:

$$\frac{d\, y_{O_2,b}}{d\, z} = \frac{A_G L_G \varepsilon_{eG} (1-\varepsilon_{bG})}{G_{CG}} k_g \left(y_{O_2,b}\ y_{O_2,e}\right) \qquad (3.40)$$

or after integration:

$$y_{O_2,b} = y_{O_2,e} + \overline{e}^{\alpha_1 z} \left(y_{O_2,f} - y_{O_2,e}\right) \qquad (3.41)$$

where $y_{O_2,f} = 1$

equation 3.41 will be

$$y_{O_2,b} = y_{O_2,e} + e^{-\alpha_1 z}\left(1 - y_{O_2,e}\right) \tag{3.42}$$

with

$$y_{O_2,b}(0) = 1$$

Energy Balance:

Applying the conservation principle:

$$\left[\left(U_a - U_{mf}\right)A_G\, L_G\right]\rho_{gG}\, C_{P_{gG}} \frac{d\overline{T}_e}{d Z_G} = V_e\, a_v h\left(\overline{T}_e - \overline{T}_b\right) \tag{3.43}$$

Normalizing the length of the regenerator by the total length of the regenerator Z_G, and the dimensional temperatures by the air feed temperature $\left(\overline{T}_{airf}\right)$. Equation (3.43) becomes after rearrangement:

$$\frac{d\,T_b}{d\,z} = \frac{\left(1-\varepsilon_{bG}\right)L_G\, A_G\, a_v h}{G_{CG}\;\rho_{gG}\, C_{P_{gG}}}\left(T_e - T_b\right) \tag{3.44}$$

The dimensionless group:

$$\frac{\left(1-\varepsilon_{bG}\right)L_G\, A_G\, a_v h}{G_{CG}\;\rho_{gG}}\, C_{P_{gG}}$$ is named α_h

Equation (3.44) will be :

$$\frac{dT_b}{dz} = \alpha_h\left(T_e - T_b\right) \tag{3.45}$$

Solving equation (3.45) analytically:

$$\int_{T_{airf}}^{T_b} \frac{dT_b}{(T_e - T_b)} = \int_0^1 \alpha_h \, dz \tag{3.46}$$

Finally equation (3.46) becomes:

$$T_b = T_e + e^{-\alpha_h z} \left[T_{airf} - T_e\right] \tag{3.47}$$

Since $T_{airf} = 1$, the bubble phase energy balance in its final form becomes:

$$T_b = T_e + e^{-\alpha_h z} \left[1 - T_e\right] \tag{3.48}$$

with $T_b(0) = 1$

3.3.4.2 Emulsion phase equations

Coke Mass Balance

The coke mass balance in emulsion phase is:

$$F_{SG} W_{CD} - F_{CG} W_{CD} = V_{SG} \rho_s \left(k_C W_{CG} C_{O_2,e}\right) \tag{3.49}$$

where V_{SG} = Volume of solid catalyst in the regenerator

$= V_G (1-\varepsilon_{bG})(1-\varepsilon_{eG})$

$= A_G (1-\varepsilon_{bG})(1-\varepsilon_{eG})$

Equation (3.49) will be :

$$F_{SG} (W_{CD} - W_{CG}) = V_G (1-\varepsilon_{bG})(1-\varepsilon_{eG}) \rho_S \left(k_C W_{CG} C_{O_2,e}\right) \tag{3.50}$$

Applying the normalization step, equation (3.50) in its final from becomes:

$$F_{SG}\left(W_{CD}-W_{CG}\right)=A_G\,L_G\left(1-\varepsilon_{bG}\right)\left(1-\varepsilon_{eG}\right)\rho_S\,C_{O_2,f}\,k_C\,W_{CG}\,y_{O_2,e} \tag{3.51}$$

CO Mass Balance

The conservation of mass equation for CO in emulsion phase taking in account that:

$$-r_{CO}=\frac{-k_C}{MW}\left(\frac{1}{1+\sigma}\right)W_{CG}\,C_{O_2,e}+k_{CO,e}\,C_{CO,e}\,C_{O_2,e}^{0.5} \tag{3.52}$$

is:

$$U_{mf}\,A_G\,C_{CO,f}+A_G\,L_G\left(1-\varepsilon_{bG}\right)\begin{bmatrix}\varepsilon_{eG}\,\rho_b\,k_{CO,e}\,C_{CO,e}\,C_{O_2,e}^{.5}\\-\left(\varepsilon_{eG}\right)\rho_S\,\frac{k_C}{MW}\,\frac{1}{(1+\sigma)}W_{CG}\,C_{O_2,e}\end{bmatrix} \tag{3.53}$$

$$=\left(U_{mf}\,A_G\right)C_{CO,e}+A_G\left(1-\varepsilon_{bG}\right)\varepsilon_{eG}\int_O^{L_G}k_g\left(C_{CO,e}-C_{CO,b}\right)dz_G$$

Normalizing equation (3.53) to give:

$$C_{O_2,f}\,U_{mf}\,y_{CO,f}+L_G\left(1-\varepsilon_{bG}\right)\begin{bmatrix}\varepsilon_{eG}\,\rho_b\,k_{CO,e}\,C_{O_2,f}^{1.5}\,y_{CO,e}\,y_{O_2,e}^{.5}\\-\left(\varepsilon_{eG}\right)\rho_S\,\frac{k_C}{MW}\,C_{O_2,f}\,\frac{1}{(1+\sigma)}W_{CG}\,y_{O_2,e}\end{bmatrix}$$

$$=C_{O_2,f}\,U_{mf}\,y_{CO,e}+\left(1-\varepsilon_{bG}\right)\left(\varepsilon_{eG}\right)C_{O_2,f}\,L_G\int_0^1\left(y_{CO,e}-y_{CO,b}\right)dz \tag{3.54}$$

The integral is solved by substituting for $y_{CO,b}$ from equation (3.39).

$$\int_0^1 k_g\left(y_{CO,e}-y_{CO,b}\right)dz=\int_0^1 k_g\left[y_{CO,e}-y_{CO,e}-\left(y_{CO,f}-y_{CO,e}\right)e^{-\alpha_1 z}\right]dz$$

$$= -k_g \int_0^1 \left(y_{CO,f} - y_{CO,e}\right) e^{-\alpha_1 z} = \frac{-k_g \left(y_{CO,f} - y_{CO,e}\right)}{-\alpha_1} e^{-\alpha_1 z} \Bigg|_0^1$$

$$= \frac{k_g \left(y_{CO,f} - y_{CO,e}\right)\left(e^{-\alpha_1} - 1\right)}{-\alpha_1} = \frac{G_{CG}\, k_g}{A_{GL_G}\, \varepsilon_{eG} (\varepsilon_{eG}) k_g} \left(y_{CO,f} - y_{CO,e}\right)\left(e^{-\alpha_1} - 1\right)$$

Substitute for the integral in equation (3.54) to give the final form of the CO mass balance in the emulsion phase:

$$\frac{\left[G_{IG} + G_{CG}\left(1 - e^{-\alpha_1}\right)\right]}{A_G\left(1 - \varepsilon_{bG}\right)\varepsilon_{eG}} \left(y_{CO\,f} - y_{CO\,e}\right) = L_G\, \rho_b\, k_{CO,e}\, C^{0.5}_{O_2,f}\, y_{CO,e}\, y^{0.5}_{O_2,e}$$

$$- L_G \frac{(1 - \varepsilon_{eG})}{\varepsilon_{eG}} \rho_S \left(\frac{1}{1+\alpha}\right) W_{CG}\, y_{O_2,e} \qquad (3.55)$$

O_2 Mass Balance

The derivation of oxygen material balance in the emulsion phase of the regenerator is similar to CO case except that

$$- r_{O_2} = \frac{k_C}{MW_C}\left(\frac{2\alpha + 1}{2\alpha + 2}\right) W_{CG}\, C_{O_2,e} + \frac{k_{CO,e}\, C_{CO,e}\, C^{0.5}_{O_2,e}}{2} \qquad (3.56)$$

The final form of the equation of O_2 in the emulsion phase is:

$$\frac{\left[G_{IG} + G_{CG}\left(1 - e^{-\alpha_1}\right)\right]}{A_G\left(1 - \varepsilon_{bG}\right)\varepsilon_{eG}} \left(y_{O_2,f} - y_{O_2,e}\right) = \frac{L_G\, \rho_b\, k_{CO,e}\, C^{0.5}_{O_2,f}\, y_{CO,e}\, y^{0.5}_{O_2,e}}{2}$$

$$+ L_G \frac{(1 - \varepsilon_{eG})}{\varepsilon_{eG}} \rho_S \left(\frac{2\alpha + 1}{2\alpha + 2}\right) W_{CG}\, y_{O_2,e} \qquad (3.57)$$

Energy balance in emulsion phase

Fig. 3.6 shows the heats entering and exiting the regenerator emulsion phase. Entering heats are provided by air flow, heterogeneous reactions and solid flow. However, the heats coming out are by air flow, solid flow and losses to surroundings.

The inner heats can be represented mathematically as :

$$U_{mf}\, A_G\, \rho_{gG}\, C_{PgG}\, \overline{T}_{air,f} + \left\{ \begin{matrix} L_G\, A_G\, (1-\varepsilon_{bG})\varepsilon_{eG}\, \rho_b \left(-r_{CO,e}\right)\left(\Delta H_{R,CO}\right) \\ + M_{SG}\, \left(-r_C\right)\left(-\Delta H_{R,C}\right) \end{matrix} \right\} + F_{SG}\, C_{PS}\, \overline{T}_D$$

while the outer heats expression is :

$$U_{mf}\, A_G\, \rho_{gG}\, C_{P_{gG}}\, \overline{T}_e + A_G\, (1-\varepsilon_{bG}) \int_0^{L_G} a_v h\left(\overline{T}_e - \overline{T}_b\right) d\,Z_G + F_{SG}\, C_{P_S}\, \overline{T}_e + \overline{H}_{\ell G}$$

Inner heats is equal to outer heats as represented in this equation:

$$U_{mf}\, A_G\, \rho_{gG}\, C_{PG}\, \overline{T}_{air,f} + \left[\begin{matrix} L_G\, A_G\, (1-\varepsilon_{bG})\rho_b \left(-r_{CO,e}\right)\left(-\Delta H_{R,CO}\right) \\ + M_{SG}\, \left(-r_C\right)\left(-\Delta H_{R,C}\right) \end{matrix} \right]$$

$$+ F_{SG}\, C_{P_S}\, \overline{T}_D = U_{mf}\, A_G\, \rho_G\, C_{P_{gG}}\, \overline{T}_e + A_G\, \left(1 - \varepsilon_{bG}\right) \int_0^{L_G} a_v h\left(\overline{T}_e - \overline{T}_b\right) d\,Z_G +$$

$$F_{SG}\, C_{P_S}\, \overline{T}_e + H_{\ell G} \qquad (3.58)$$

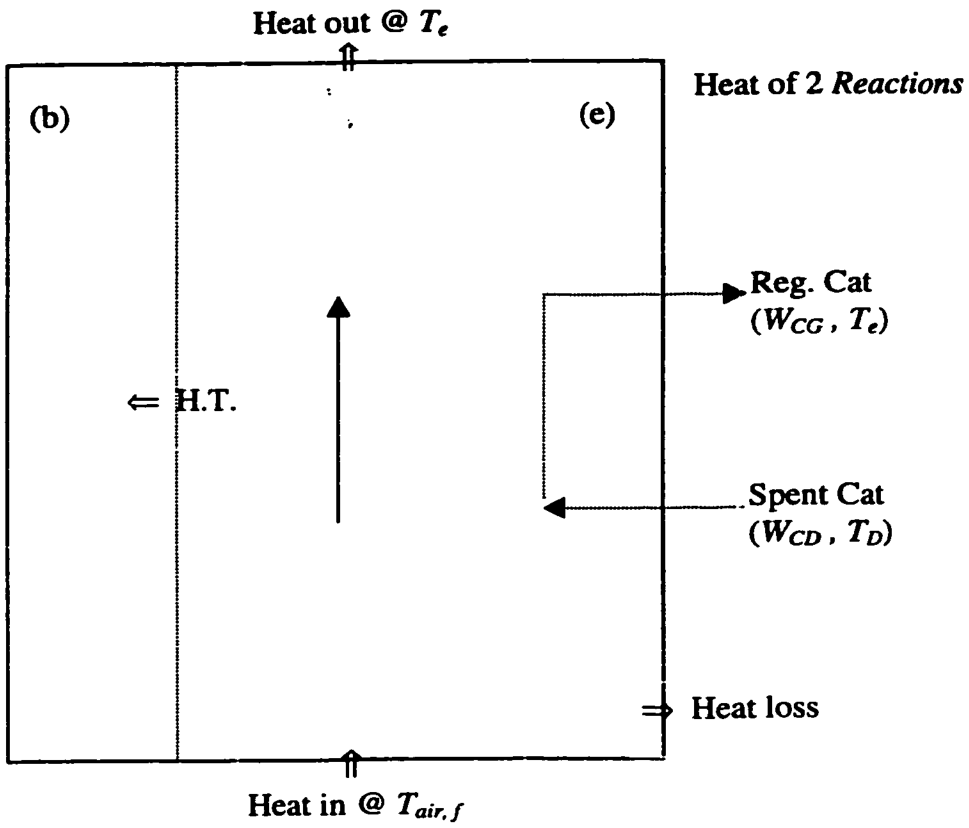
Heat out @ T_e
Heat of 2 *Reactions*
(b)
(e)
Reg. Cat
(W_{CG} , T_e)
⇐ H.T.
Spent Cat
(W_{CD} , T_D)
⇒ Heat loss
Heat in @ $T_{air,f}$

Fig. 3.6 Energy balance in the regenerator emulsion phase

Normalizing temperatures by $T_{ref,\,G}$ and Z_G *by* L_G, and integrating to give the final form of energy balance in the emulsion phase:

$$\frac{\left[G_{IG} - G_{CG}\left(e^{-\alpha_h} - 1\right)\right]\rho_{gG}\,C_{PgG}}{F_{SG}\,C_{PS}}\left(T_{air,f} - T_e\right) + \left(T_D - T_e\right) + \frac{L_G\,A_G\,\varepsilon_{eG}\,\rho_b}{\overline{\overline{T}}_{ref}\,F_{SG}\,C_{PS}}$$

$$\left[k_{CO,e}\left(C_{O_2,f}\right)^{1.5} y_{CO,e}\, y_{O_2,e}^{0.5}\right]\left(-\Delta H_{R,CO}\right) + \frac{M_{SG}}{\overline{\overline{T}}_{ref}\,F_{SG}\,C_{PS}}\left[k_C\,W_{CG}\,C_{O_2,f}\,y_{O_2,e}\right]$$

$$\left(-\Delta H_{R,C}\right) - H_{\ell G} = 0 \qquad (3.59)$$

In conclusion, our regenerator model is similar to the model developed by Ali & Rohani (1996) since the assumptions used in our work are similar to a great extent to what they assumed in their model development except that we have steady state assumption.The detailed derivation is shown in Appendix B.

CHAPTER 4

SIMULATION RESULTS & DISCUSSION

4.1 Introduction

One of distinguished features of the model developed in Chapter 3 is that it combines both the reactor, which is in this case downer, and the regenerator reactor. In fact, the model represents what is happening actually in the FCC-downer unit. The open literature models proposed for downer reactor lack our model advantage. *They deal only with downer reactor without considering the effect of regenerator on the performance of the whole unit.* For example, Bolkan-Kenny et al. (1994) developed a model that only solves the conversion and different aspects in the downer without considering the regenerator effects on the whole units. *Moreover, our model considers non-isothermal operation in the reactor while the models presented in the literature assume isothermal operation.*

The kinetic parameters used in our model for FCC-reaction are obtained for the same catalyst utilized in the pilot plant. Usually, the simulation studies of FCC-units in literature depend on values taken from the literature.

The pilot plant (P.P) gives the temperature profiles inside the downer and the regenerator. Also it supplies product yields from the downer and the coke left on the regenerated catalyst. The presence of such data gives confidence when comparing the model with the actual outputs.

The comparison between the model and Pilot Plant outputs indicates that the model predicts the Pilot Plant data reasonably well. It gives close values for output of the downer (i.e. conversion and yields of gasoline and other components), plus good prediction for regenerator temperature and percentage of carbon on the regenerated catalyst. This shows that the model assumptions presented in Chapter 3 are reasonable.

4.2 Parameters used in simulation

In order to model and simulate the FCC-downer unit, the parameters related to the model should be obtained. Our model depends upon a lot of parameters since they relate to the downer, and a fluidized bed in the regenerator where there are two phases to deal with. In fact, the parameters of this model can be conveniently divided into different groups:

1. Operational parameters for downer and regenerator reactors.
2. Physical properties for downer and regenerator reactors.
3. Reaction kinetic for downer and regenerator reactors.
4. Thermodynamic properties for downer and regenerator reactors.
5. Bubble and emulsion phase properties for regenerator reactor.

The operational parameters used are taken from the operation of the Pilot Plant since one of the main objectives of this work is to test the model results against the Pilot Plant data. The operational parameters are listed in Table 4.1.

Table 4.1 Operational Parameters used to the FCC-downer unit simulation

Parameters	Value	Unit
L_D	1.0	m
D_D	10.9×10^{-3}	m
L_G	1.037	m
D_G	73.9×10^{-3}	m
F_{gD}	2.778×10^{-4}	Kg/s
F_{SD}	6.94×10^{-3} for C/O = 25	Kg/s
F_{SG}	6.94×10^{-3} for C/O = 25	Kg/s
$\bar{T}_{airf}$	298.15	K
$\bar{T}_{oilf}$	523.0	K
U_a	57.0×10^{-3}	m/s

The physical properties of both the catalyst used (HS-FCC5 in this case) and the gas oil are supplied by the HS-FCC project team mentioned earlier. Other physical properties are obtained using CHEMSHARE package which uses correlations to calculate physical and thermodynamics properties (Chemshare, 1996). The sets of physical properties used in simulation are listed in Table 4.2.

The reaction kinetics data for the FCC reactions carried out in the downer are given by HS-FCC project team for the HS-FCC5 catalyst used in operation of the pilot plant. However, the reaction kinetics for the coke burning reaction in the regeneration are obtained from the work of Moorley & de Lasa (1987). All of the reaction kinetics parameters are listed in Table 4.3.

The heats of cracking reactions are obtained by fitting technique. They were obtained by fitting the model to a certain run in the Pilot Plant and then they were used in the rest of simulation. These adjusted values are in the same order of magnitude as values presented in the literature as shown in Table 4.4. Whereas, the heats of coke burning reactions in the regenerator are obtained from the literature (Sadegbeige, 1995). These parameters are listed in Table 4.4.

Other parameters related to voidage in the downer or the bubble and emulsion phase in the regenerator, are listed in Table 4.5. The procedure for determining values for (ε_{gD}, ε_{bG}, ε_{eG}) and (h, k_g) was discussed in section 3.3.1.

Table 4.2 Physical and thermal properties used in the simulation of the FCC-downer unit

Properties	Value	Unit	Ref.
$C_{P\ell}$	2.10	kJ/(kg.K)	HS-FCC Project Team
$C_{P_{gD}}$	2.04	kJ/(kg.k)	Ali (1995)
$C_{P_{gD}}$	1.149	kJ/(kg.K)	CHEMSHARE
ρ_{oil}	882.0	kg/m^3	HS-FCC Project Team
ρ_{gD}	8.40	kg/m^3	Ali & Rohani (1997)
ρ_{gG}	0.71	kg/m^3	CHEMSHARE
C_{P_S}	1.108	kJ/(kg.K)	HS-FCC Project Team
ρ_S	1500	kg/m^3	HS-FCC Project Team
ρ_b	820	kg/m^3	HS-FCC Project Team
C_{P_a}	1.44	kJ/(kg.K)	CHEMSHARE
ρ_a	0.678	kg/m^3	CHEMSHARE
d_P	70.0	µm	HS-FCC Project Team

Table 4.3 **Kinetic and deactivation parameters for reactions in the downer and the regenerator used in the simulation of the FCC unit**

Reaction	Pre-exponential constant	Activation Energy $\left[{}^{kJ}/_{mol}\right]$
k_{AB} *	620.0 s^{-1}	47.626
k_{AC} *	88.0 s^{-1}	60.275
k_{AD}*	60.0 s^{-1}	39.781
k_{BC}	0.0 s^{-1}	0.0
k_{BD}	3400.0 s^{-1}	76.366
α (coking)	2.4 s^{-1}	32.728
k_C	1.4×10^8 $m^3/(kmol \cdot s)$	125
$k_{CO,e}$	247.75 $(m^3)^{1.5}/(kmol^{0.5} \cdot s)$	70.74

** k_{AB} , k_{AC} , k_{AD} values given are multiplied by ρ_b*

Table 4.4 Heats of reaction and vaporization used in the simulation of the FCC-downer unit

Heat of reaction	Values	Ali (1995)	Units
ΔH_{AB}	0.5×10^3	1.647×10^3	kJ/kg
ΔH_{AC}	$- 3.00 \times 10^3$	-10.89×10^3	kJ/kg
ΔH_{AD}	3.50×10^3	5.40×10^3	kJ/kg
ΔH_{BC}	-3.0×10^3	-12.53×10^3	-
ΔH_{BD}	2.20×10^3	3.75×10^3	kJ/kg
ΔH_{C}	$-25/.0 \times 10^3$	-	kJ/mol
$\Delta H_{CO,e}$	-282.0×10^3	-	kJ/mol
ΔH_{vap}	270	-	kJ/kg

Table 4.5 Other simulation parameters

Parameters	Value	Unit	Ref.
ε_{gD}	0.997	-	Zhu et al. (1995)
ε_{bG}	0.571	-	Equation 3.20
ε_{eG}	0.510	-	Kunii & Levenspiel (1991)
h	2.34	kJ/(m^2.s.K)	Equation 3.27
k_g	3.37	s^{-1}	Equation 3.26
a_v	0.08	m^2/m^3	Equation 3.25
$T_{ref,\, D}$	523.0	K	HS-FCC project team
$T_{ref,\, G}$	298.15	K	HS-FCC project team

4.3 Numerical Procedure

As shown in Chapter 3, we ended up with five ODE's for the downer and seven non-linear algebraic equations for the regenerator. The first set represents the profiles in the downer while the second solves for different unknowns inside the regenerator. Both sets have dependence on positions except the emulsion phase equations in the regenerator because the emulsion phase is considered as a well-mixed tank reactor.

The differential equations are solved by fourth-order Runga-Kutta method (RK4). Then, the output of this solution is given as an input to the non-linear algebraic equations in the regenerator which are solved using Newton-Raphson technique. The output is then moved to the differential equations as an input. This iterative procedure continues until we get steady values in both units (i.e. the downer and the regenerator).

The codes developed to solve the problem numerically are written by a new version of Fortran language. It is called Fortran 90. The codes utilize some IMSL library sub-routines such as IVPRK and NEQNF. All codes used in our simulation are given in Appendix C.

4.4 Model results and comparison with P.P. data

The model was solved using the parameters listed earlier in Tables 4.1 to 4.5. Two runs in the pilot plant are used to reveal the deviation between model results and actual data, namely runs # 39 and # 62. Table 4.6 lists the model results and actual data for both runs. The definition of conversion of gas oil in the Pilot Plant is given by:

$$\text{Conversion (wt.\%)} = 100 - \text{HCO} - \text{LCO} \tag{4.1}$$

where HCO and LCO are the heavy and light cycle oil respectively exiting with products of the cracking reactions.

It can be inferred from Table 4.6 that the model predicts downer yields that are good particularly gasoline. The model predicts the yields and outputs for Run # 62 better than Run # 39. That means that the model predictions are better at higher catalyst to oil ratio cases.

Fig. 4.1 shows the conversion and concentration profiles predicted by the FCC-downer model for Run# 39. It is obvious that the model predicts the gasoline yield rather well. The deviation between the model and actual Pilot Plant data is about 4%. While the deviation in predicting gases yield is about 20%.

The temperature profile for Run # 39, presented in Fig. 4.2, reveals a typical view for endothermic reactions which is the same as our case. In fact, there is a significant deviation between the model and the Pilot Plant data for the temperature at the entrance of the downer. This happens due to trying to maintain the P.P. reactor at fixed temperature (isothermal) while in our case we have changing temperature profile (non-isothermal).

Figs. 4.3 and 4.4 show the temperature and coke on catalyst profiles inside the regenerator. They are constant a long the regenerator due to CSTR approximation assumed for the emulsion phase. The deviation between the model and actual results for the regenerator temperature is about 6%. The difference between the actual and model results for the regenerated catalyst results from the assumptions made when modeling the regenerator.

Table 4.6 Model results vs. pilot plant data

		Conversion %	Gasoline%	Coke %	Gases	DOT (C)	Wcc %	Trg
Run # 39 C/O = 20	Model	79.04	47.89	1.625	29.52	600	0.0013	684.2
	P.P.	70.1	45.81	1.430	22.79	600	0.0053	730.0
Run # 62 C/O = 30	Model	78.7	47.98	1.59	29.12	602.0	0.0018	661.7
	P.P.	74.6	46.27	2.06	32.17	600	0.0048	719.0

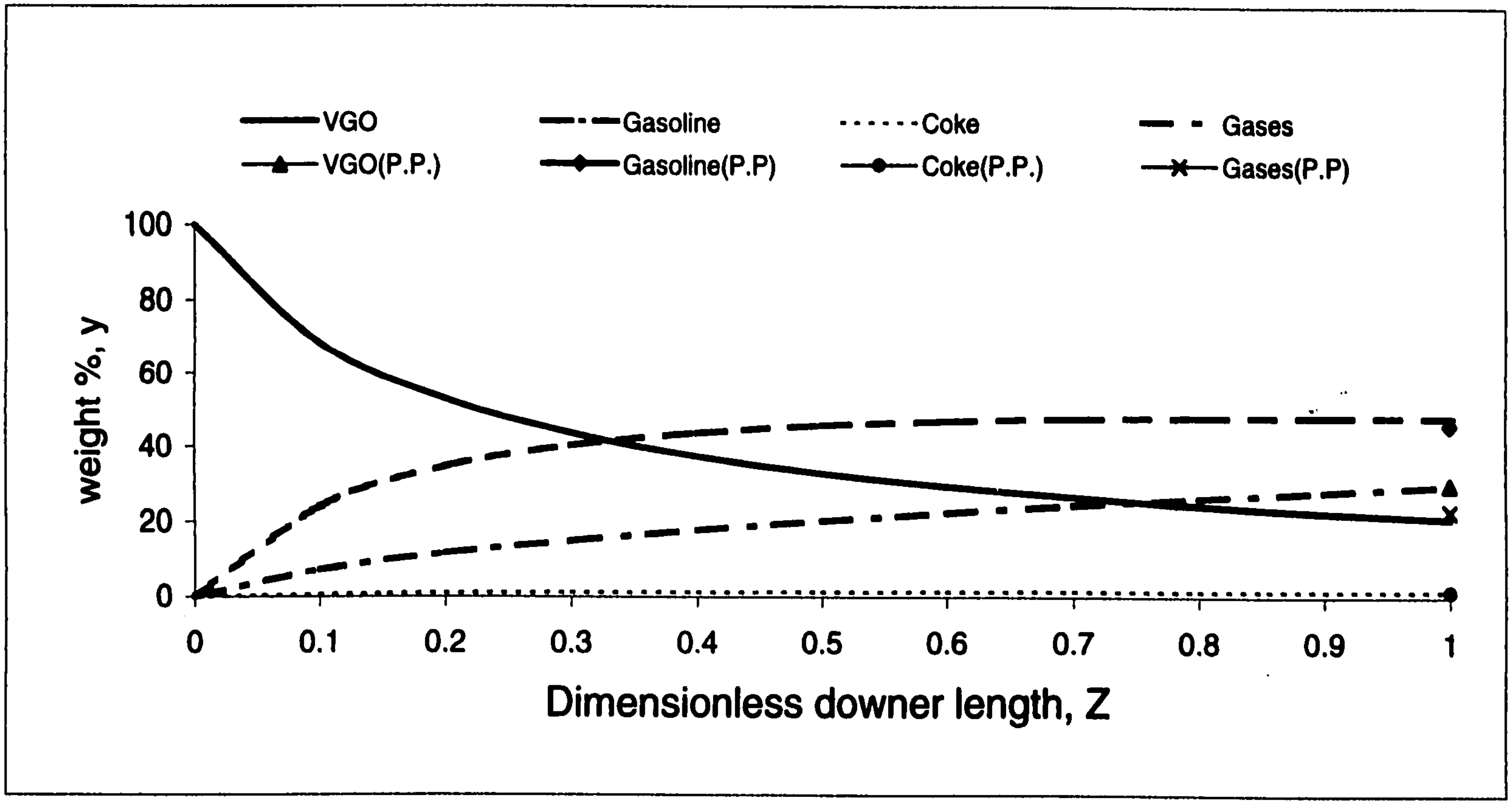

Fig. 4.1: Comparison of model predictions and pilot plant data for conversion and yields in the downer(Run#39)

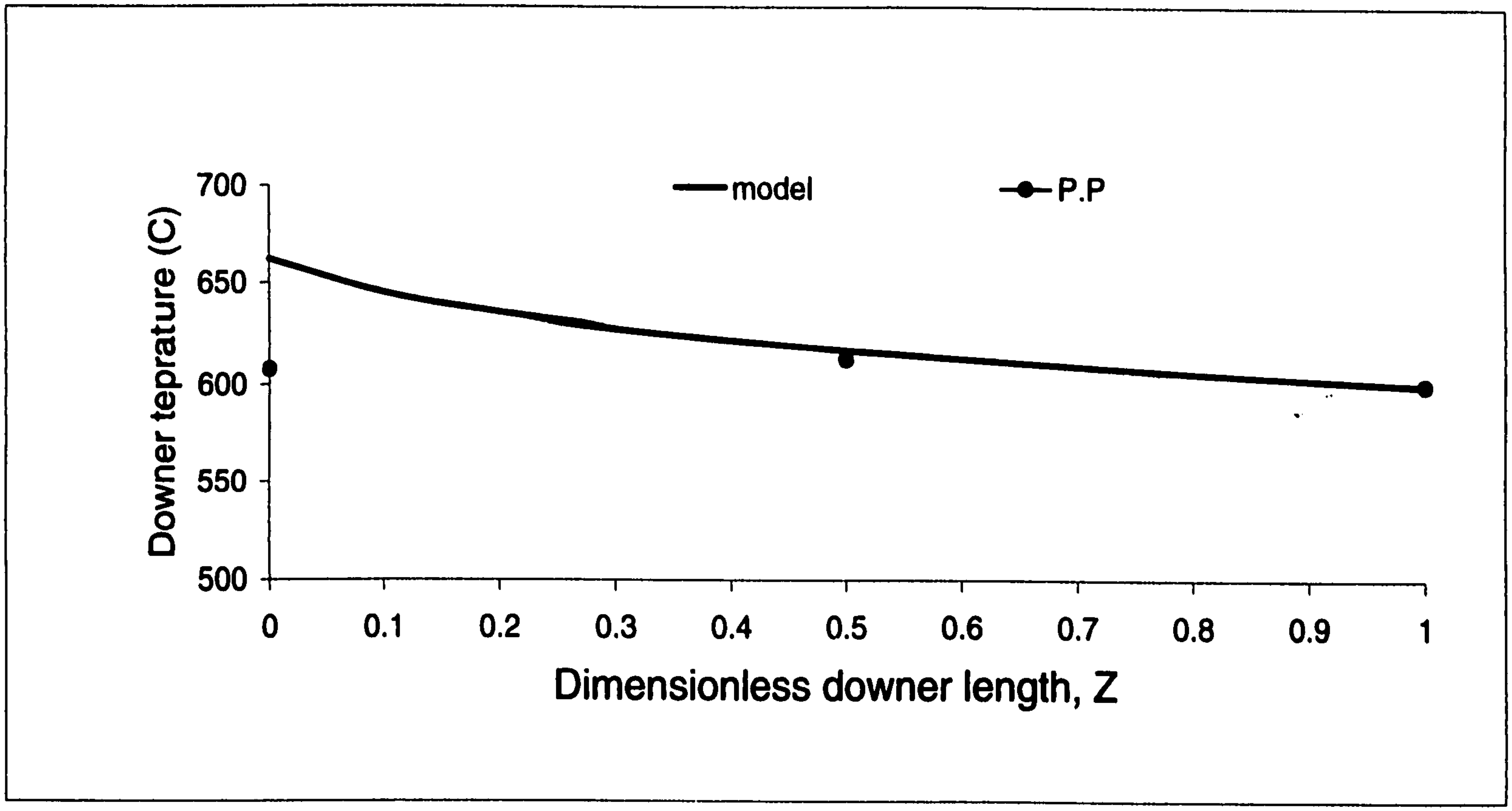

Fig. 4.2: Comparison of model predictions and pilot plant data for temperature in the downer(Run#39)

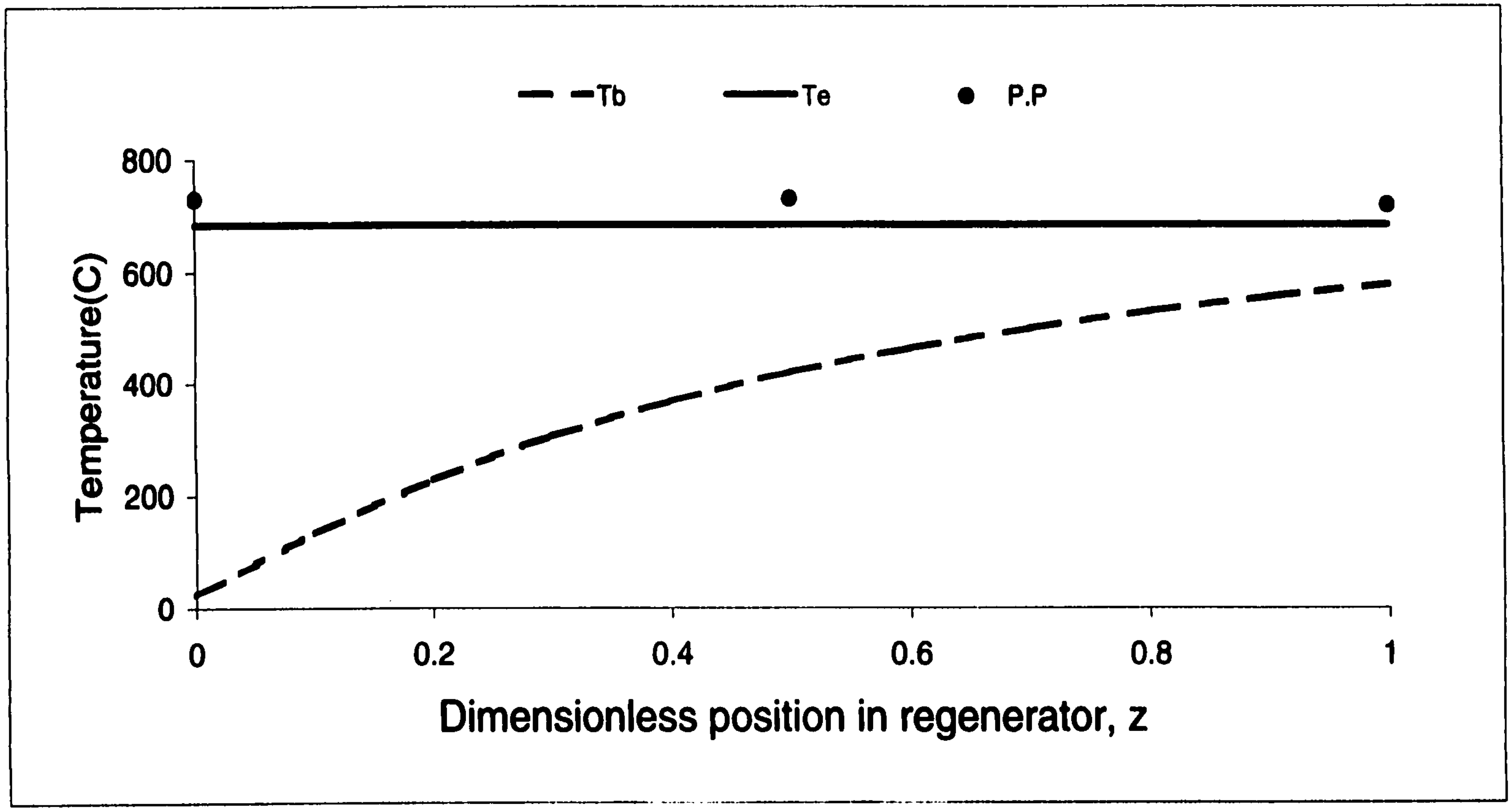

Fig.4.3: Comparison of emulsion and bubble phase temperatures with P.P. data for regenerator (Run#39)

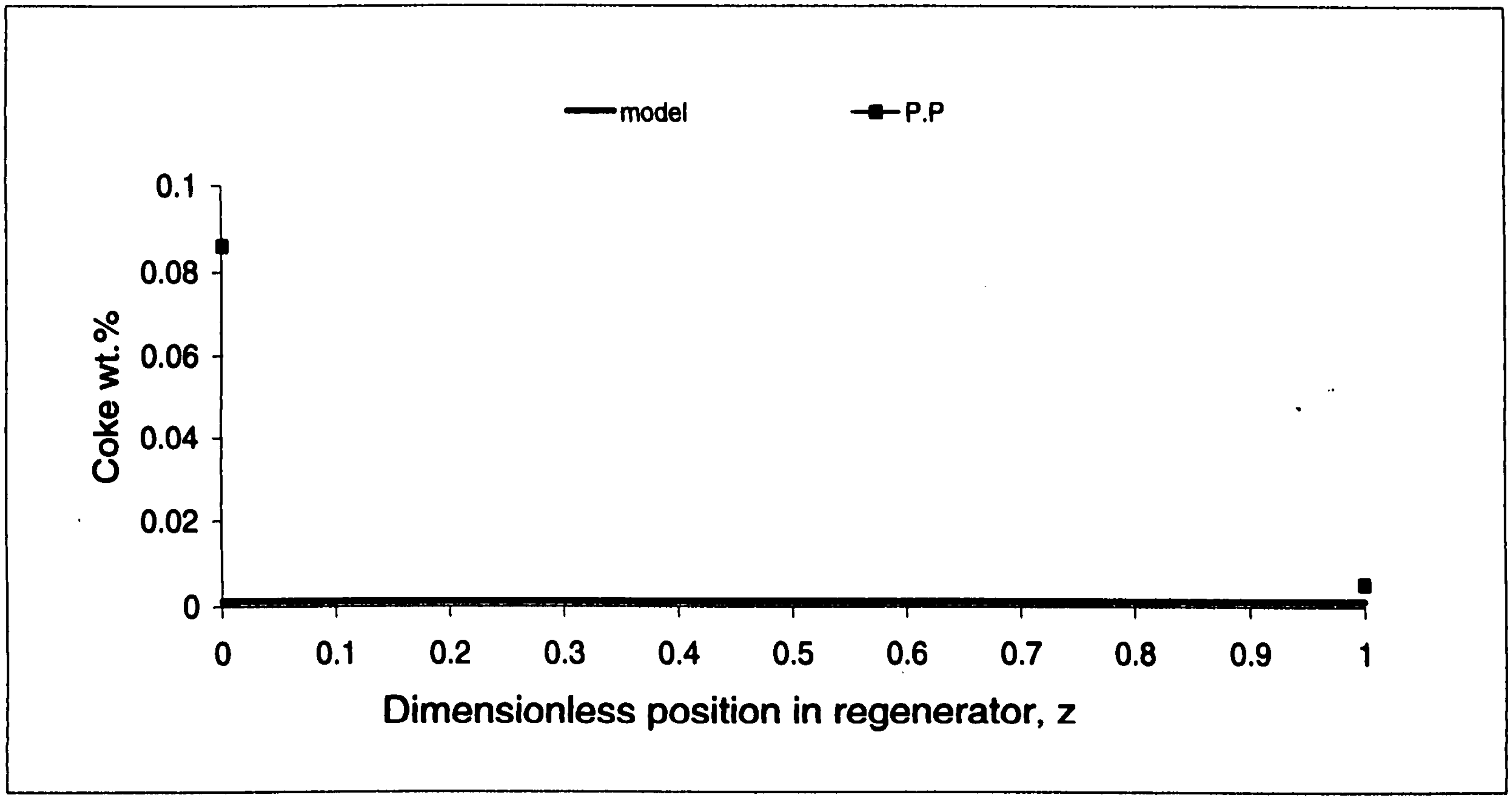

Fig. 4.4: Comparison of coke on regenerated catalyst with P.P. data for regenerator (Run#39)

The model was projected for Run# 62 conditions and gave Figs. 4.5 and 4.6 inside the downer, and Figs. 4.7 and 4.8 in the regenerator. The deviations between the model results and actual data for gasoline yield, light gases yield, and regenerator temperature are 3.5%, 10.5%, and 8.6%, respectively.

The discrepancy between the model predictions and the Pilot Plant is attributed to several factors. The simplifying assumptions imposed on the model could be one factor. The nature of the methods used to determine the physical parameters together with the heats of reactions could be another factor.

The direct use of kinetic parameters is another possible source of error because they were obtained using the MAT unit which is generally used for screening catalysts purposes but not obtaining kinetic parameters. Moreover, the heat added to the Pilot Plant unit to keep the whole unit heat-balanced could cause deviation between model and Pilot Plant data. The model does not consider the role of steam or nitrogen introduced to the unit which might cause deviation between our model results and the Pilot Plant data.

4.5 Parametric study for some operational parameters

In this section, the effect of some parameters, namely operational and design parameters, on the FCC-downer unit using our model will be presented. The effects considered are upon the conversion and different yields in the downer, the temperature, and coke on the catalyst in the regenerator. These are the most important variables which show the performance of the whole unit.

The parametric study includes effects of changing catalyst to oil ratio (C/O), length of the downer, cross sectional area of the downer, and flow of air to the regenerator. The effects of these parameters on the performance of the whole unit will be presented next.

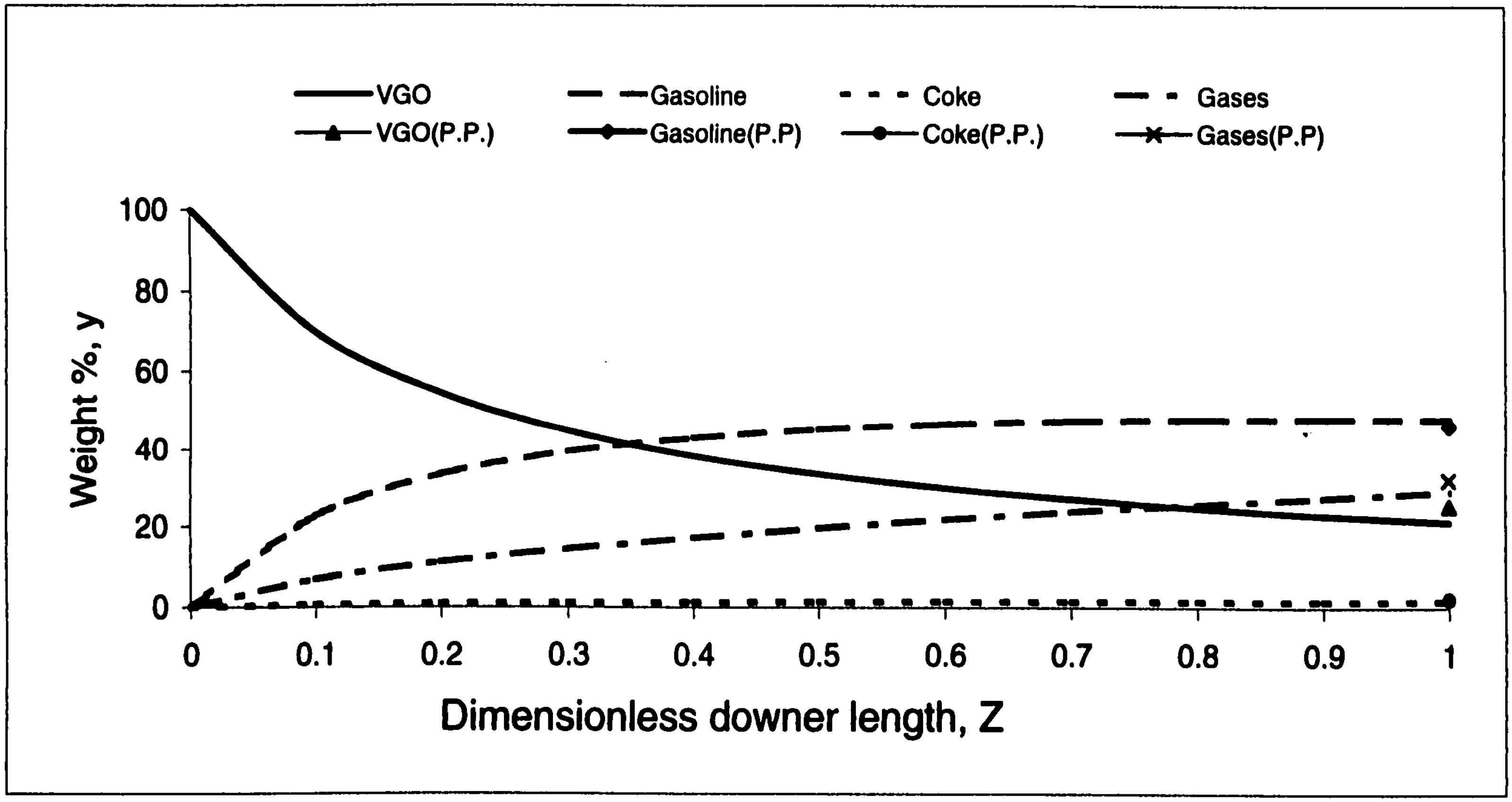

Fig. 4.5: Comparison of model predictions and pilot plant data for conversion and yields in the downer(Run#62)

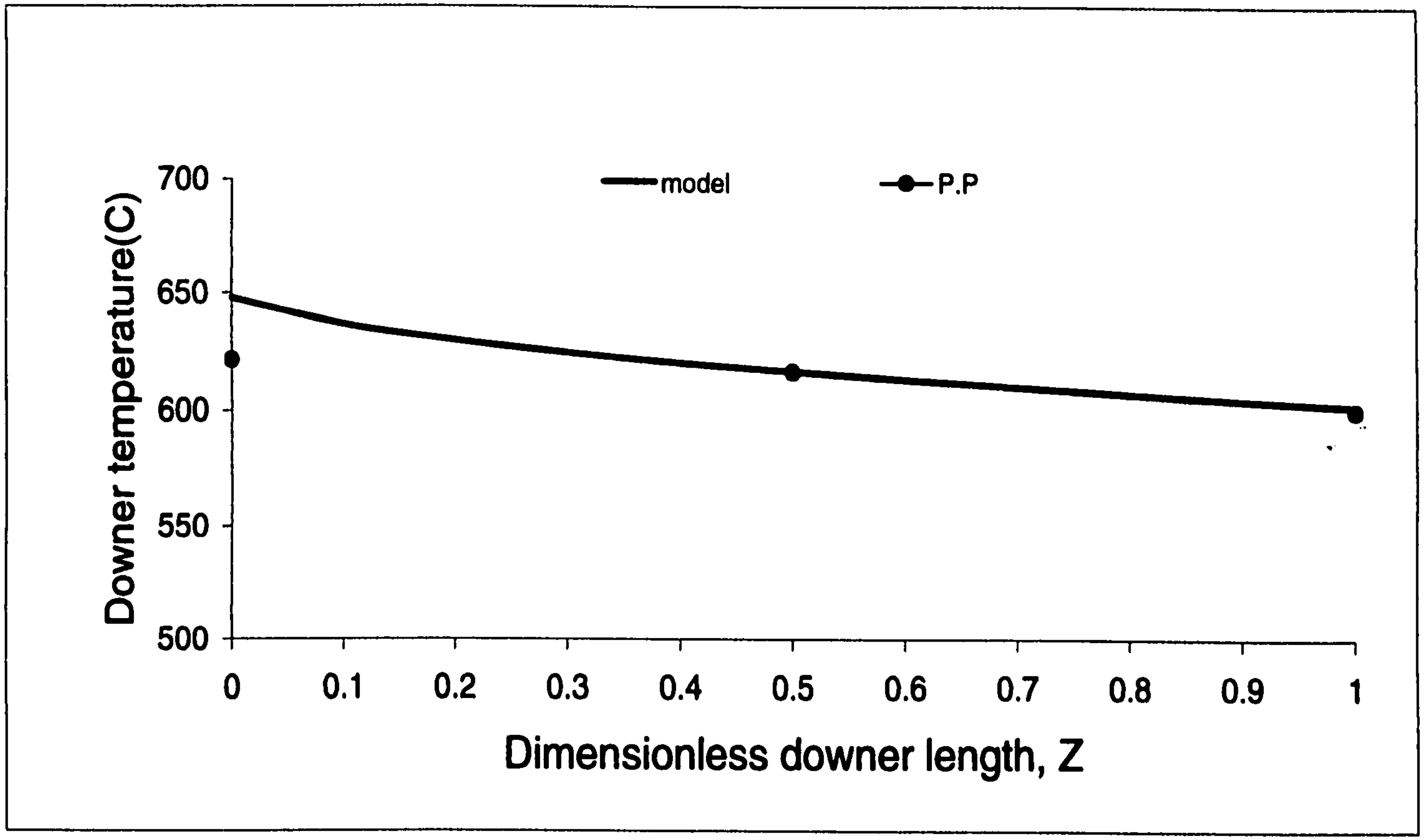

Fig. 4.6: Comparison of model predictions and pilot plant data for temeprature in the downer(Run#62)

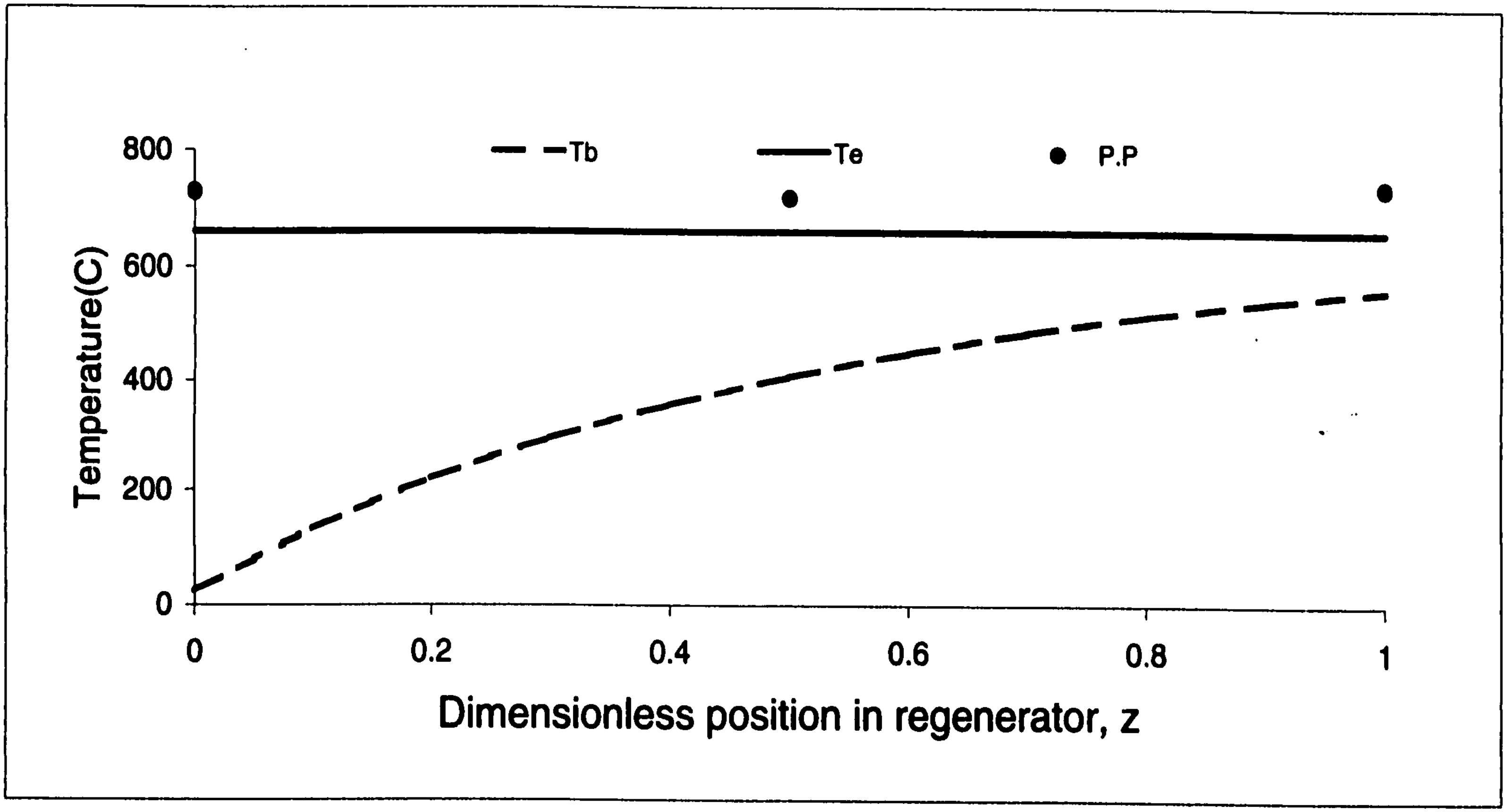

Fig.4.7: Comparison of emulsion and bubble phase temperatures with P.P. data for regenerator (Run#62)

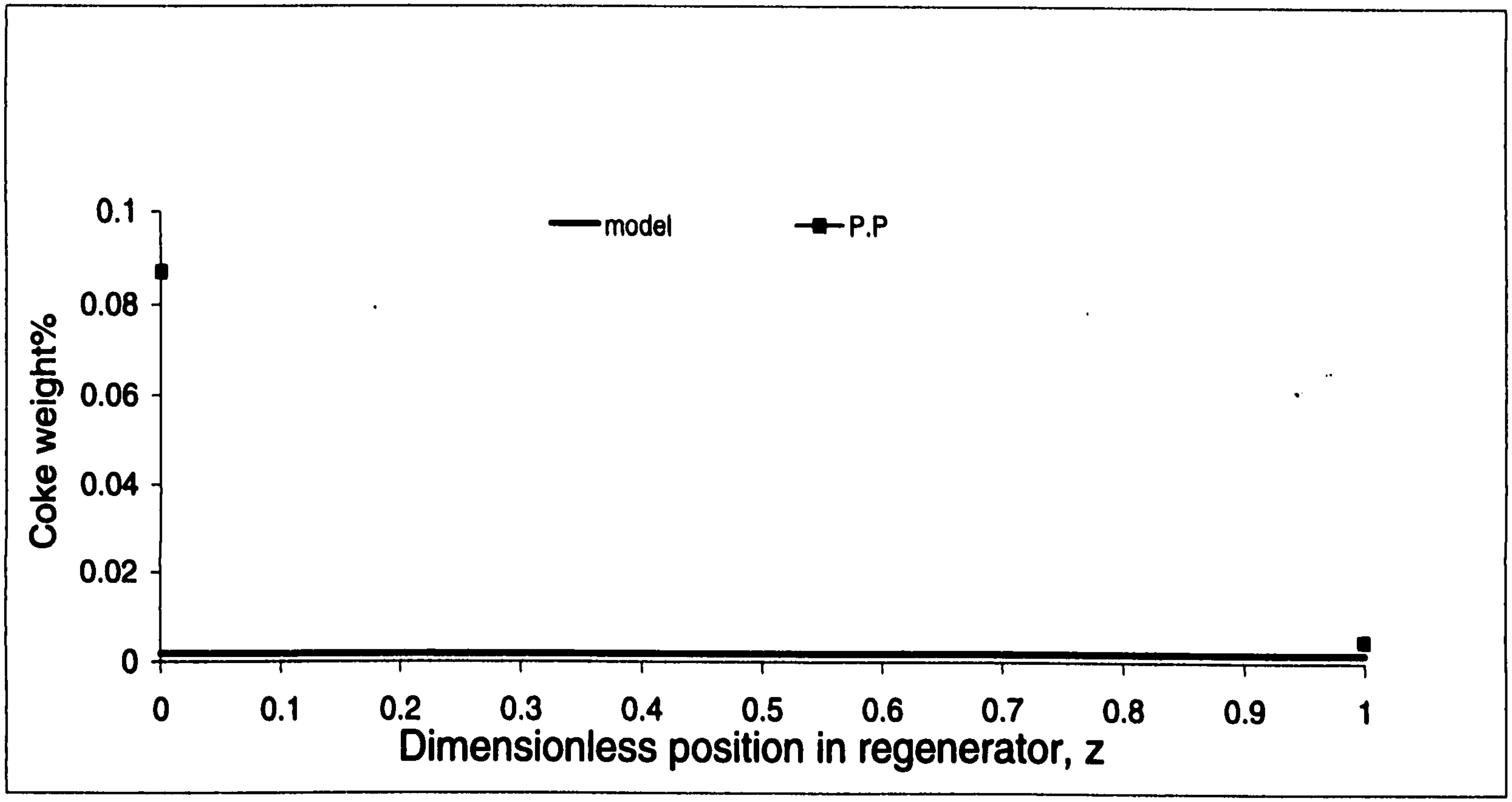

Fig. 4.8: Comparison of coke on regenerated catalyst with P.P. data for regenerator (Run#62)

4.5.1 Effect of changing Catalyst/Oil ratio

The catalyst to oil ratio is changed by either increasing the catalyst flow rate or flow rate of oil vapors in the downer. The oil fed to the unit is kept constant here. For instance, the rate of oil is one kilogram per hour while the rate of catalyst is changed depending on the C/O. The C/O can be represented mathematically as :

$$C/O = \frac{F_{sD}}{F_{gD}}$$

In our case, the C/O is changed in the range of 10 to 30. The comparison for each variable in the unit is conducted at three different downer outlet temperatures (DOT), namely 550, 600 and 650°C.

Figs. 4.9 – 4.16 summarizes the effect of varying C/O on the unit variables and yields. The conversion does not vary significantly with C/O for all DOT's under study as shown in Fig. 4.9. This is expected because the DOT is maintained constant which means that the temperature profile inside the downer is approximately the same that gives nearly the same conversion. It can be seen from Fig. 4.9 that increasing DOT favors the conversion of gas oil. This behavior is compatible with famous LeChatelier's Principle which states that supplying heat to an endothermic reaction favors the reaction progress.

According to Fig. 4.9, the gasoline yield percentage is improved by increasing of C/O ratio. So operating at higher C/O is better if the objective is to improve the intermediate product gasoline. Moreover, Fig. 4.10 gives a notification of which DOT is better to obtain gasoline. In fact, the yield of gasoline is much better at DOT's of 550 and 600°C. The difference in the yield between mentioned DOT's and DOT of 650°C is 7-10% which is significant especially if intended for a commercial unit. This is exactly what the pilot plant tells. For example, that

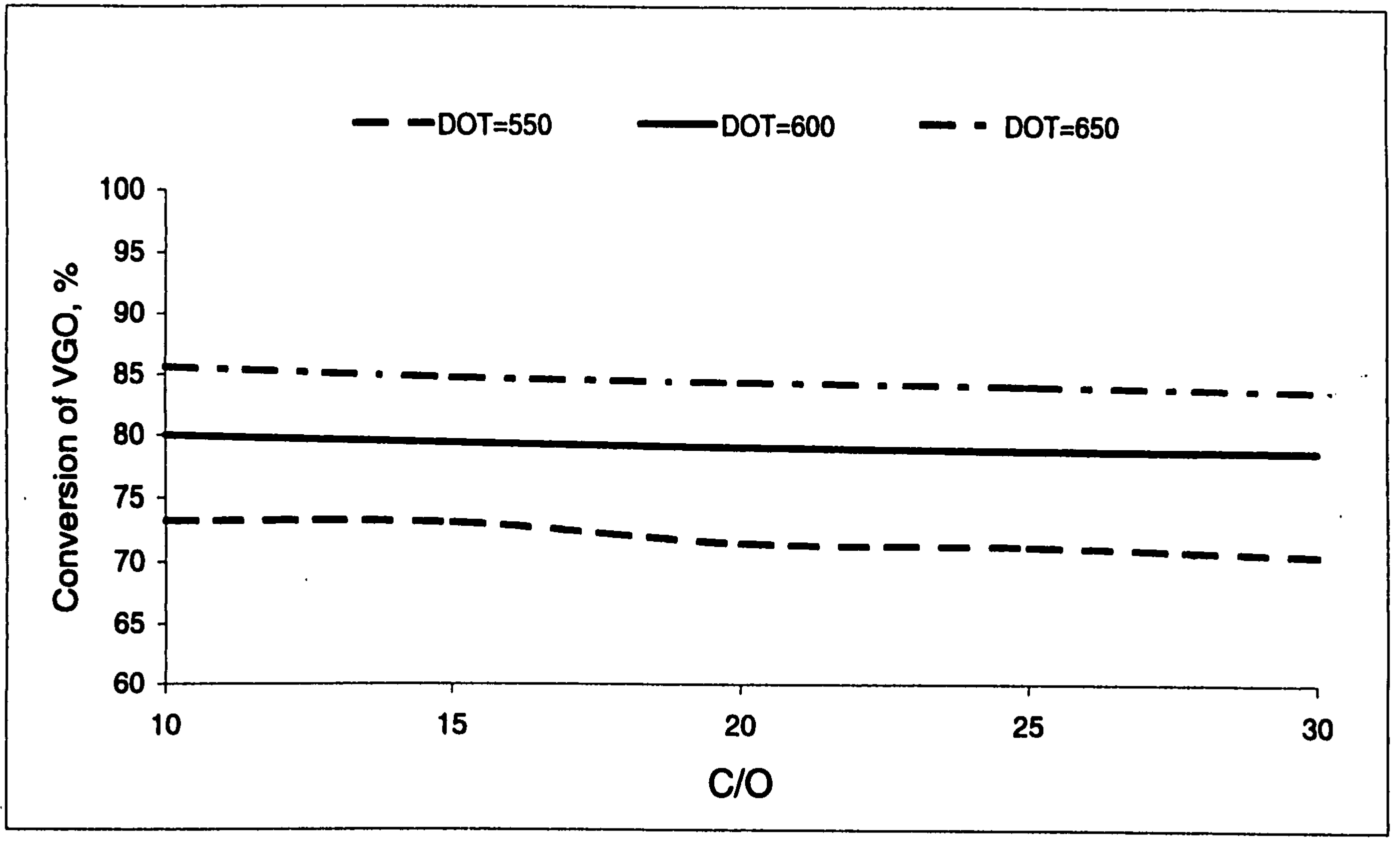

Fig. 4.9: Effect of changing catalyst to oil ratio on conversion of gas oil

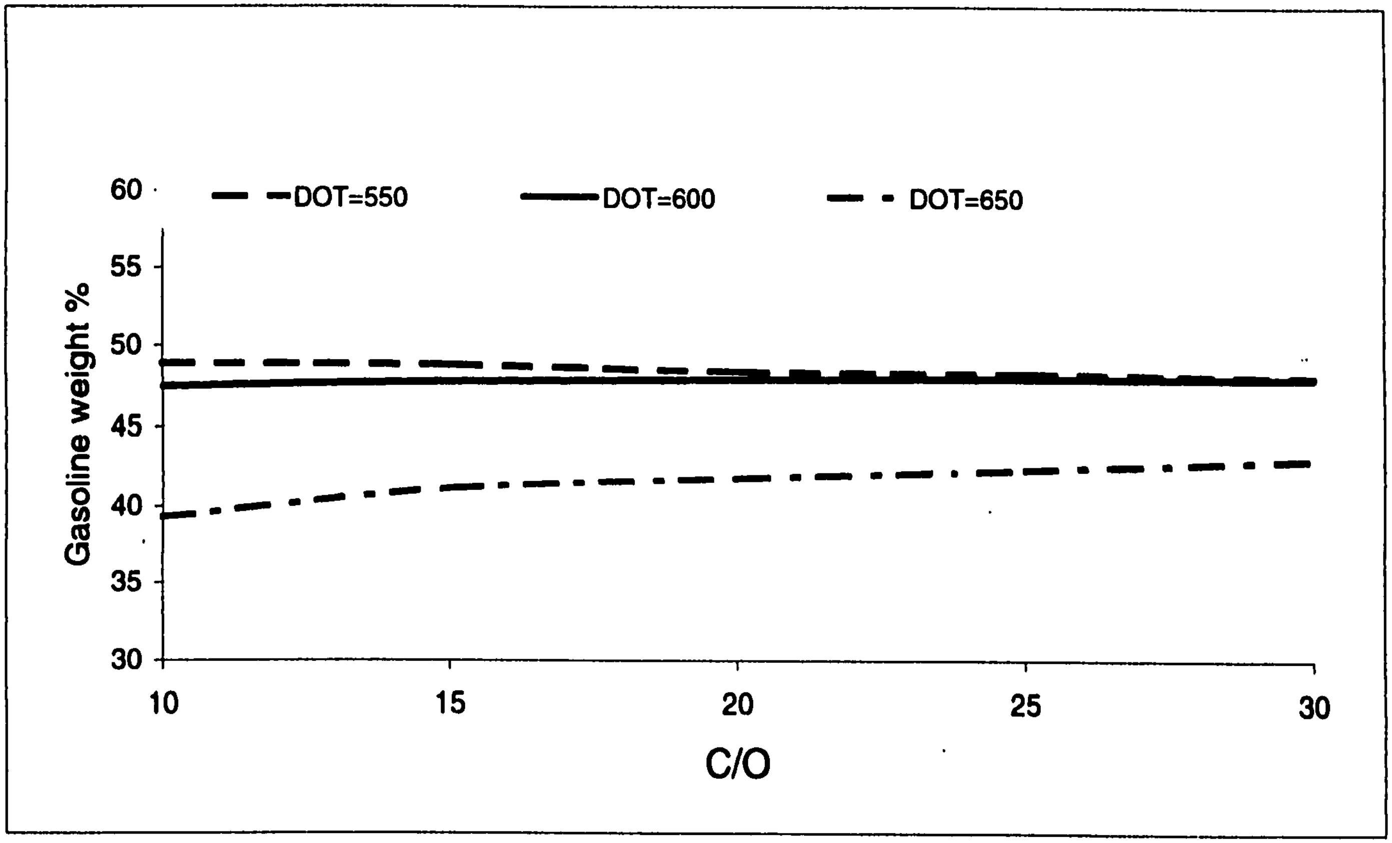

Fig. 4.10: Effect of changing catalyst to oil ratio on gasoline yield

gasoline yield in Run # 42 where DOT of 550°C is 49.78% while it is 38.64%, in Run # 41 with DOT of 650°C. In conclusion, the optimum gasoline yield is obtained at higher C/O and lower DOT.

The gases yield decreases slightly when we increase the C/O ratio. The decrease is more obvious when operating at DOT of 650°C as shown in Fig. 4.11. In addition, the gases profile versus DOT's shows that operating at higher DOT gives higher gases yield. In the pilot plant runs, the same conclusion is obtained. For instance, Run # 42 where DOT is 550°C, the gases yields is 25.0% while it is 40.49% in Run # 41 where DOT is 650°C. The difference between the two values is about 15%.

The increase in gases yields with increasing DOT can be explained by the effect of more conversion at higher DOT as shown in Fig. 4.11. So, the optimum gases yield results when operating at high DOT. Coke yield in the downer is semi-stable with changing C/O as shown in Fig. 4.12 due to fixing DOT. But it increases when the DOT is more. This behavior is expected since more gas oil and more gasoline are converted to coke at higher temperature profiles in the downer.

The behavior of the regenerator temperature and coke on the regenerated catalyst against C/O is shown in Figs. 4.13 and 4.14. The regenerator temperature goes down significantly with feeding more catalyst for all DOT's under study. This is attributed to more heat removal from the regenerator by the solid phase when enlarging the amount of the catalyst. Subsequently, the regeneration process is affected negatively because lower burning reactions carried out at lower regenerator temperature. Fig. 4.14 shows how the regeneration process is inhibited with further increase of C/O.

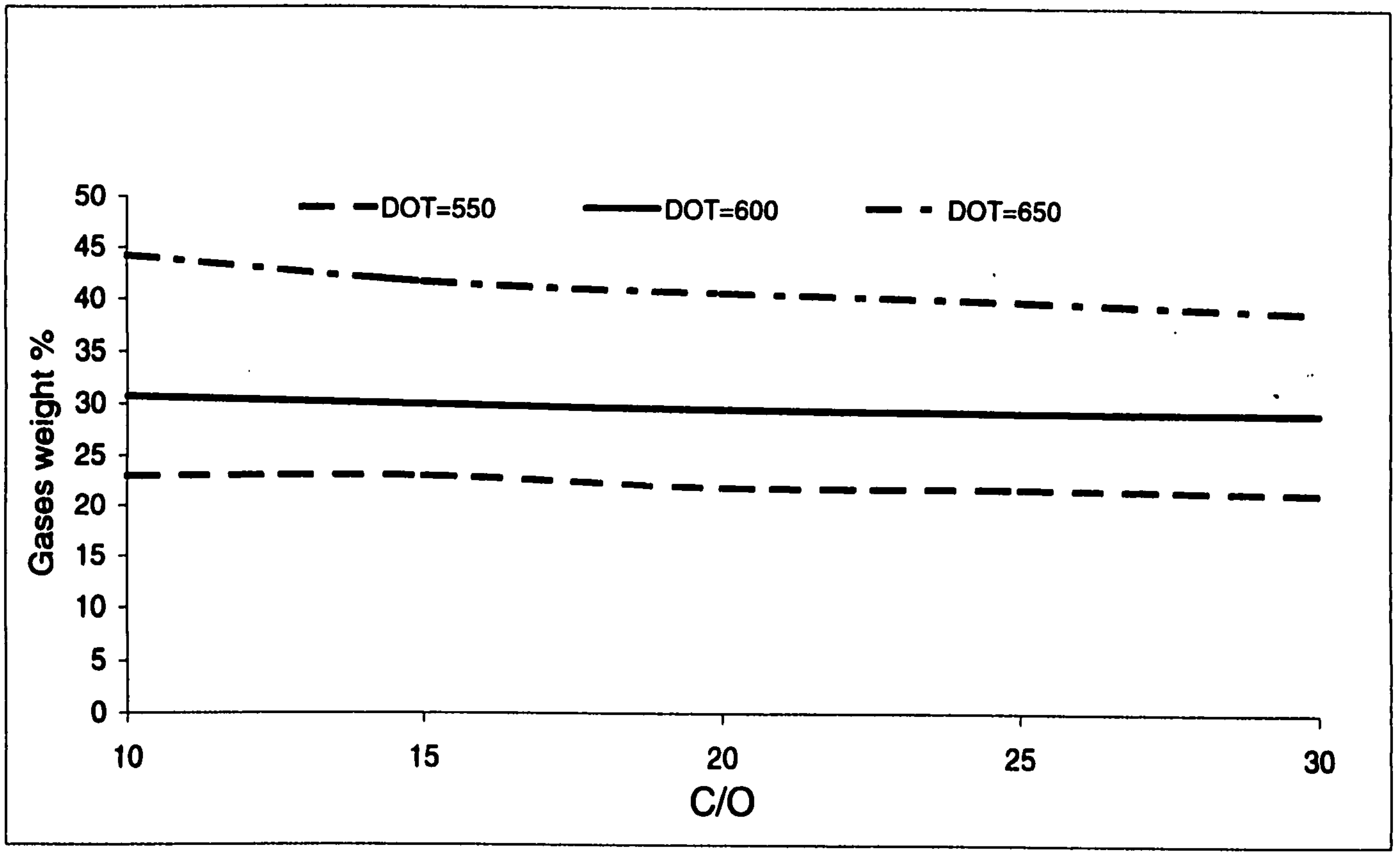

Fig. 4.11: Effect of changing catalyst to oil ratio on gases yield

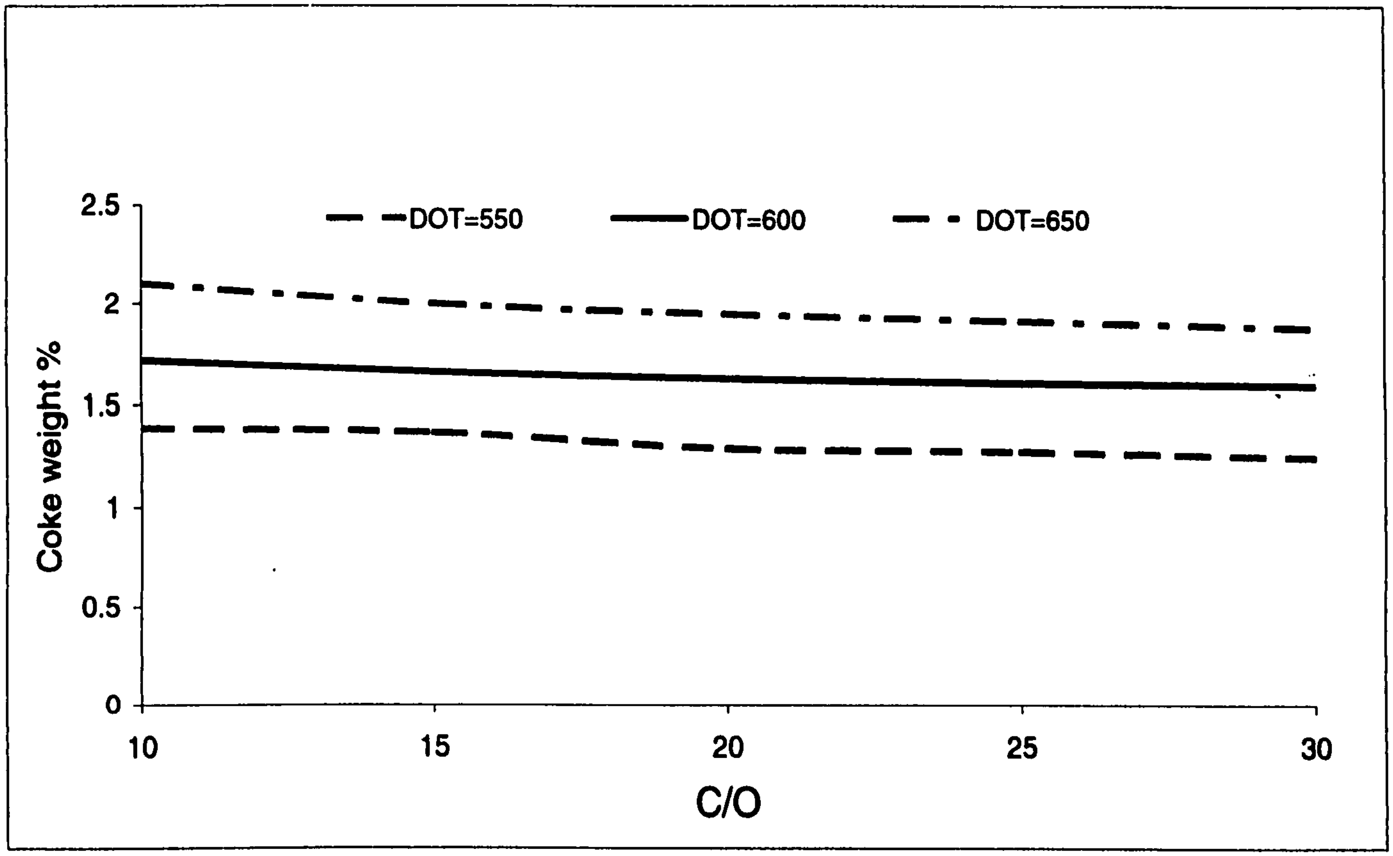

Fig. 4.12: Effect of changing catalyst to oil ratio on coke yield in the downer

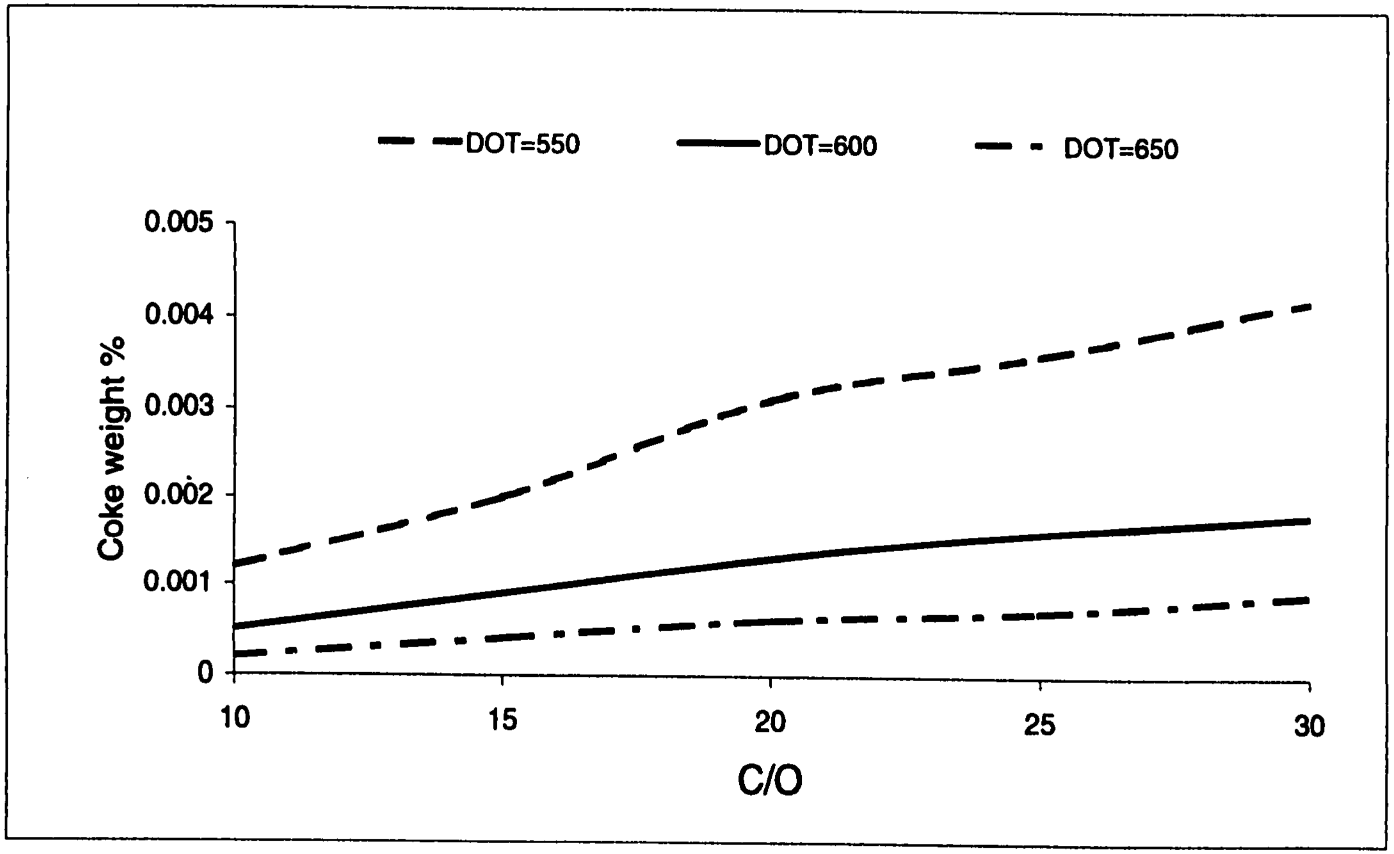

Fig. 4.13: Effect of changing catalyst to oil ratio on coke on regenerated catalyst

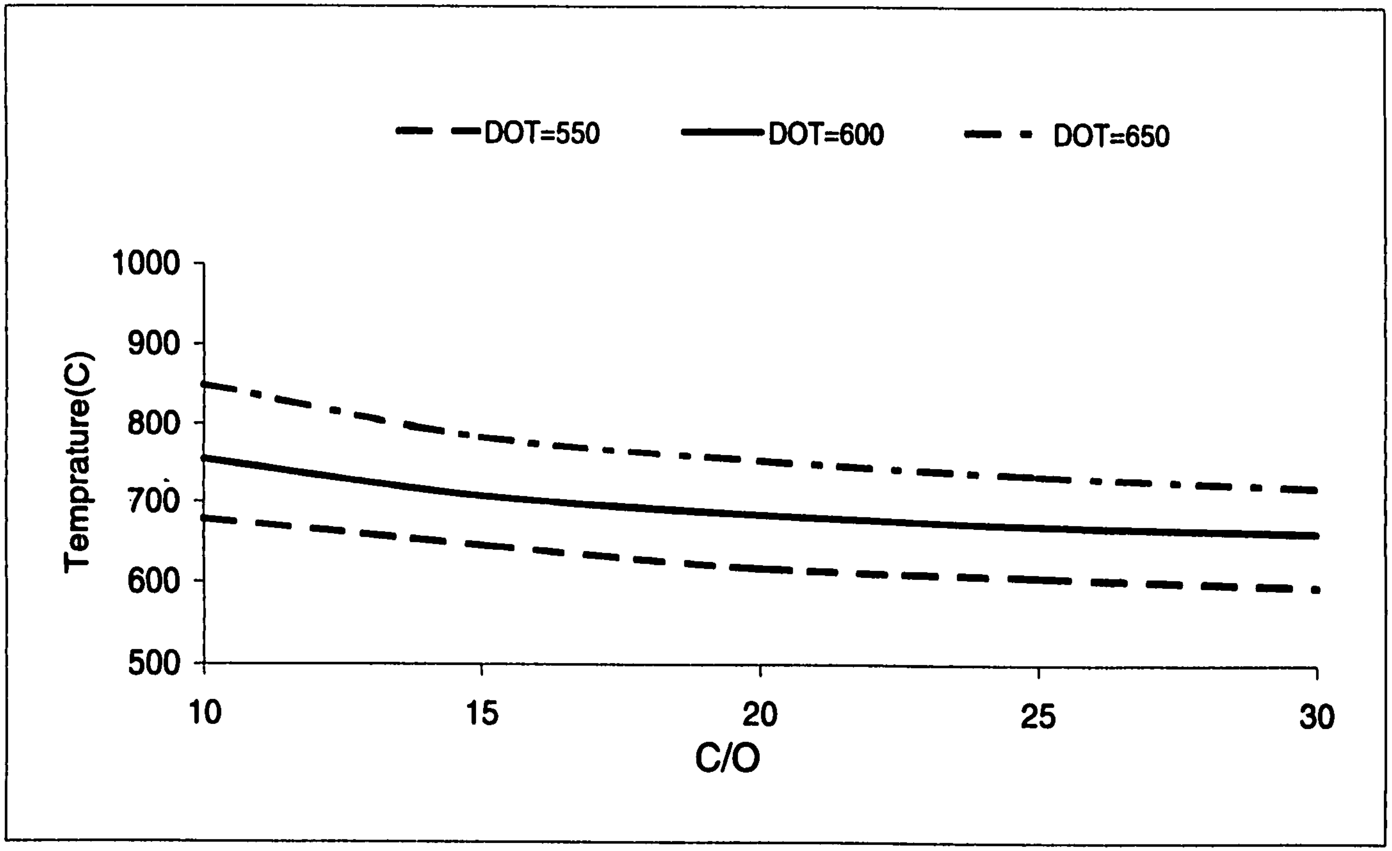

Fig. 4.14: Effect of changing catalyst to oil ratio on the emulsion phase temprature(regenerator temprature)

4.5.2 Effect of changing cross sectional area of the downer

The cross sectional area of the downer (A_D) is an important design parameter because it is related to the volume of the reactor which is a term in the reactor design equation. So increasing or decreasing the volume of the reactor affects the residence time of the reactor.

It is obvious that the conversion of the gas oil increases with enlargement of A_D as shown in Fig. 4.15 for L_D of 1 m and in Fig 4.16 for L_D of 2 m for all DOT cases under study. So operating at higher A_D gives higher conversion of gas oil.

Gasoline is an intermediate product. It is expected that there is an optimum point for gasoline yield. Fig 4.17 shows that the maximum gasoline yield for L_D of 1 m and DOT of 600°C is obtained at about A_D of 0.80 cm^2 while optimum A_D for producing gasoline is 1.6 cm^2 at DOT of 550°C and 1 m length. Fig. 4.18 shows the same trend for L_D of 2 m. The optimum gasoline yields for different A_D and L_D are summarized in Table 4.7.

After reaching the optimum A_D, the gasoline yield returns to lower values with expanding the reactor cross sectional area. Specifically, at L_D of 2 m, the gasoline yield decreases at large A_D's.

Coke yield increases gradually when A_D is enlarged. The slight increase demonstrated is due to more gas oil converted to coke when the reaction is allowed to occur in longer residence time. The increase is approximately 0.5% from a small to large A_D for all cases at different lengths, as shown in Figs. 4.19 & 4.20. So at larger cross sectional area of the downer, the deactivation of the catalyst is higher as a result of more coke deposits on the catalyst.

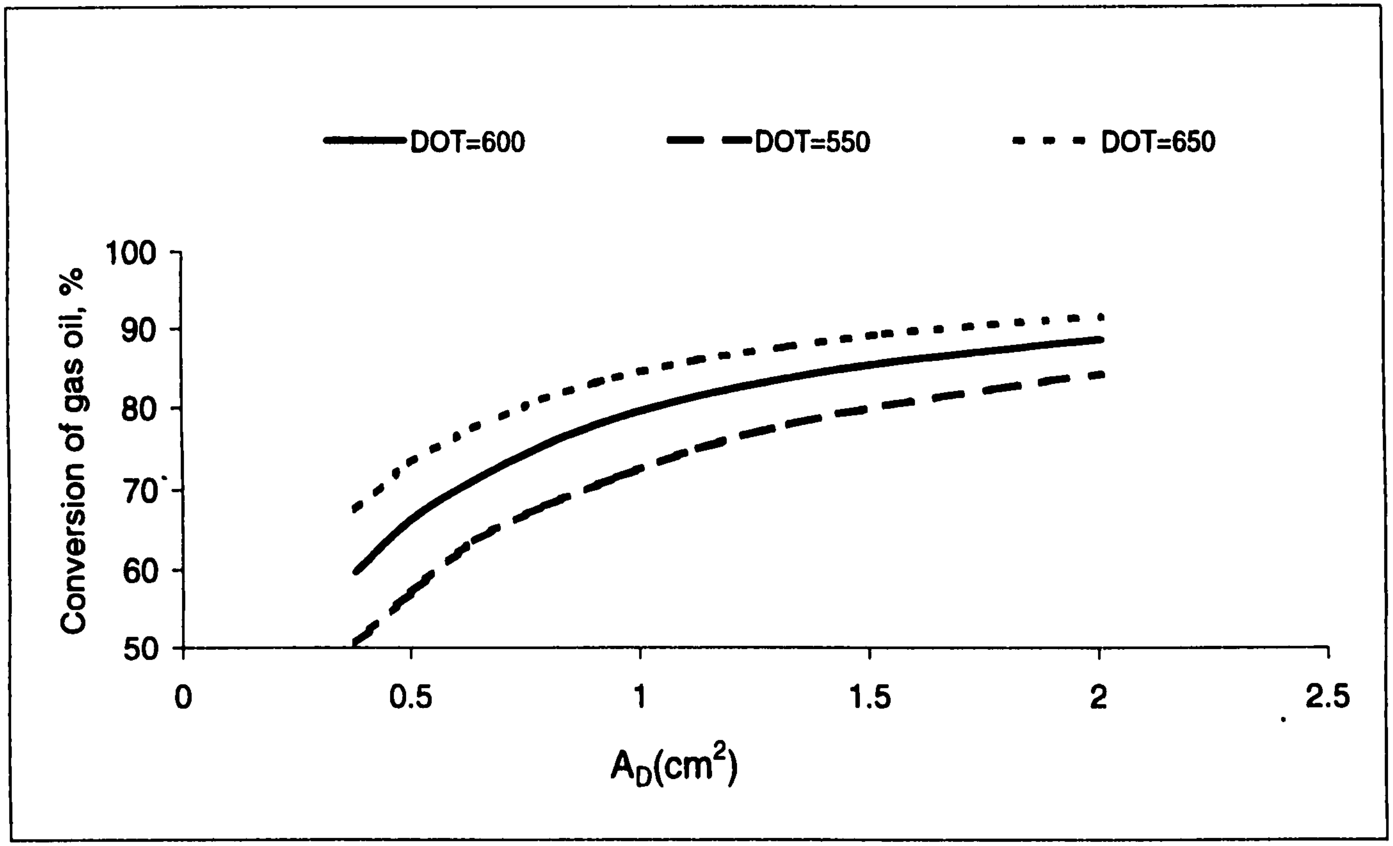

Fig. 4.15: Effect of changing downer cross-section area on conversion of gas oil, L_D=1 m

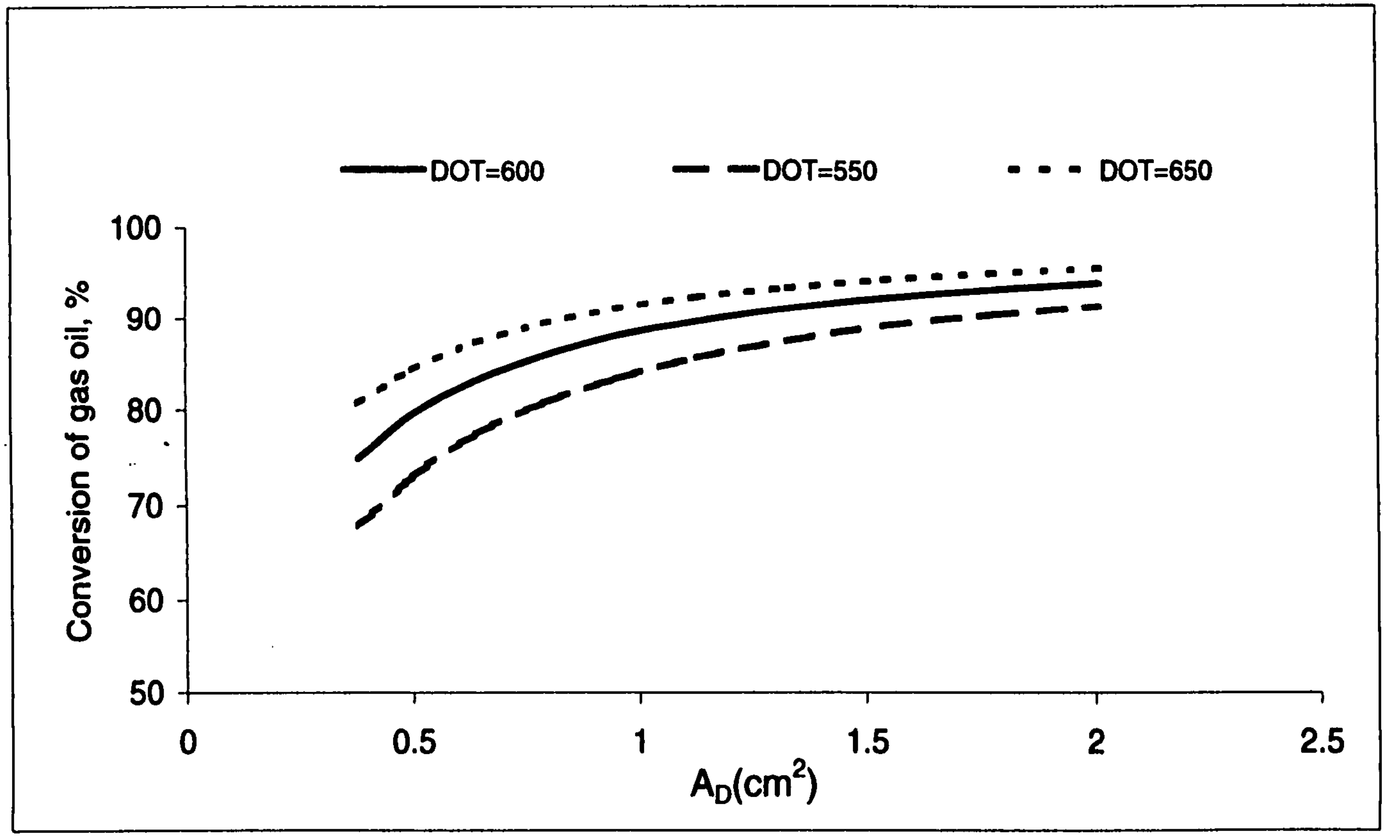

Fig. 4.16: Effect of changing downer cross-section area on conversion of gas oil, L_D=2 m

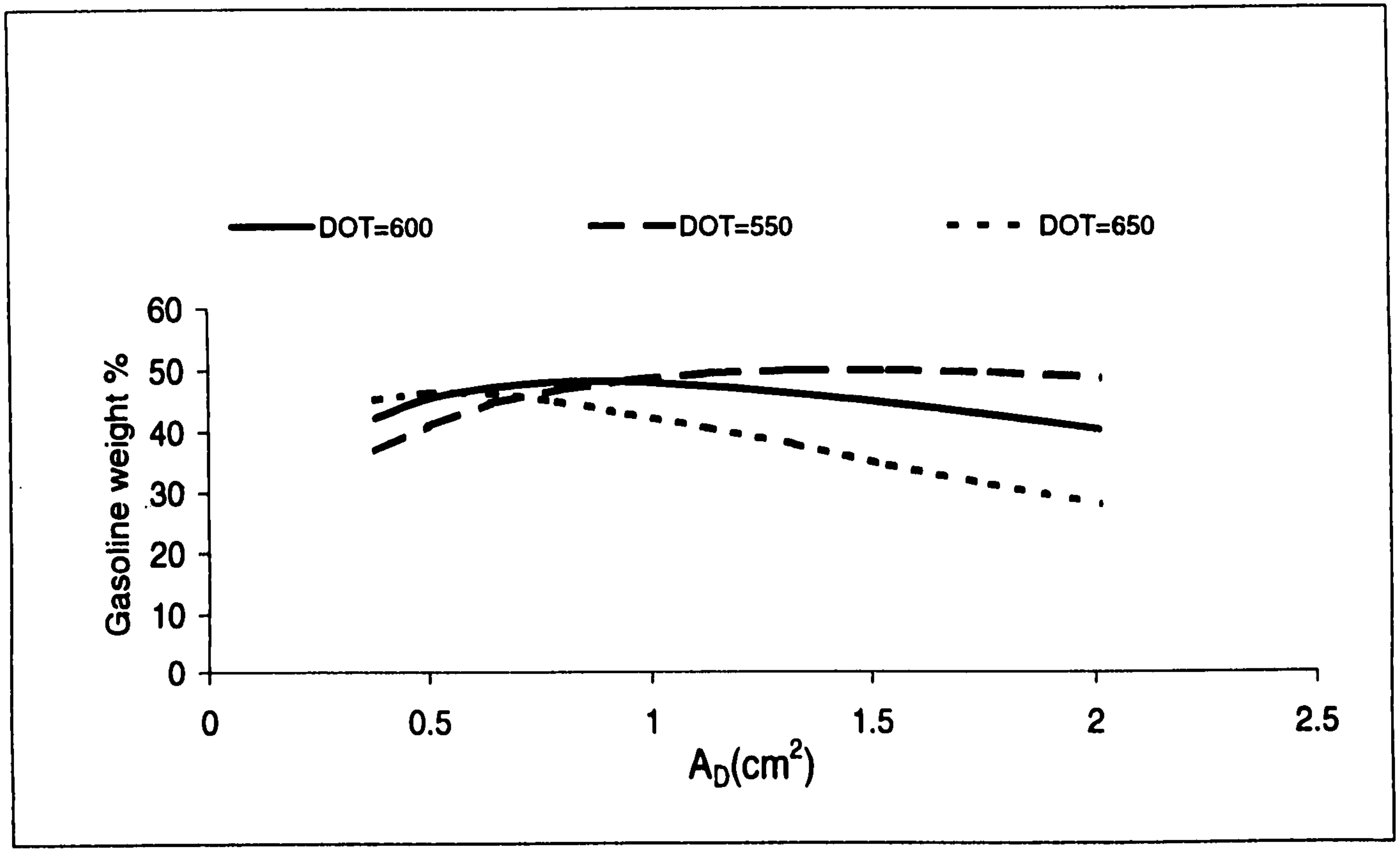

Fig. 4.17: Effect of changing downer cross-section area on gasoline yield, L_D=1 m

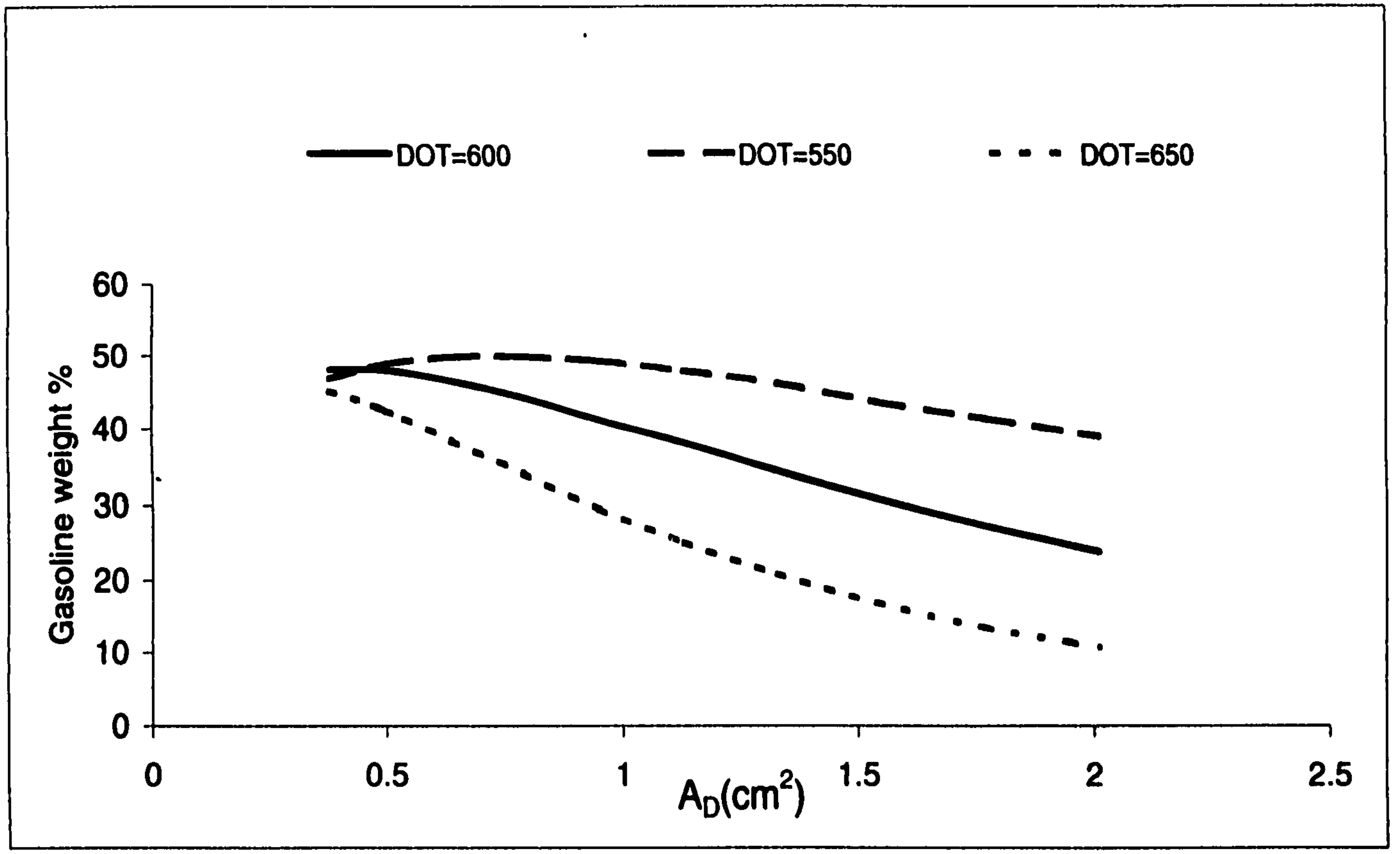

Fig. 4.18: Effect of changing downer cross-section area on gasoline yield, L_D=2 m

Table 4.7 Optimum A_D to produce gasoline at different DOT and L_D

L_D (m)	DOT (°C)	Opt. A_D (m^2)
1.0	550	1.6
	600	0.820
	650	0.530
2.0	550	0.75
	600	< 0.5
	650	<0.5

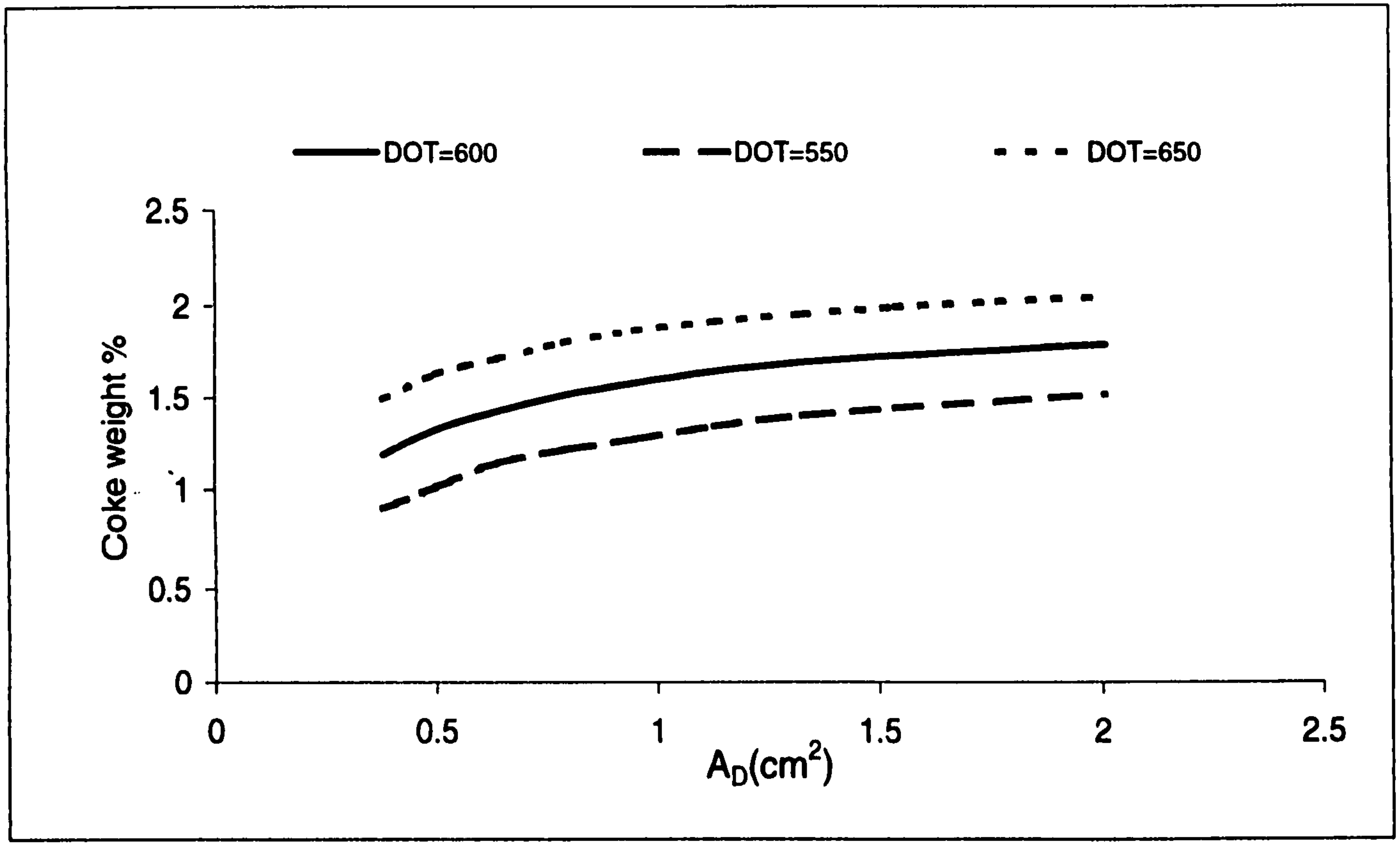

Fig. 4.19: Effect of changing downer cross-section area on coke yield, L_D=1 m

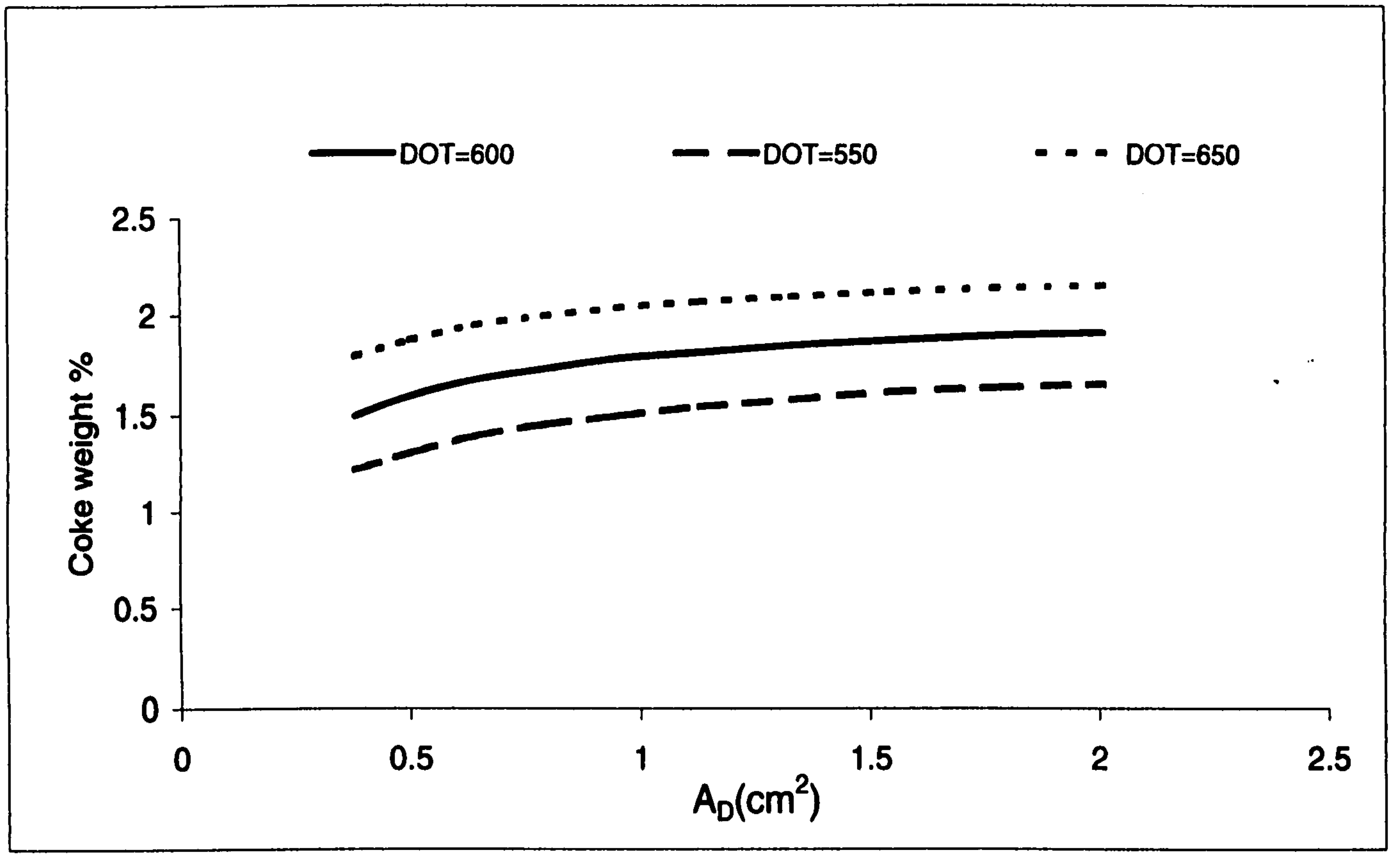

Fig. 4.20: Effect of changing downer cross-section area on coke yield, L_D=2 m

Gases yield exhibits steady increasing profiles with enlarging the cross sectional area of the downer. In Figs. 4.21 and 4.22 this behavior is similar for both L_D's under study. The increase in the gases yield happens due to move gas oil and gasoline conversion to gases with enlargement of the downer volume or in other words extending the residence time.

As seen in Figs. 4.23 and 4.24 for coke % on the regenerated catalyst and Figs. 4.25 and 4.26 for the regenerator temperature, changing of the cross sectional area of the downer does not have a strong effect upon the profiles inside the regenerator. This can be explained as a result of maintaining DOT constant, which keeps the regenerator temperature the same and the efficiency of the regenerator to be the same also.

4.5.3 Effect of changing the length of the downer (L_D)

The length of the downer is a very important design parameter because it is related to the volume of the reactor which is a term in the design equation. Changing the downer length implies changes in the reactor volume. Therefore an increase in the downer length will affect residence time. Fig. 4.27 shows that conversion is higher at larger lengths which is expected due to increasing reactor residence time.

However, the gasoline yield exhibits a maximum with respect to the downer length. This profile is shown in Fig. 4.28. The optimum L_D to produce gasoline is listed in Table 4.8.

Coke and gases yields in the downer increase as the downer length becomes larger as shown in Figs. 4.29 and 4.30. The explanation is that more gas oil and gasoline is transformed to both coke and gases.

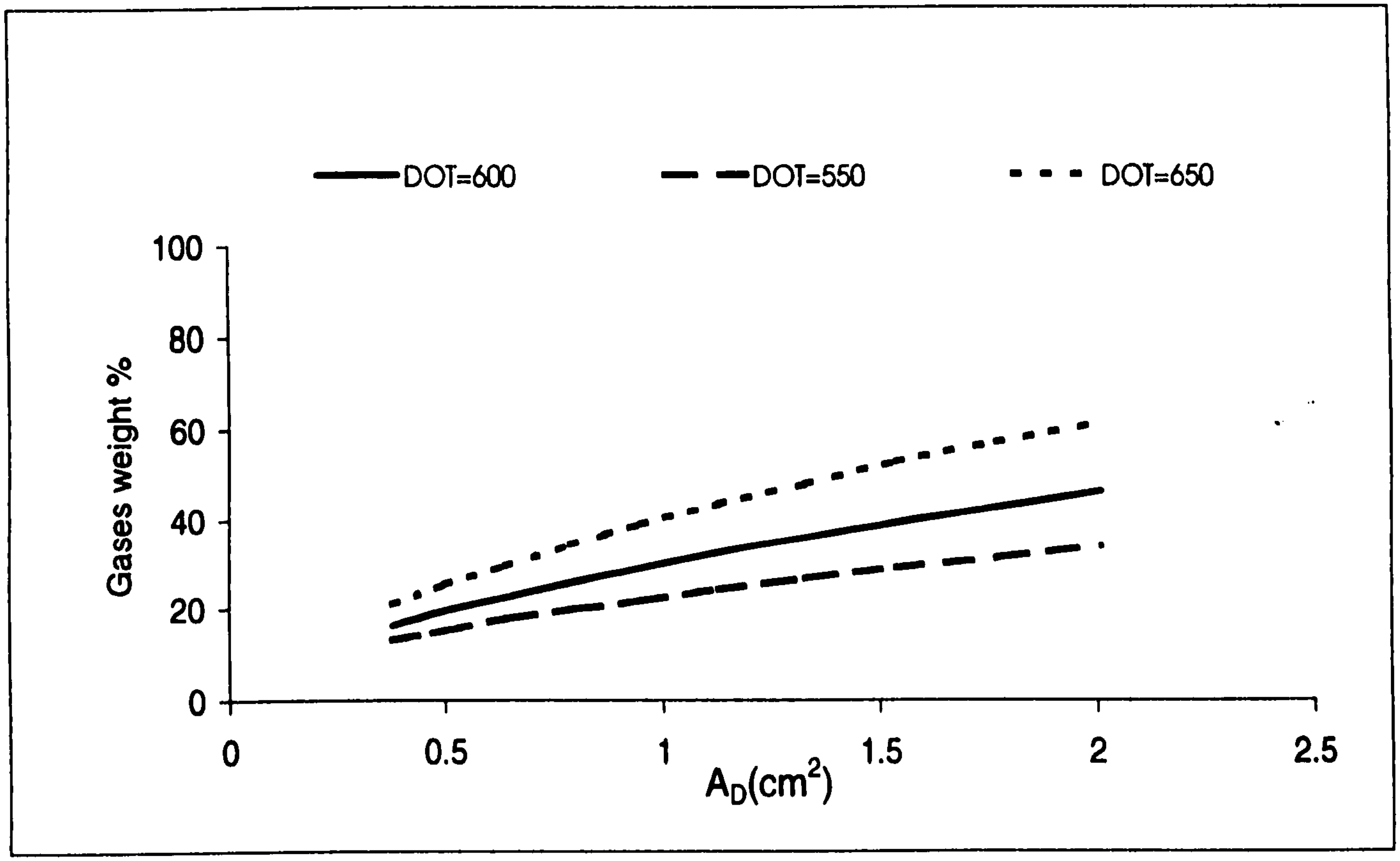

Fig. 4.21: Effect of changing downer cross-section area on gases yield, L_D=1 m

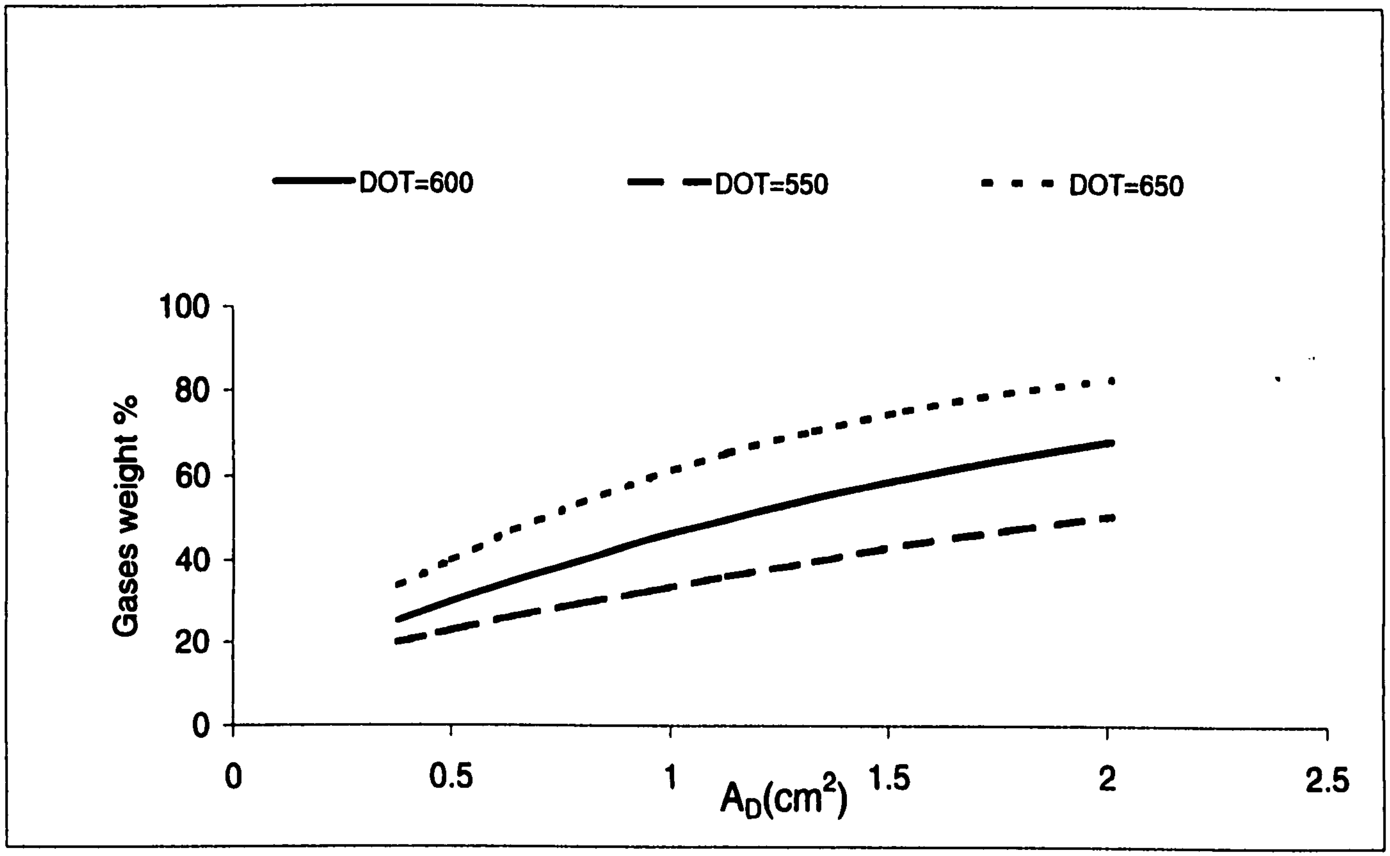

Fig. 4.22: Effect of changing downer cross-section area on gases yield, L_D=2 m

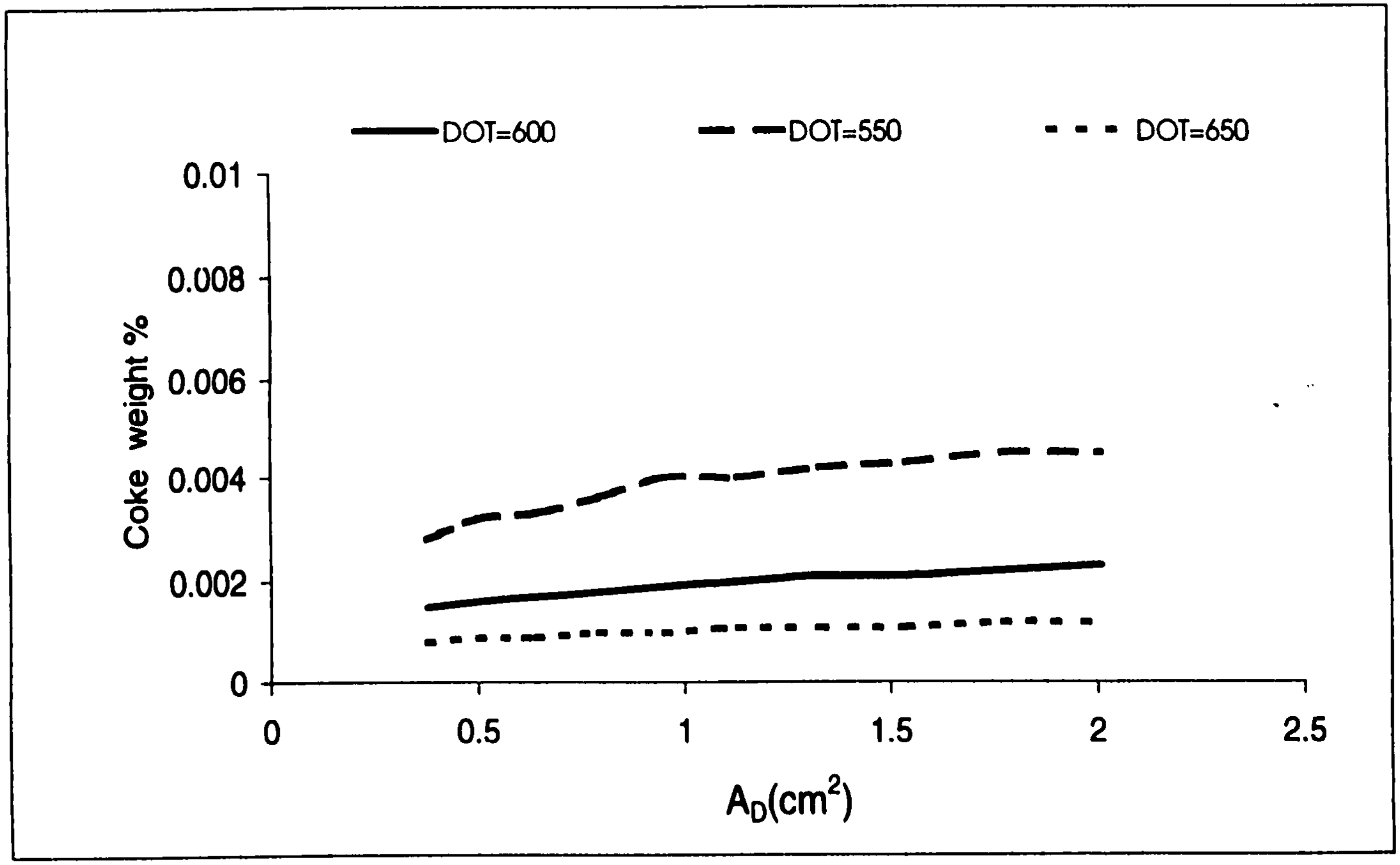

Fig. 4.23: Effect of changing downer cross-section area on coke on regenerated catalyst, L_D=1m

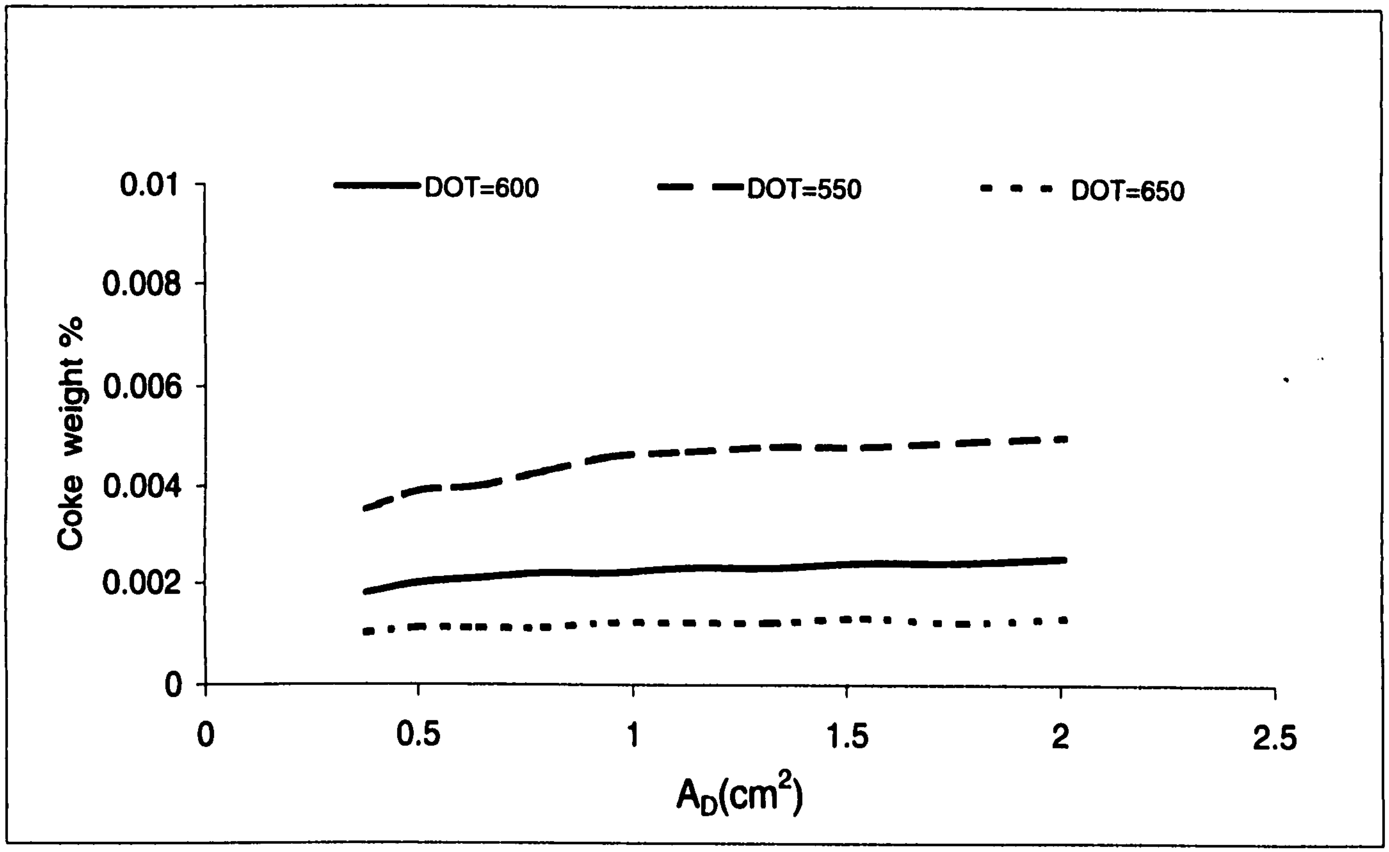

Fig. 4.24: Effect of changing downer cross-section area on coke on regenerated catalyst, L_D=2m

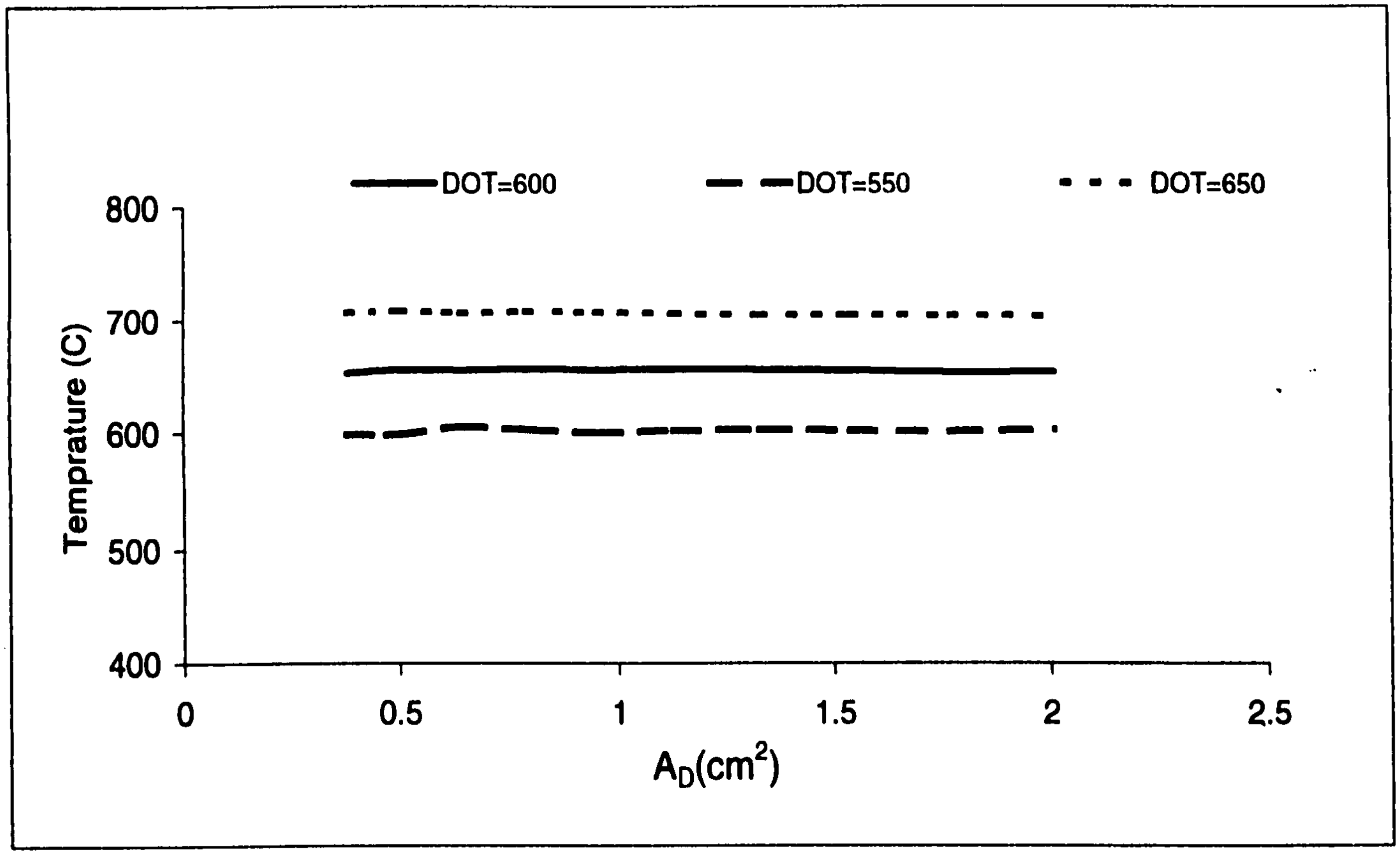

Fig. 4.25: Effect of changing downer cross-section area on emulsion phase temperature (regenerator temperature), L_D=1 m

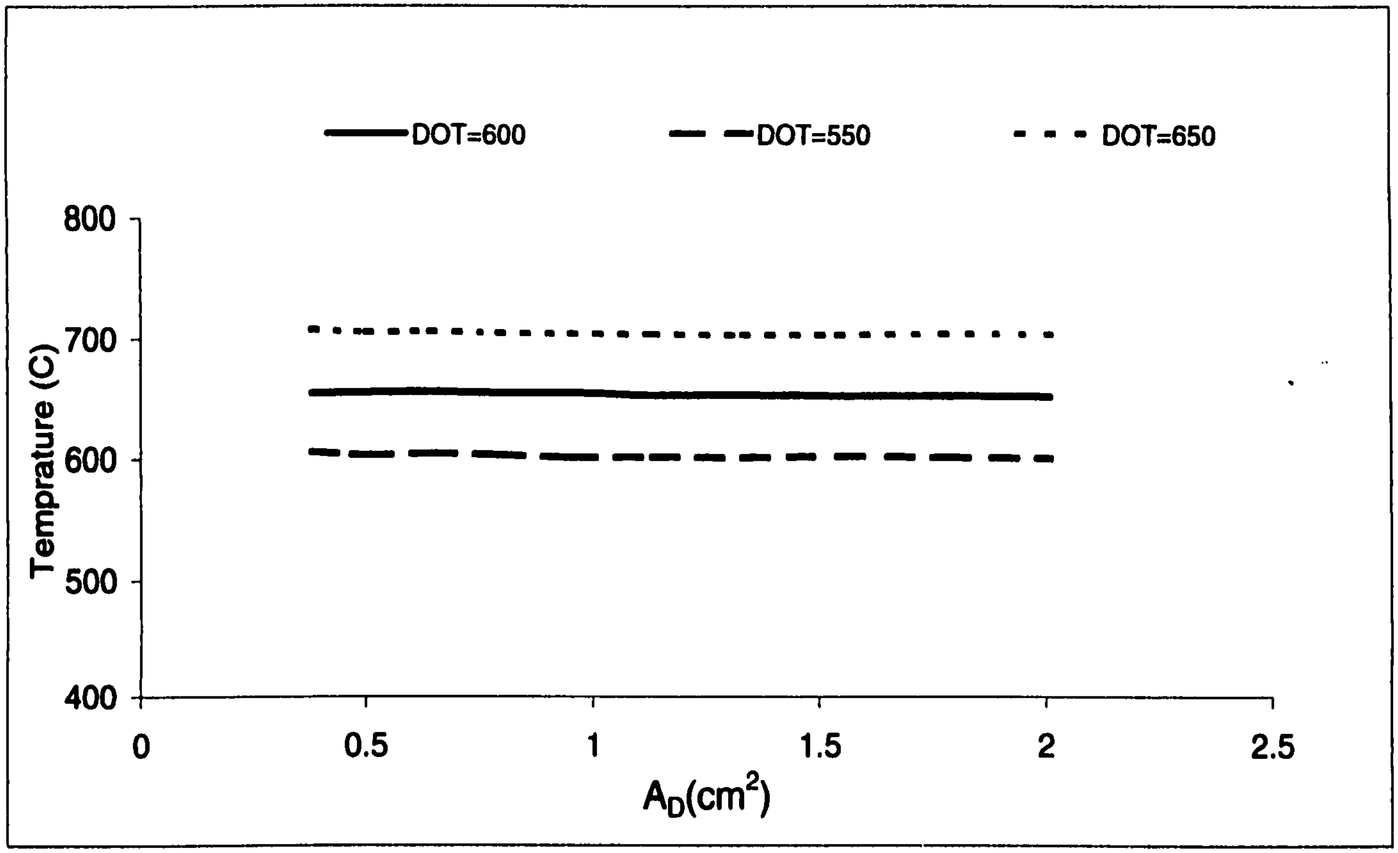

Fig. 4.26: Effect of changing downer cross-section area on emulsion phase temperature (regenerator temperature), L_D=2 m

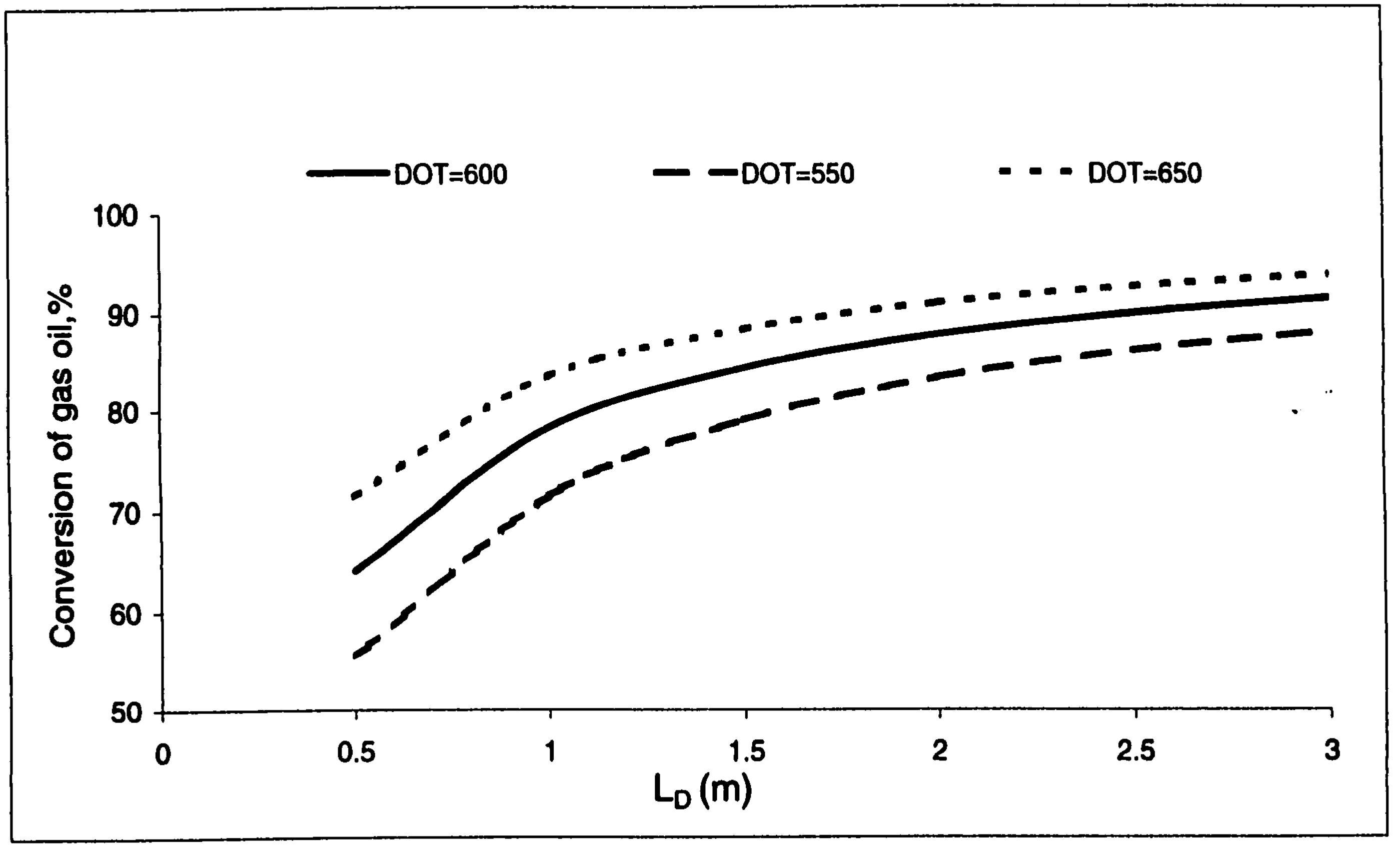

Fig. 4.27: Effect of changing length of the downer on conversion of gas oil

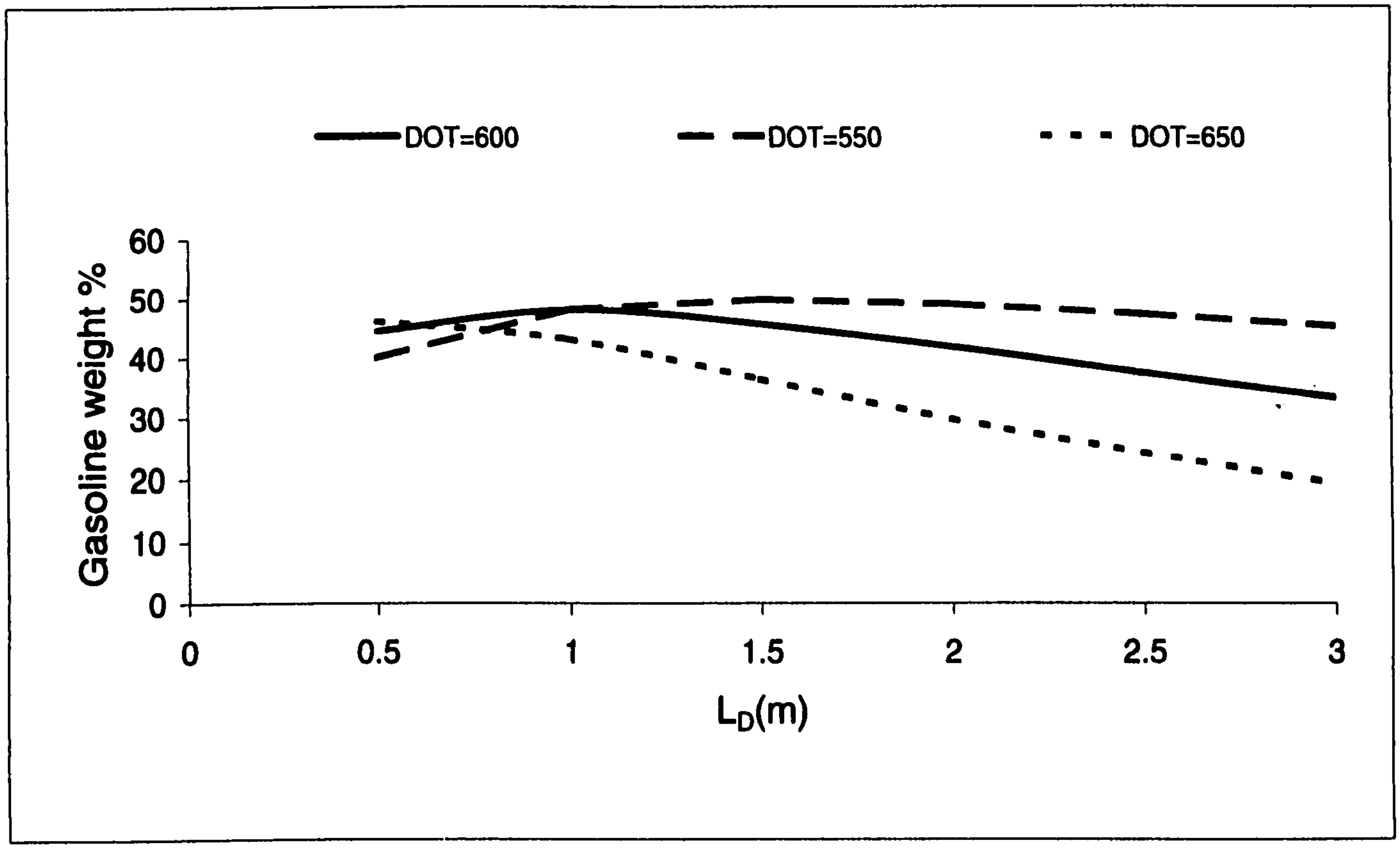

Fig. 4.28: Effect of changing length of the downer on gasoline yield

Table 4.8 Optimum L_D at fixed A_D to produce gasoline at different DOT's

DOT (°C)	Maximum Gasoline Yield (wt %)	Optimum L_D [illegible]
550	51	1.5
600	48	1.0
650	40 – 45	< 0.5

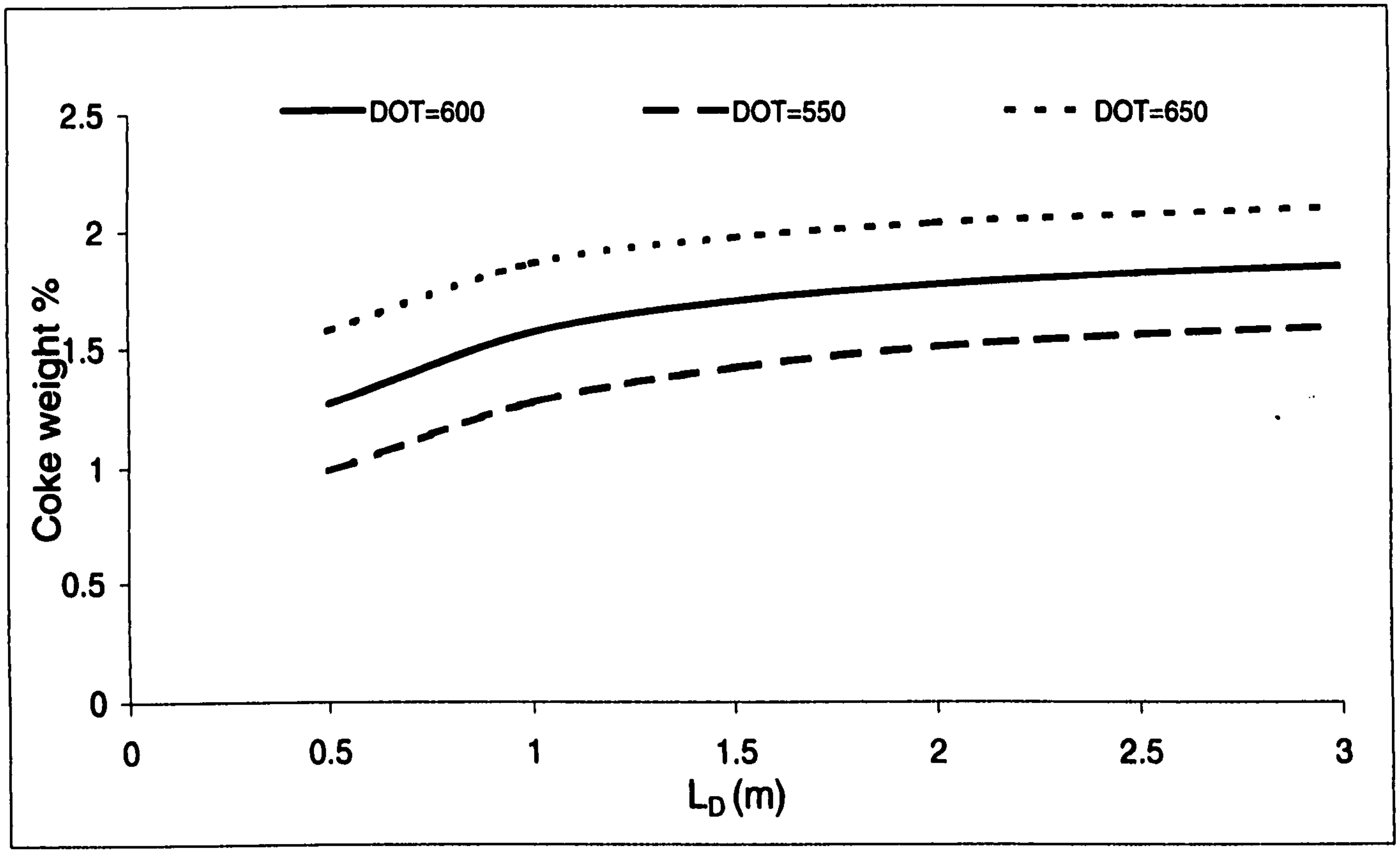

Fig. 4.29: Effect of changing length of the downer on coke yield

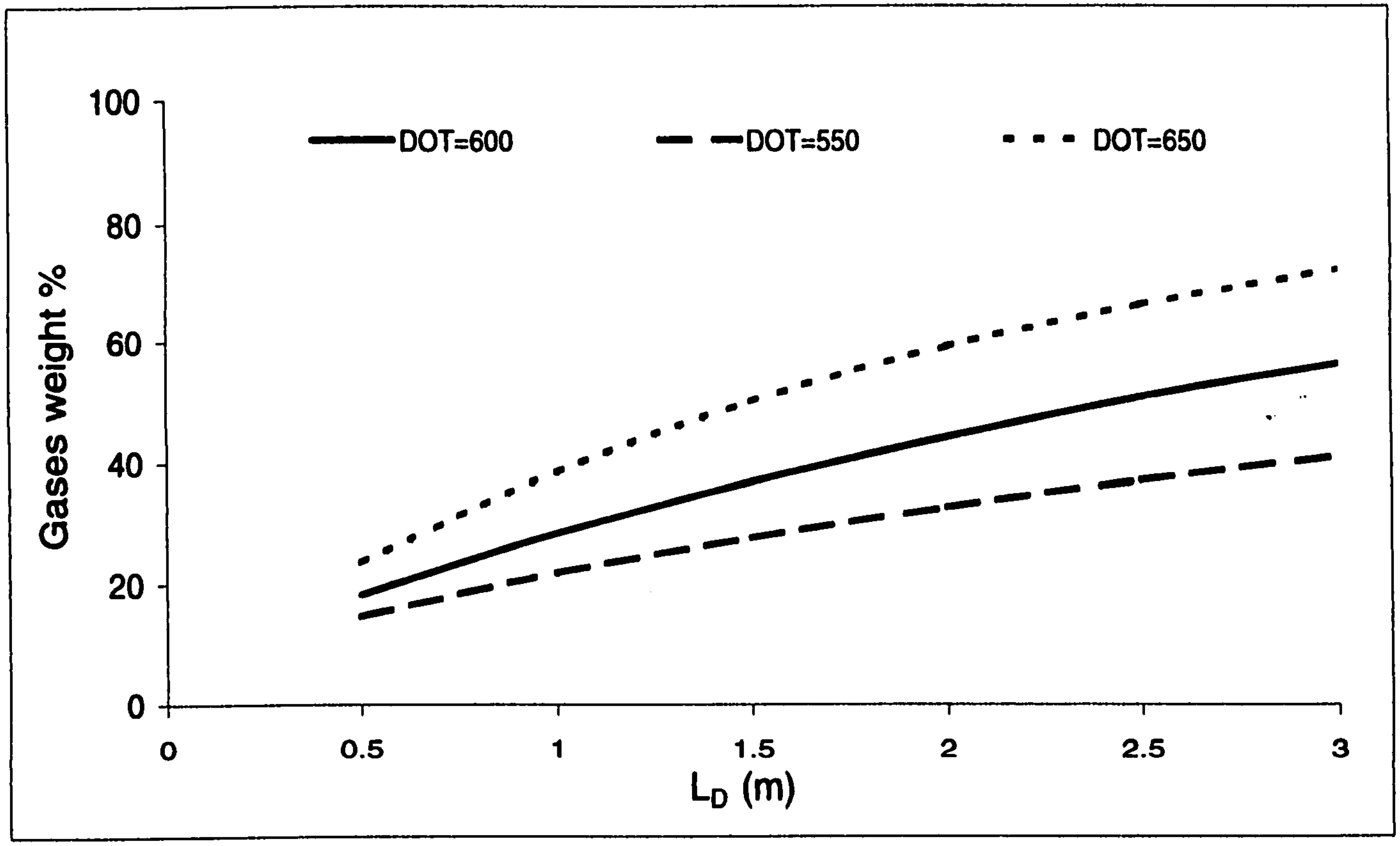

Fig. 4.30: Effect of changing length of the downer on gases yield

Coke on the regenerated catalyst Fig 4.31 increases slightly with the downer length due to more coke deposited on the spent catalyst coming from the downer. The regenerator temperature as shown in Fig. 4.32 is constant due to maintaining the DOT or the temperature of the spent catalyst introduced to the regenerator.

4.5.4 Effect of changing flow rate of air to the regenerator

The previously discussed parameters are directly related to the downer operation and design. In this section, the effect on the whole unit is viewed by changing a parameter in the regenerator. It is the air flow rate introduced in the regeneration process. Air supplies oxygen which burns the coke deposits on the catalyst. It can be inferred from Figs. 4.33 – 4.38 that the conversion and product yields reveal semi-constant behavior against the air velocity. Moreover, coke on the regenerated catalyst and regenerator temperature show constant profiles.

In the FCC-downer unit under study, the experimental data indicates that the unit is operated with complete combustion mode which requires feed of excess air in order to achieve this type of combustion. Therefore, the flow of air will not affect the regeneration process and hence the performance of the whole unit. This comment is supported by the different figures either for the downer or the regenerator, Figs. 4.33 – 4.38, because more air means more burning of carbon deposits on the catalyst. If the unit were operated in partial combustion mode, then it would be expected that the air flow would play a major role to give effective regeneration.

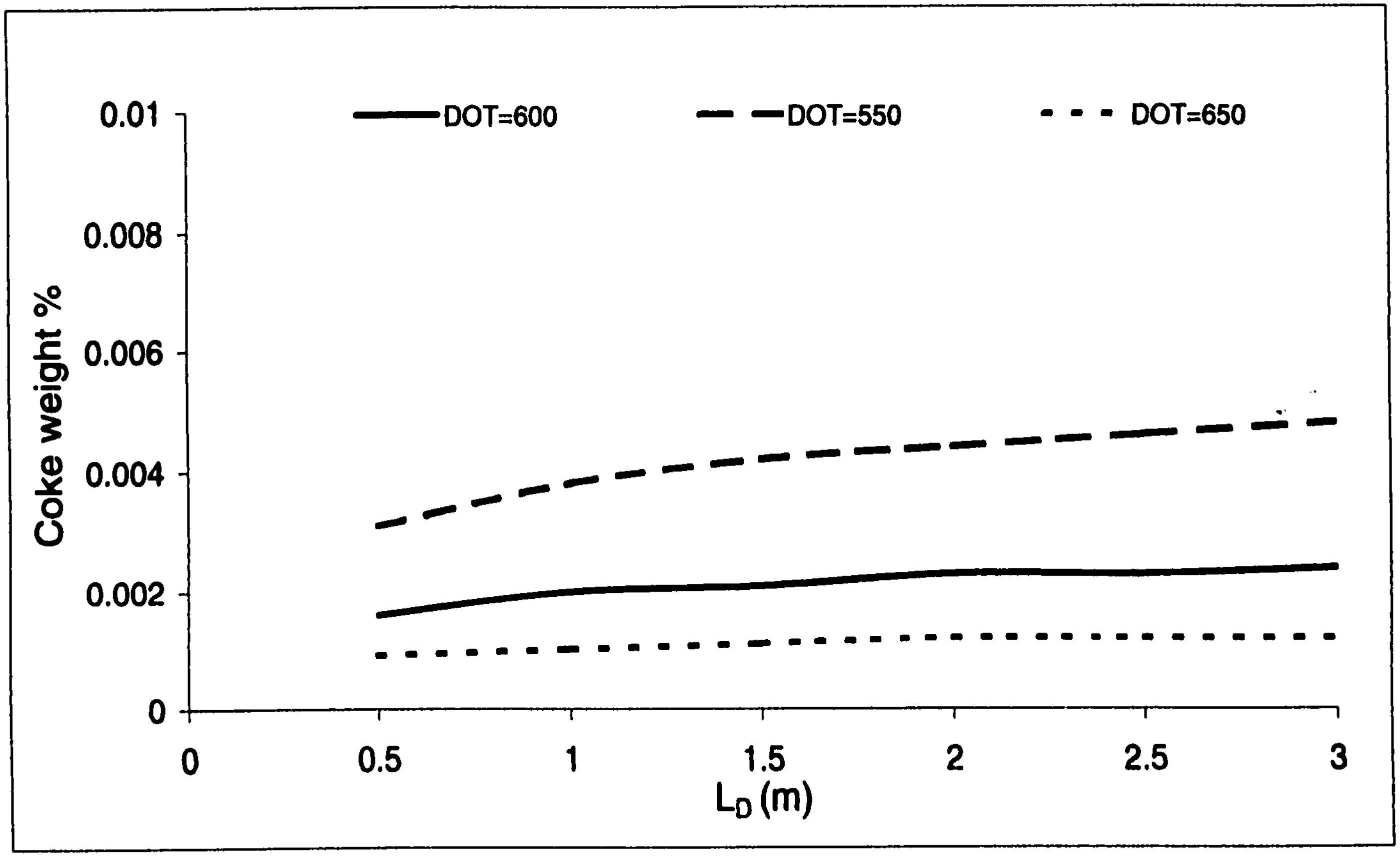

Fig. 4.31: Effect of changing length of the downer on coke on regenerated catalyst

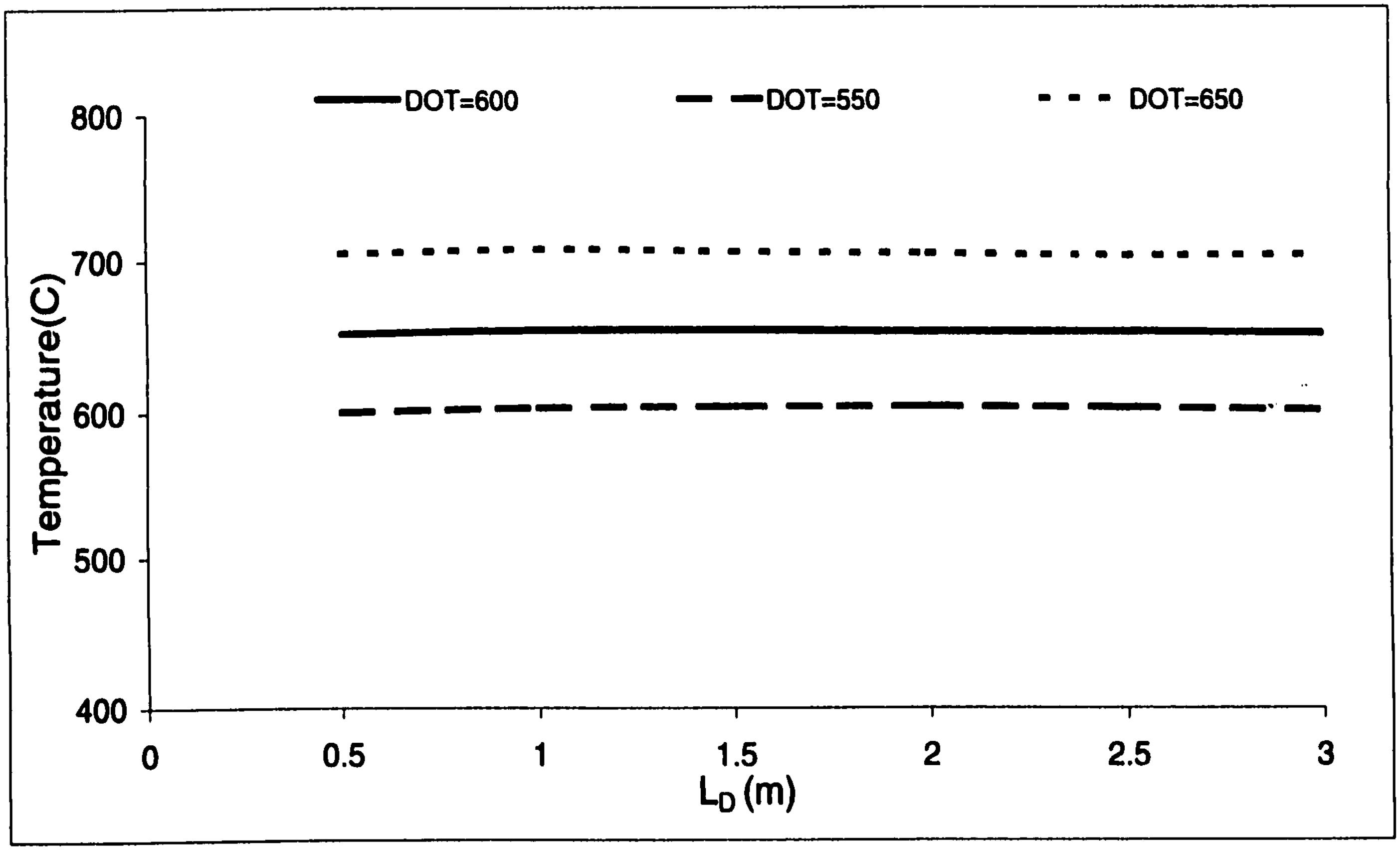

Fig. 4.32: Effect of changing length of the downer on coke on emulsion phase temperature(regenerator temperature)

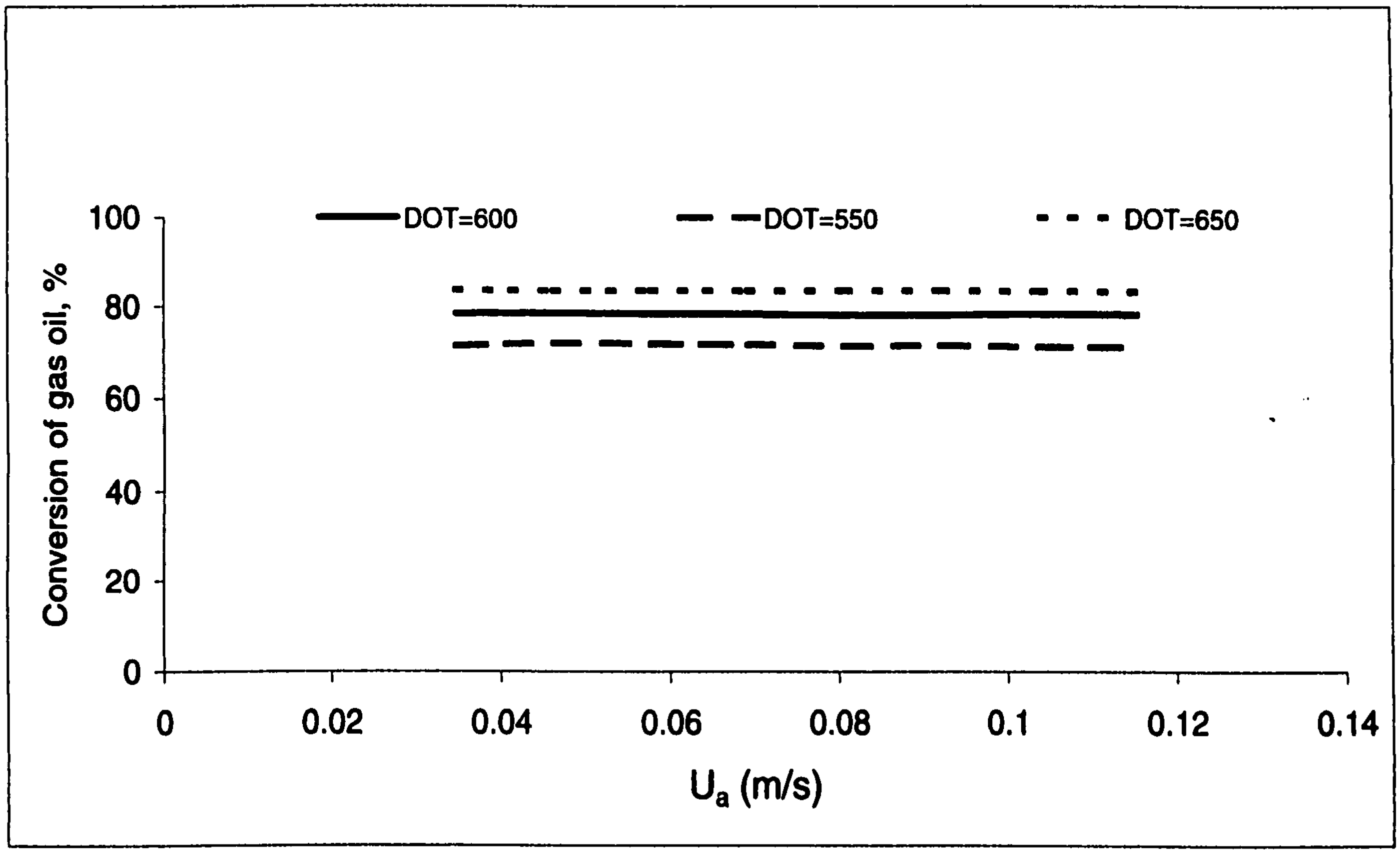

Fig. 4.33: Effect of changing the air flow on conversion of gas oil

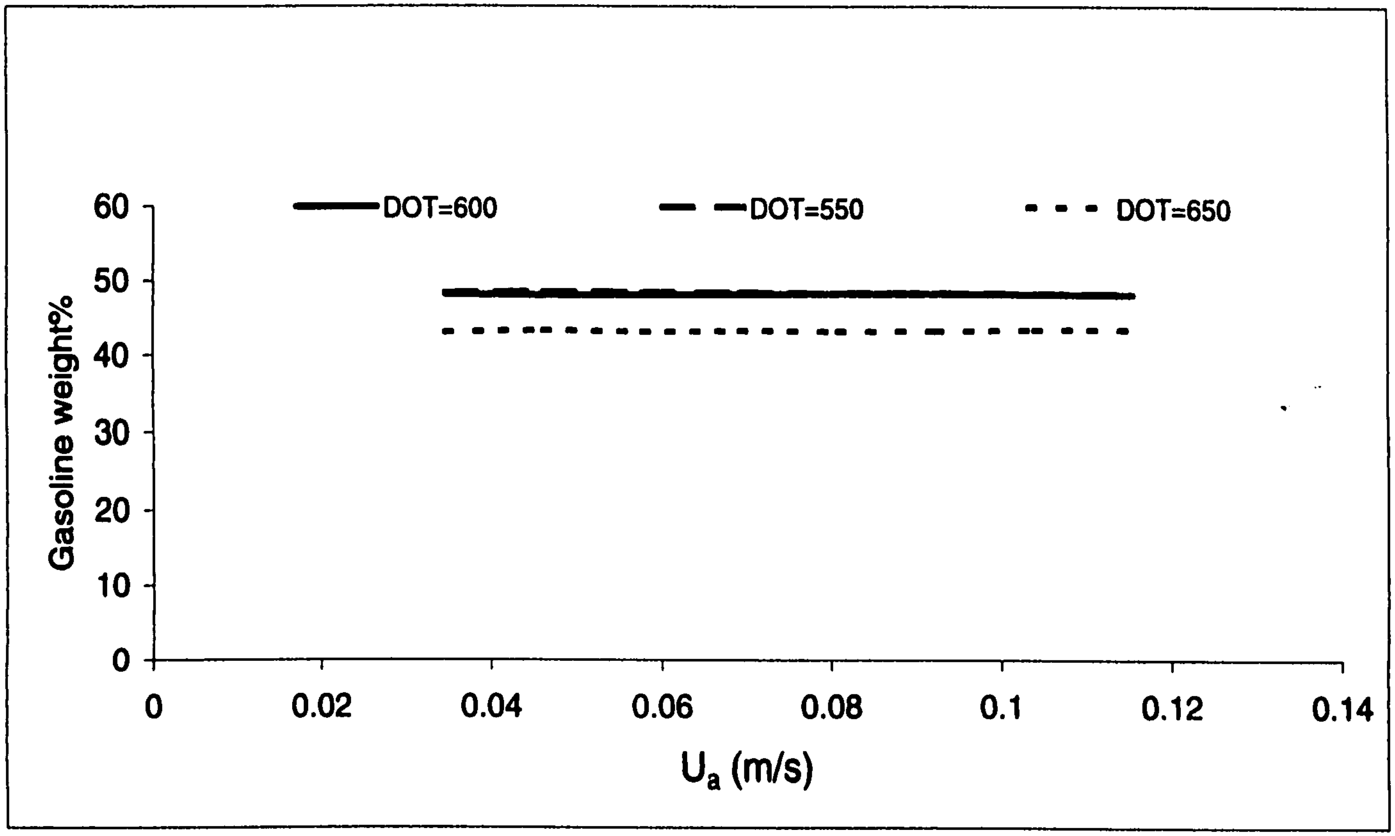

Fig. 4.34: Effect of changing the air flow on gasoline yield

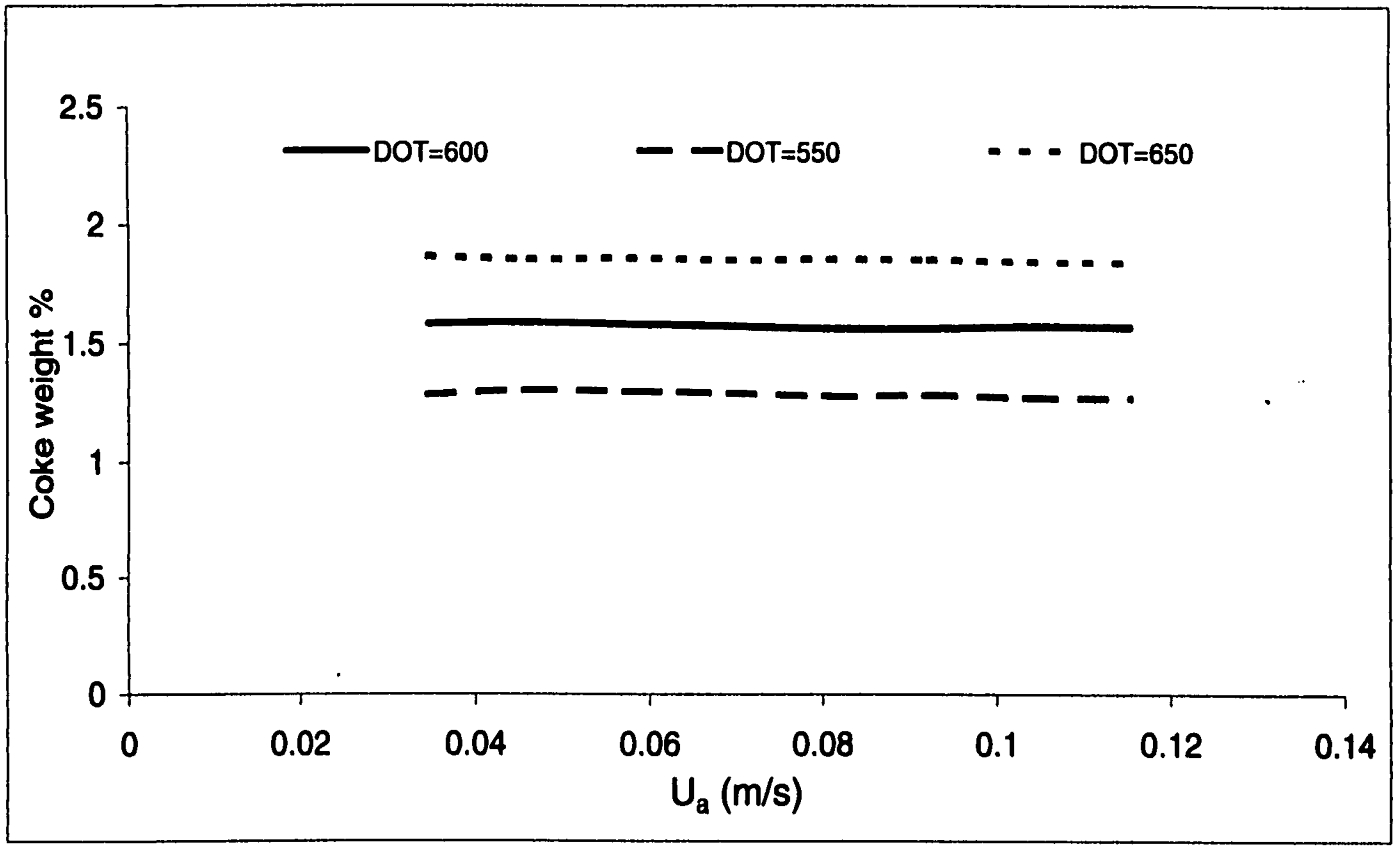

Fig. 4.35: Effect of changing the air flow on coke yield in the downer

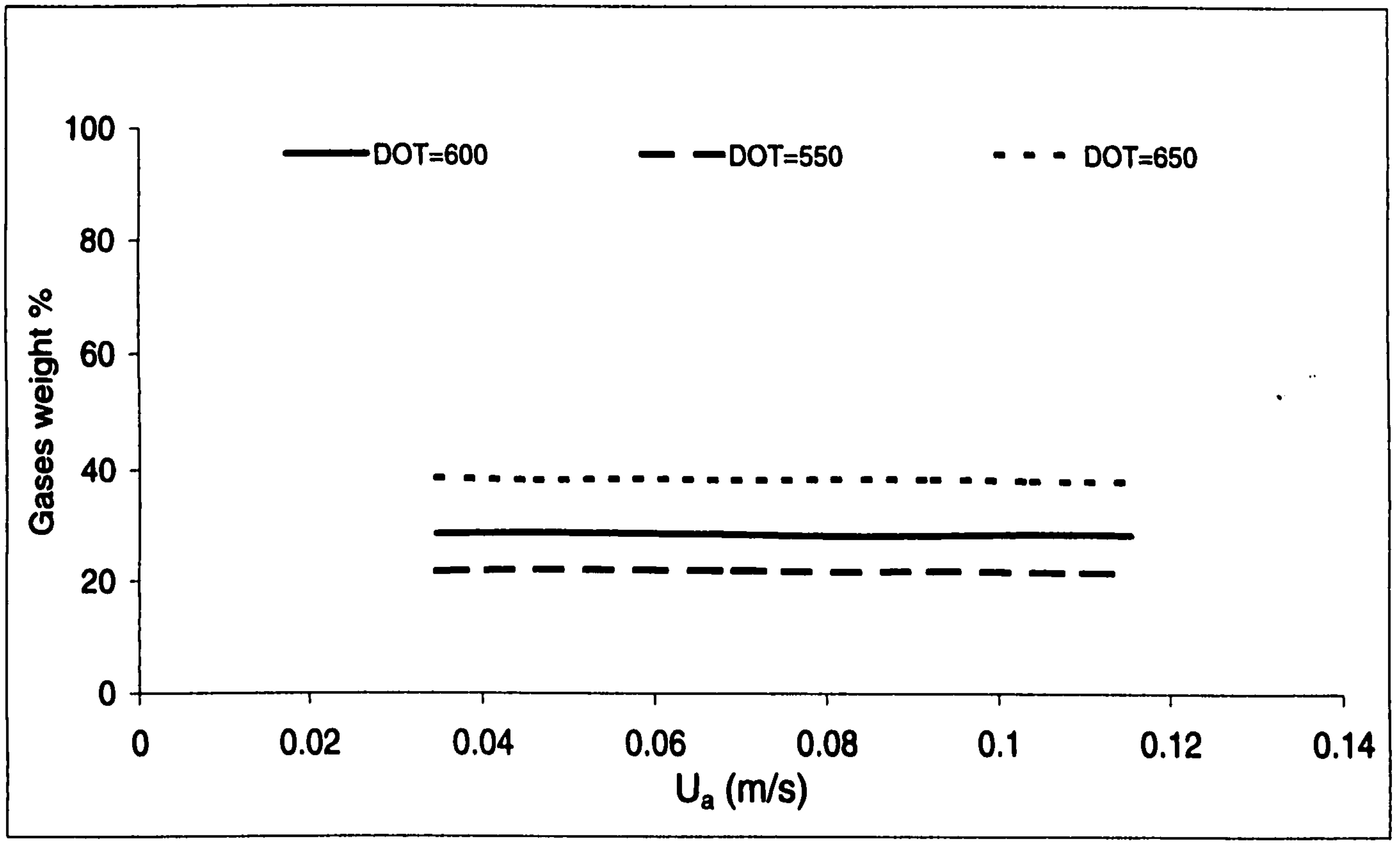

Fig. 4.36: Effect of changing the air flow on gases yield

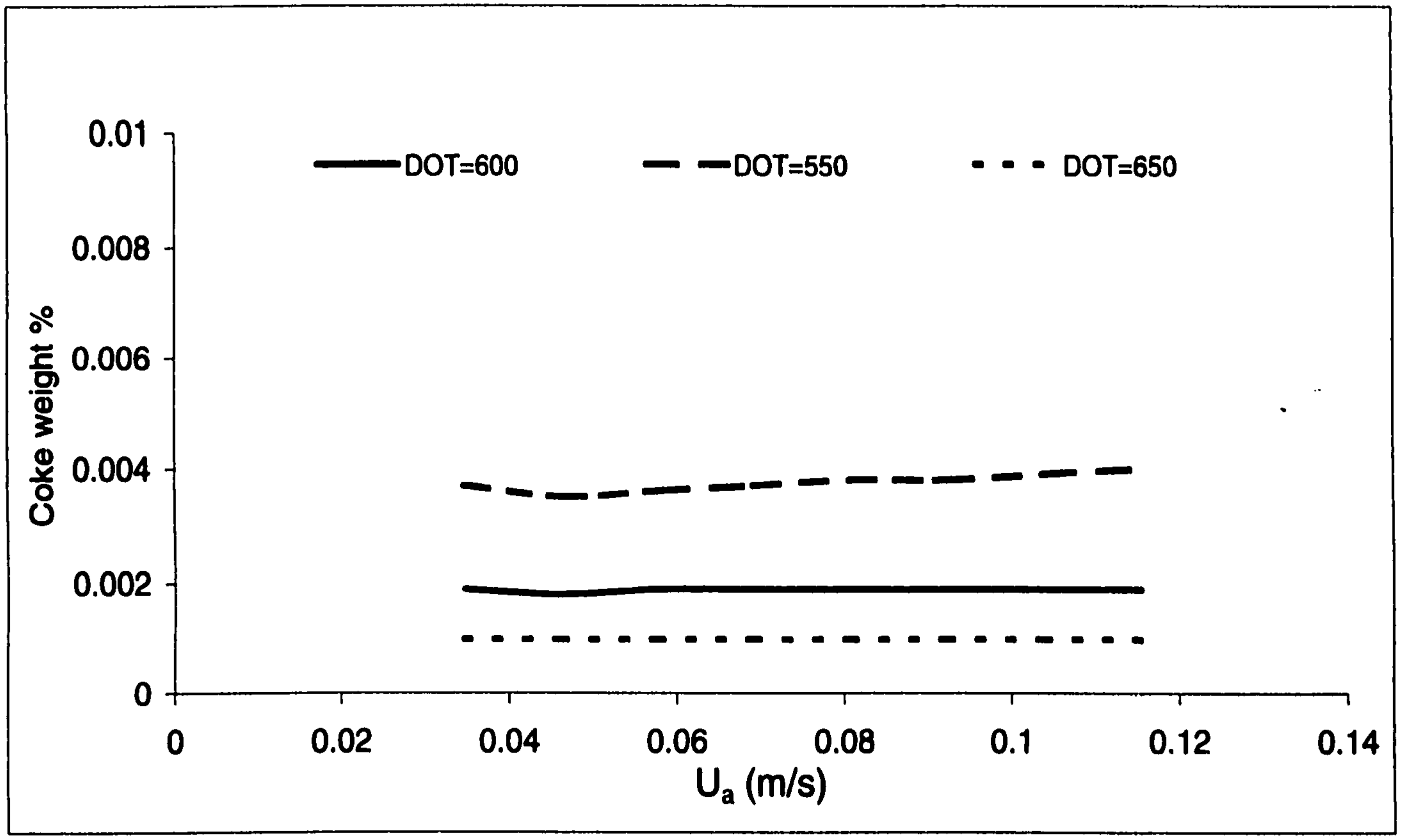

Fig. 4.37: Effect of changing the air flow on coke on regenerated catalyst

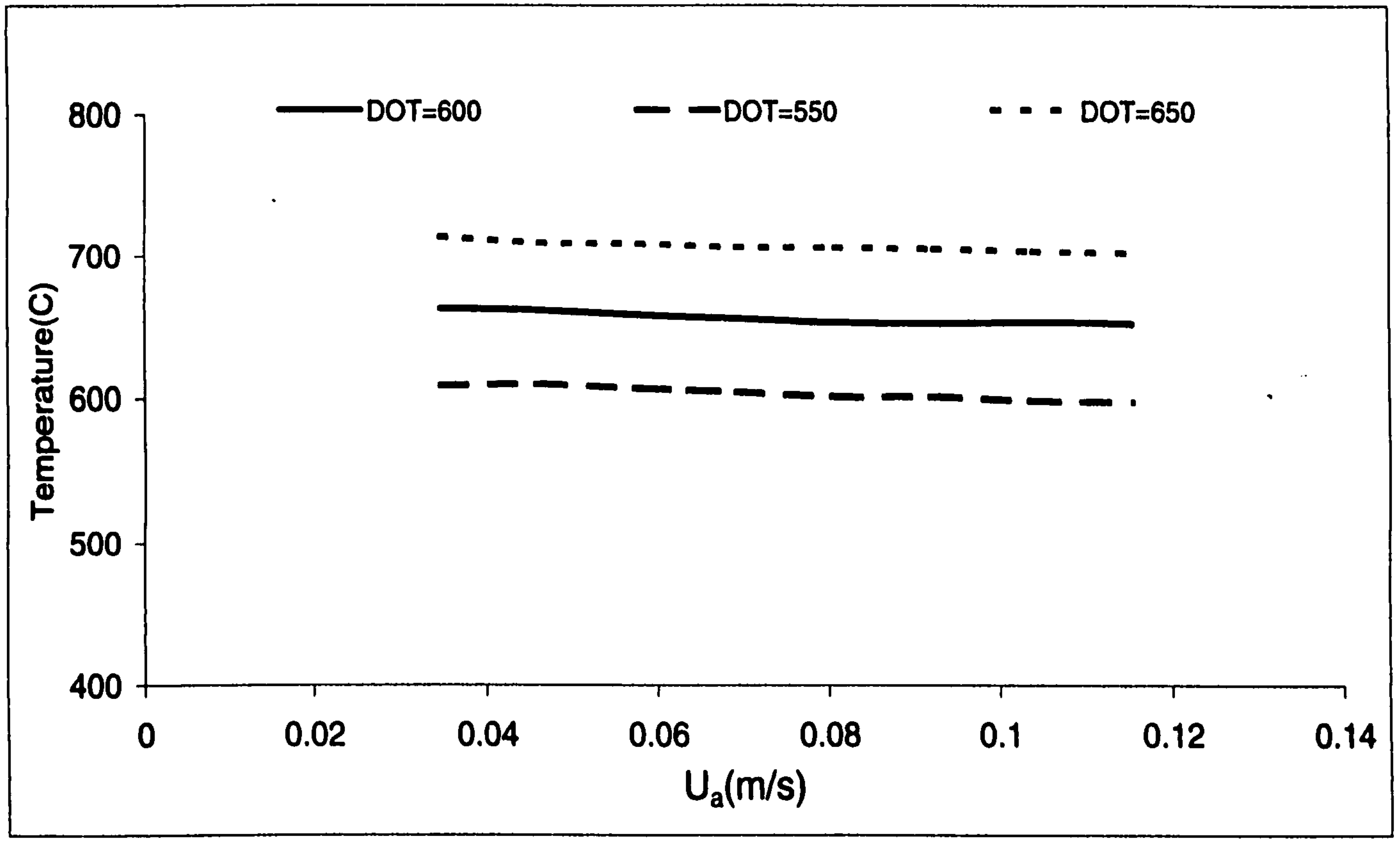

Fig. 4.38: Effect of changing the air flow on emulsion phase temperature(regenerator temperature)

4.6 Parametric sensitivity of the FCC-downer

The transfer of heat and mass between bubble and emulsion phases in the dense region of the regenerator is a very important phenomenon. The exchange of gases (reactants and products) and heat transfer between the two phases plays a major role in the mass and heat balances of the regeneration process. In this section we discuss the effect of mass transfer coefficient between *bubble-emulsion* (k_g), and the effect of heat transfer coefficient between *bubble-emulsion* phases (h) on the conversion and product yields in the downer and the temperature profiles in the downer. Moreover, the sensitivity of the FCC-downer model is studied against the heat transfer area between the two phases (a_v).

4.6.1 Model sensitivity to the bubble-emulsion mass transfer coefficient

It is clear from Figs. 4.39 and 4.40 that the model is sensitive to k_g at values of k_g below 0.2 s^{-1}. All the profiles in the downer and regenerator become constant for k_g value > 0.2 s^{-1}. Thus, the model is sensitive to k_g in a certain range (i.e. low values of k_g) and not sensitive at k_g larger than 0.2 s^{-1}. Similarly, % of coke on regenerated catalyst is changing sharply at k_g values of less than 0.2s^{-1} as shown in Fig.4.41.

4.6.2 Model sensitivity to the bubble-emulsion heat transfer coefficient

The heat transfer coefficient between bubble and emulsion phases, h, does not have a large effect on conversion and coke yield in the downer. Instead, the gasoline and gases yields vary significantly against h values, as shown in Fig. 4.42. Moreover, the temperature profiles in the downer and the regenerator decreases widely with increasing h as shown in Fig. 4.43. That means that the model is sensitive to h. Coke on regenerated catalyst increases with higher values of h as

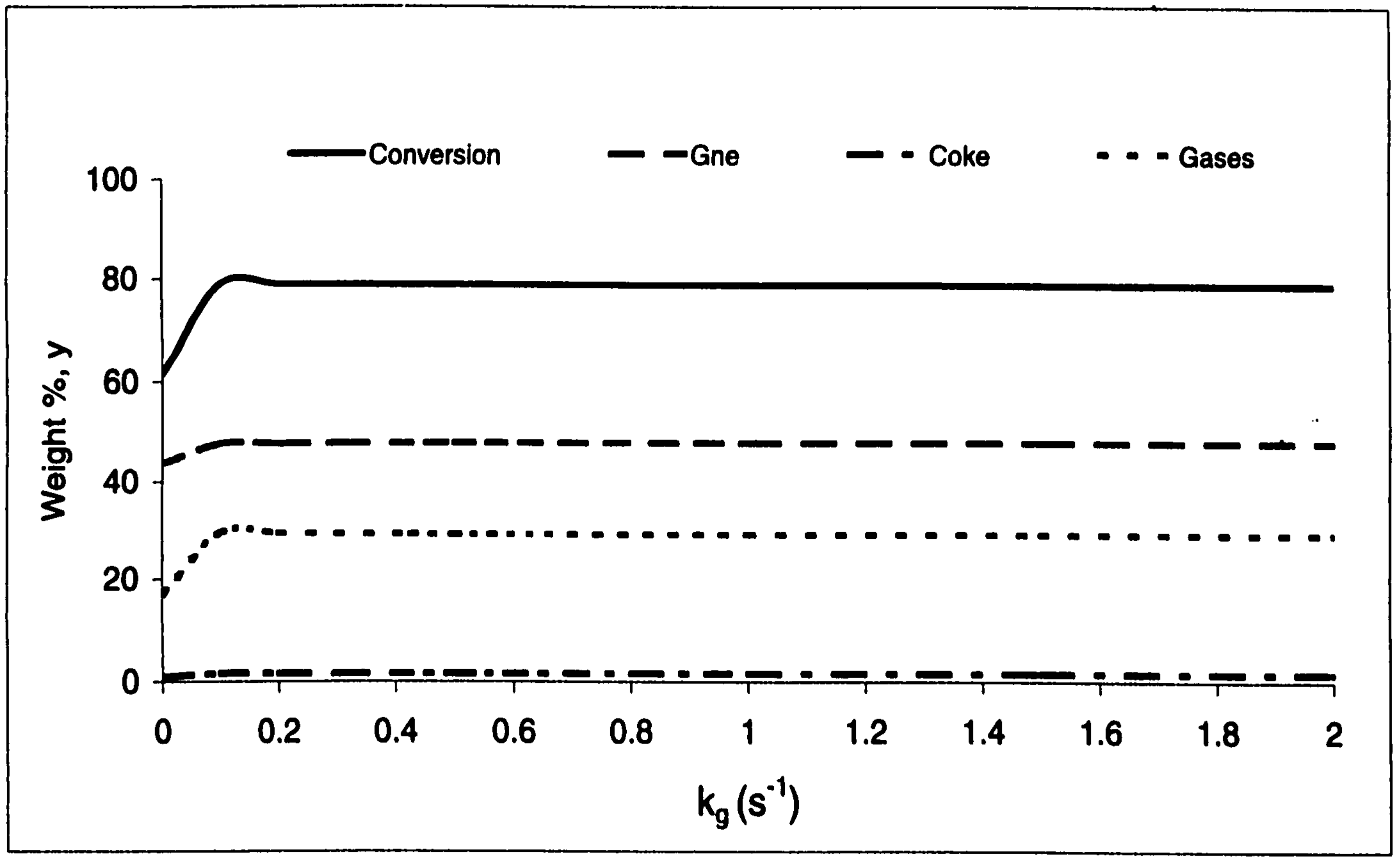

Fig. 4.39: Sensitivity of the conversion of gas oil and product yields to k_g

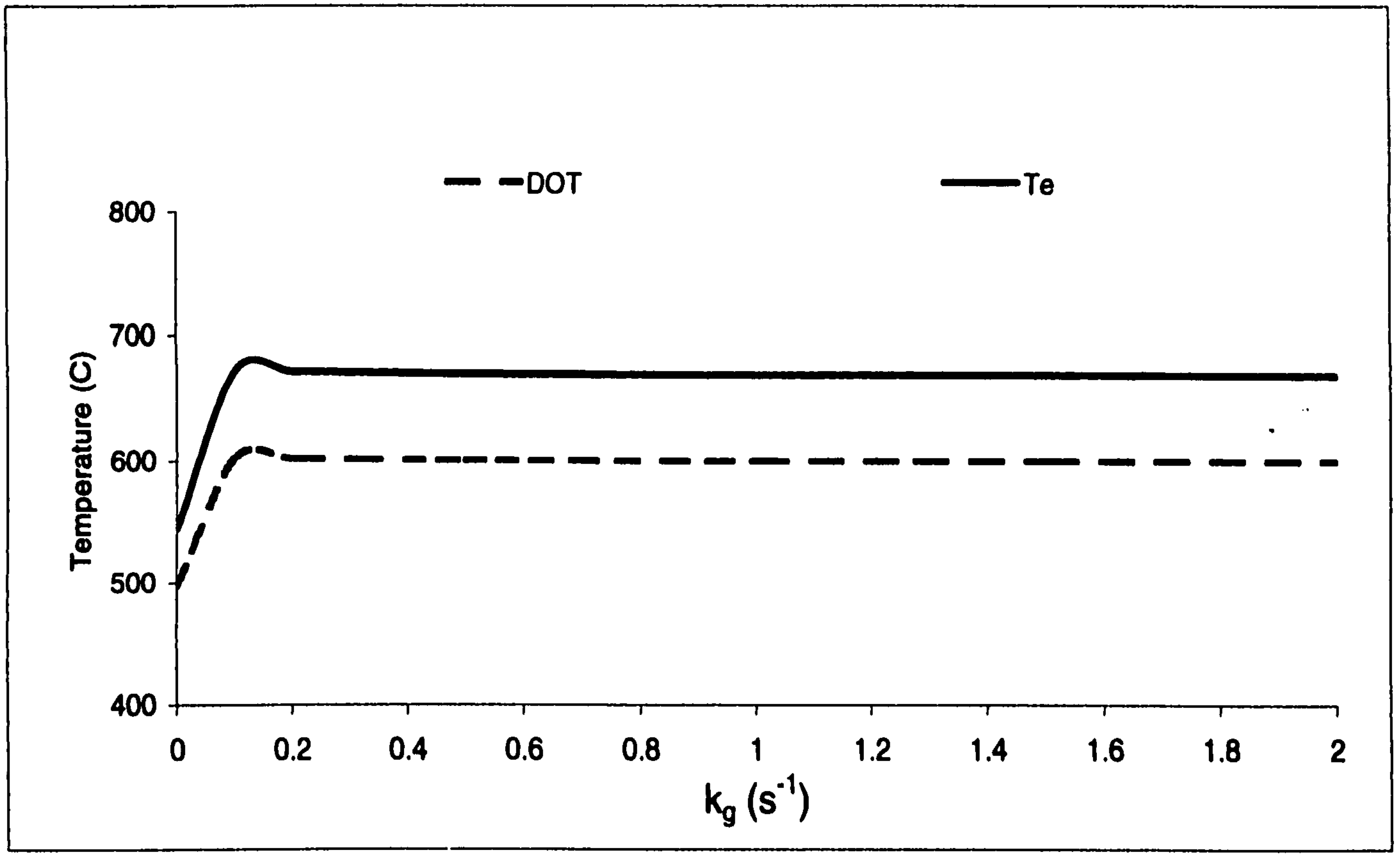

Fig. 4.40: Sensitivity of the downer outlet temperature and emulsion phase temperature(regenerator temperature) to k_g

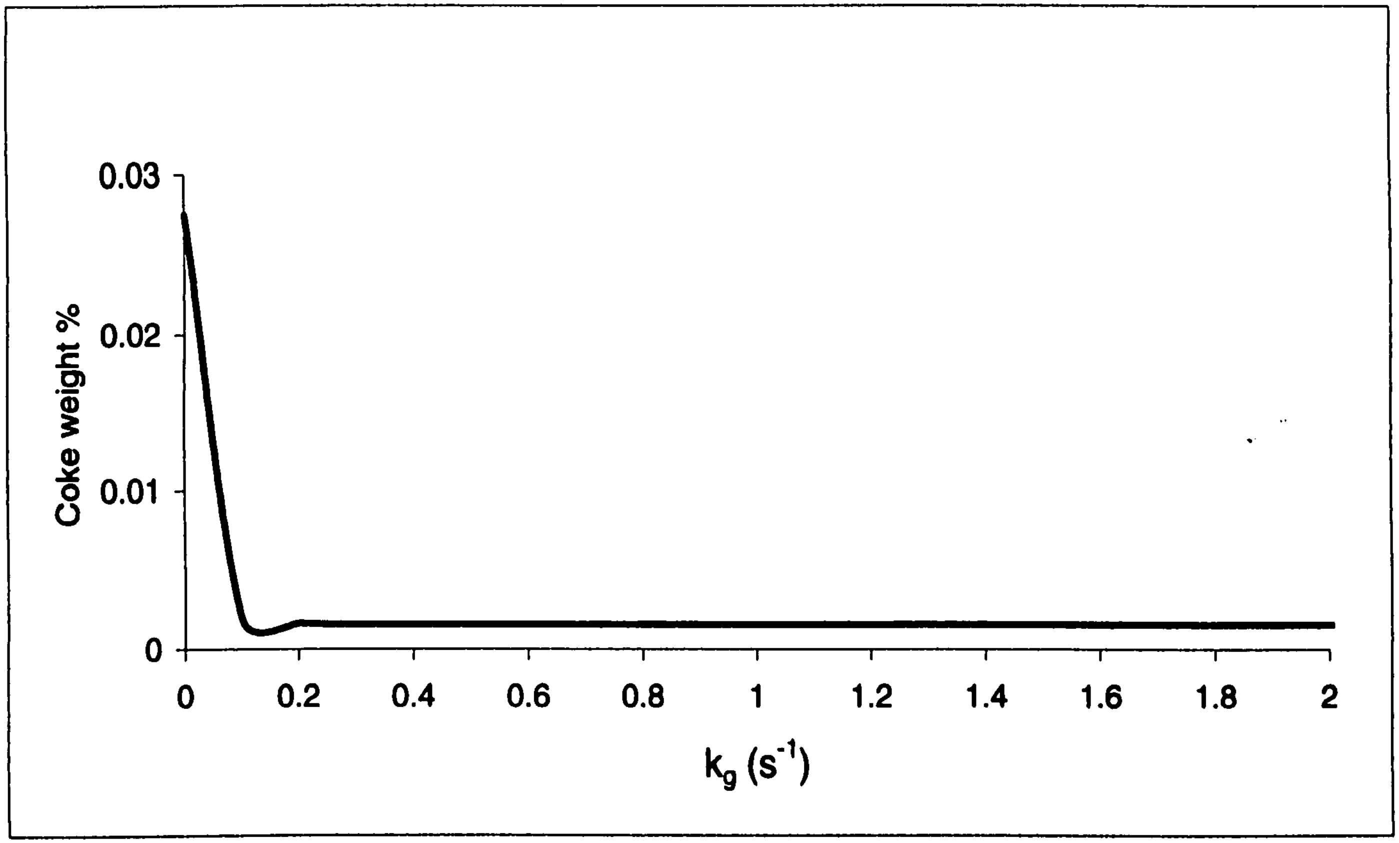

Fig. 4.41: Sensitivity of the coke on regenerated catalyst to k_g

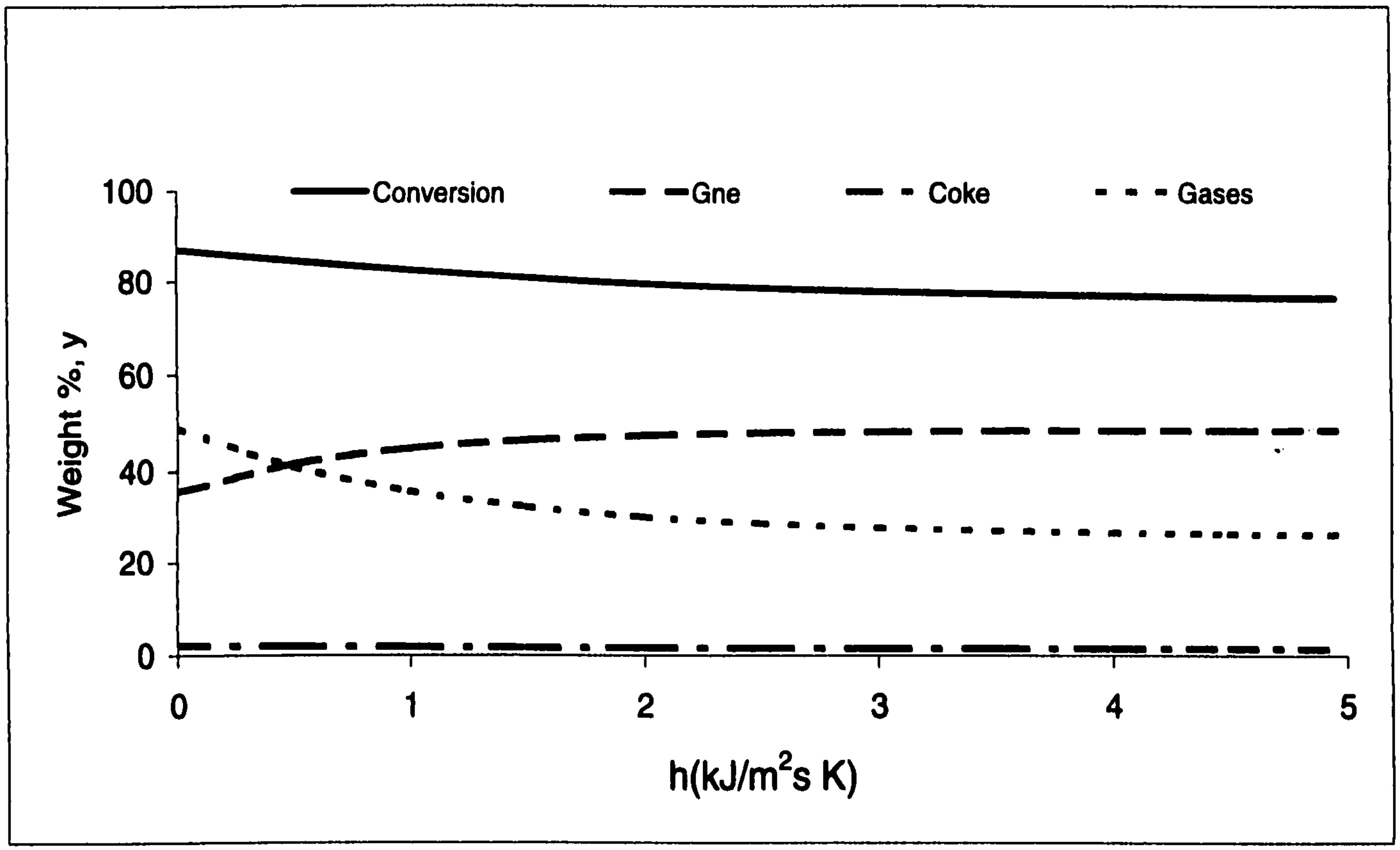

Fig. 4.42: Sensitivity of conversion of gas oil and product yields to h

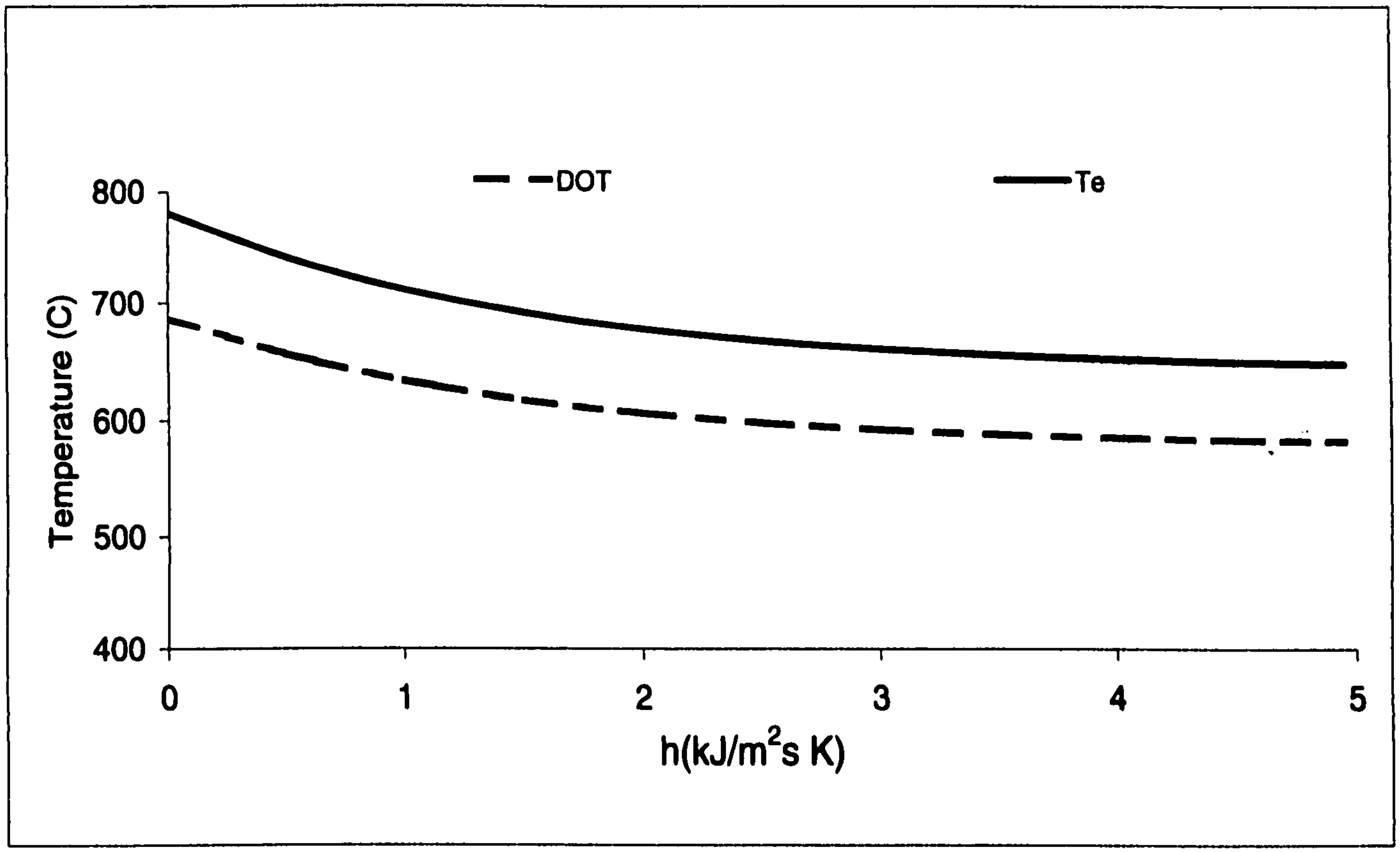

Fig. 4.43: Sensitivity of the downer outlet temperature and emulsion phase temperature(regenerator temperature) to h

shown in Fig. 4.44. Subsequently, evaluation of *h* should be done precisely with the most recent and dependent correlations.

4.6.3 Model sensitivity to the heat transfer area between bubble and emulsion phases

The heat transfer area between bubble and emulsion phases, a_v, effect on the profiles inside the downer and the regenerator will be discussed in this section. It is clear from Fig. 4.45 that changing a_v does not have a strong effect on conversion of gas oil and product yields.

Similarly the temperatures in the downer and the regenerator show steady behavior versus a_v as shown in Fig. 4.46. However, the coke on the regenerated catalyst is sensitive to changing a_v especially in the range of a_v below 0.2 m^{-1} as shown in Fig. 4.47

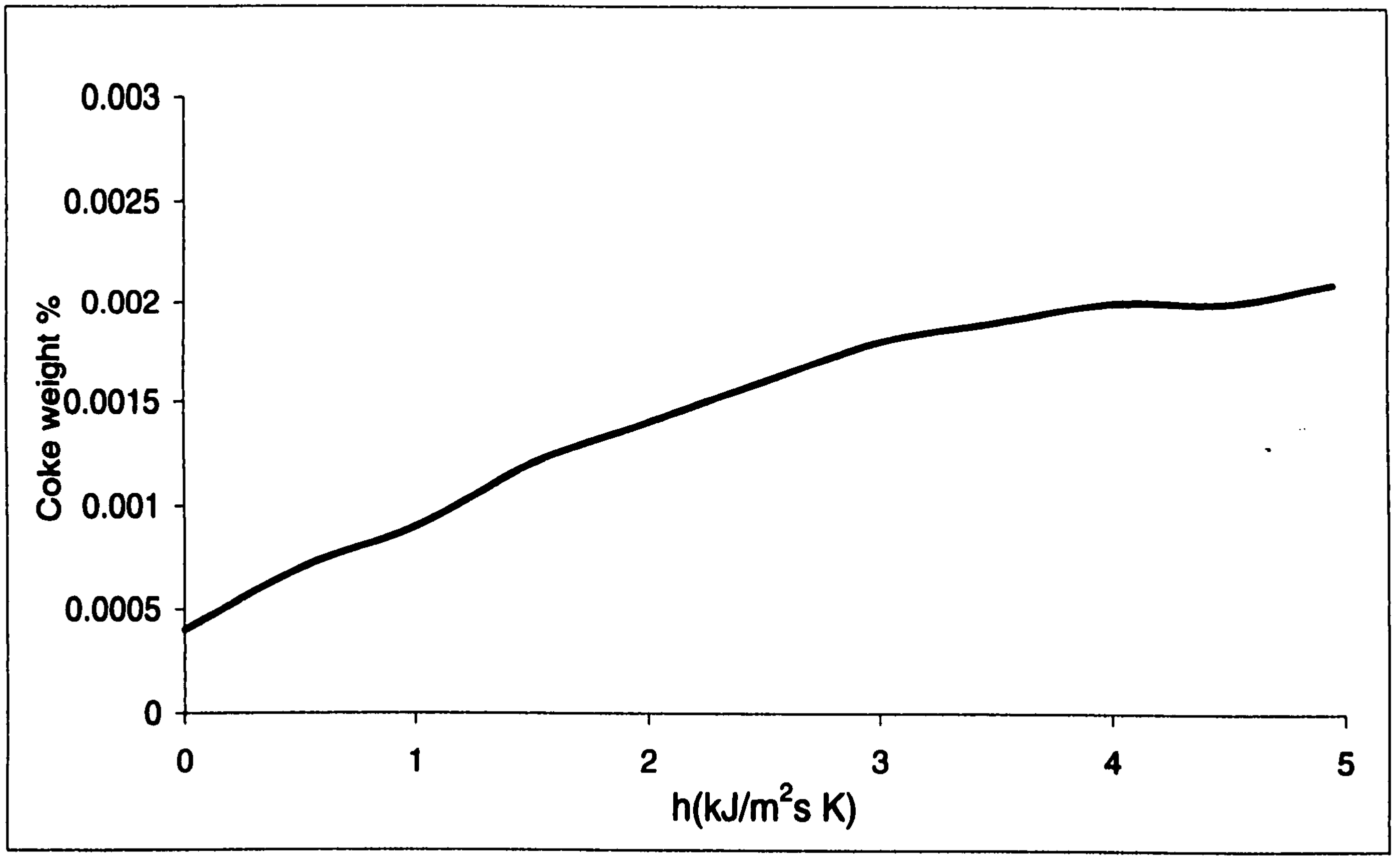

Fig. 4.44: Sensitivity of coke on regenerated catalyst to h

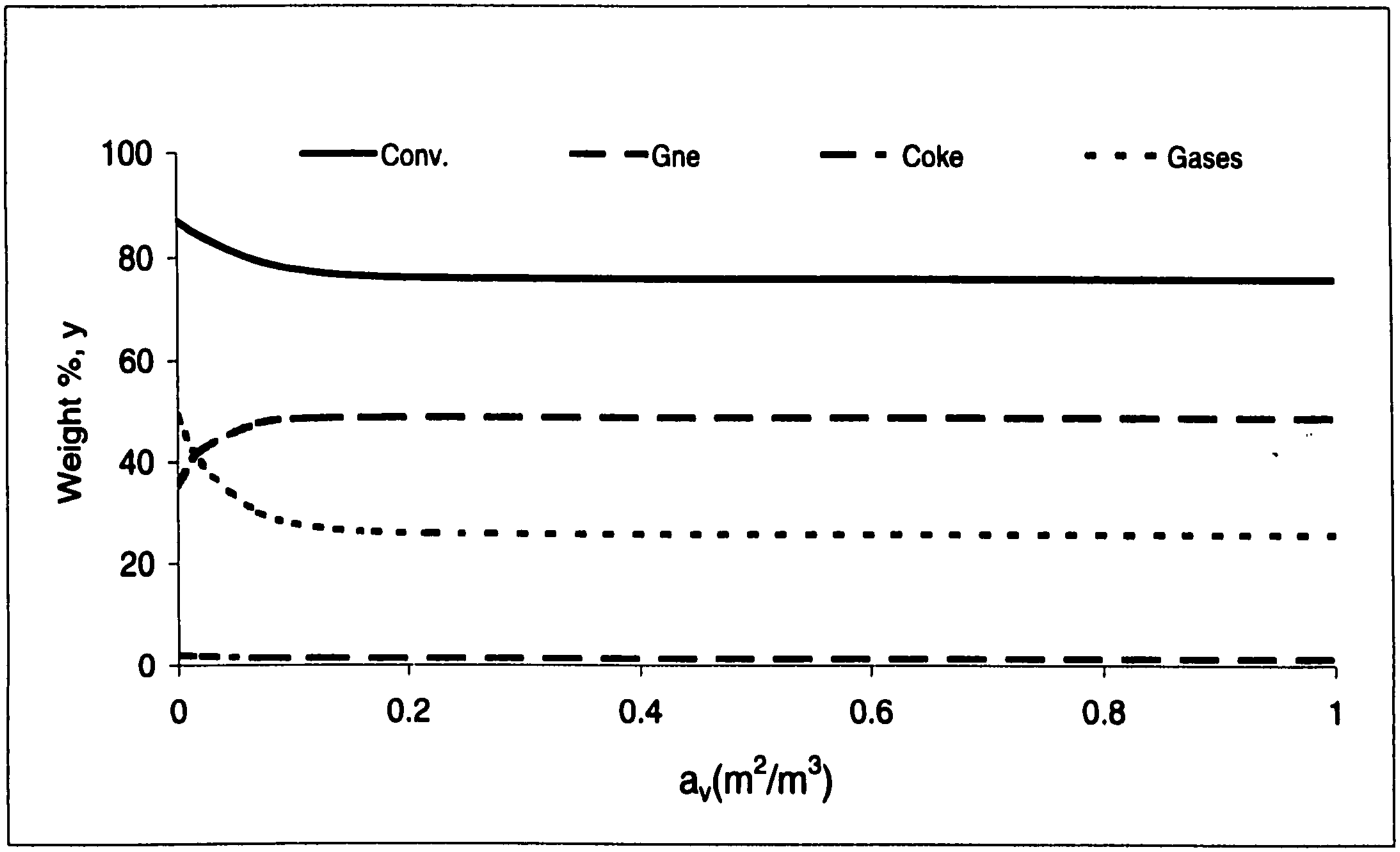

Fig. 4.45: Sensitivity of conversion of gas oil and product yields to a_v

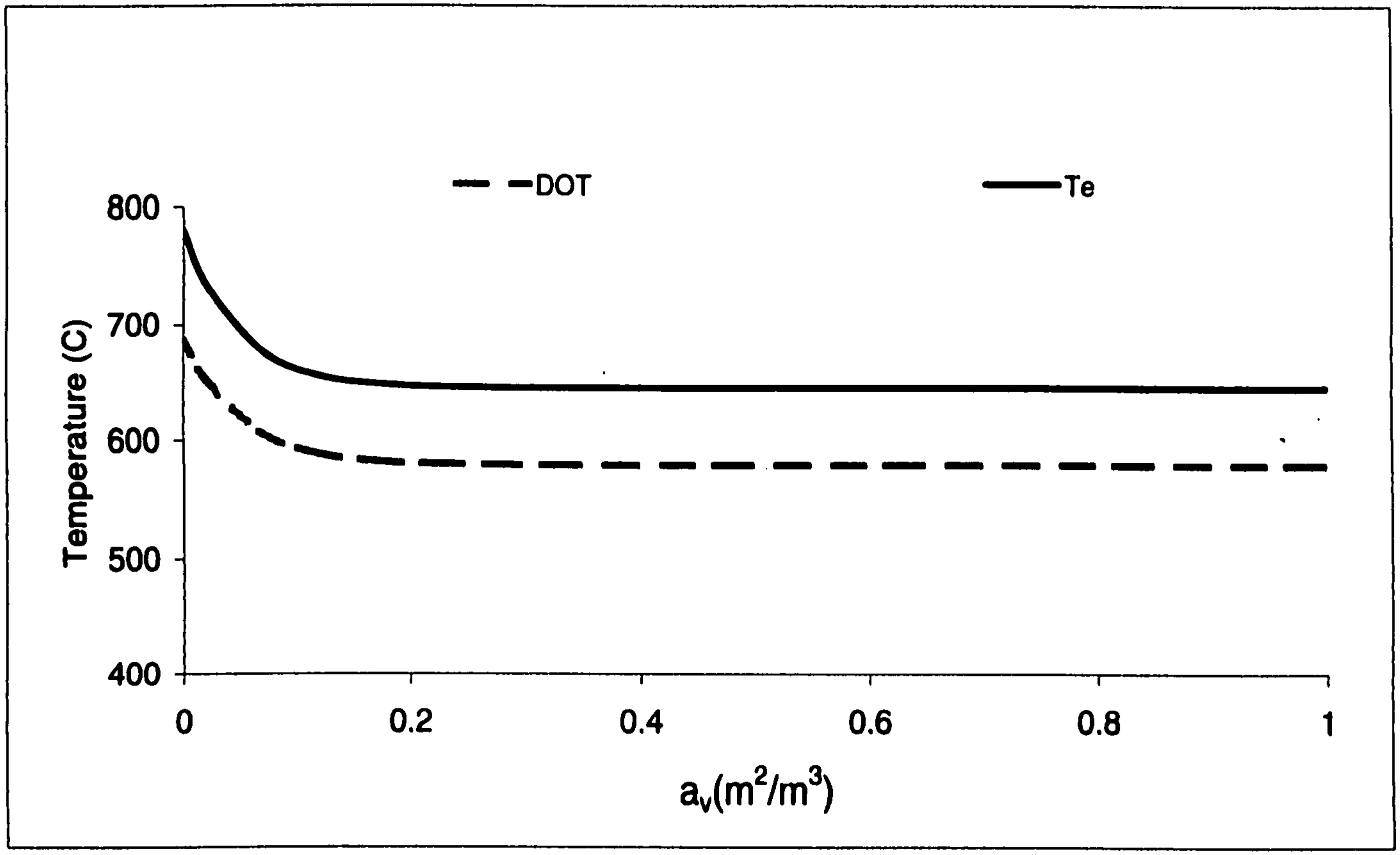

Fig. 4.46: Sensitivity of the downer outlet temperature and emulsion phase temperature(regenerator temperature) to a_v

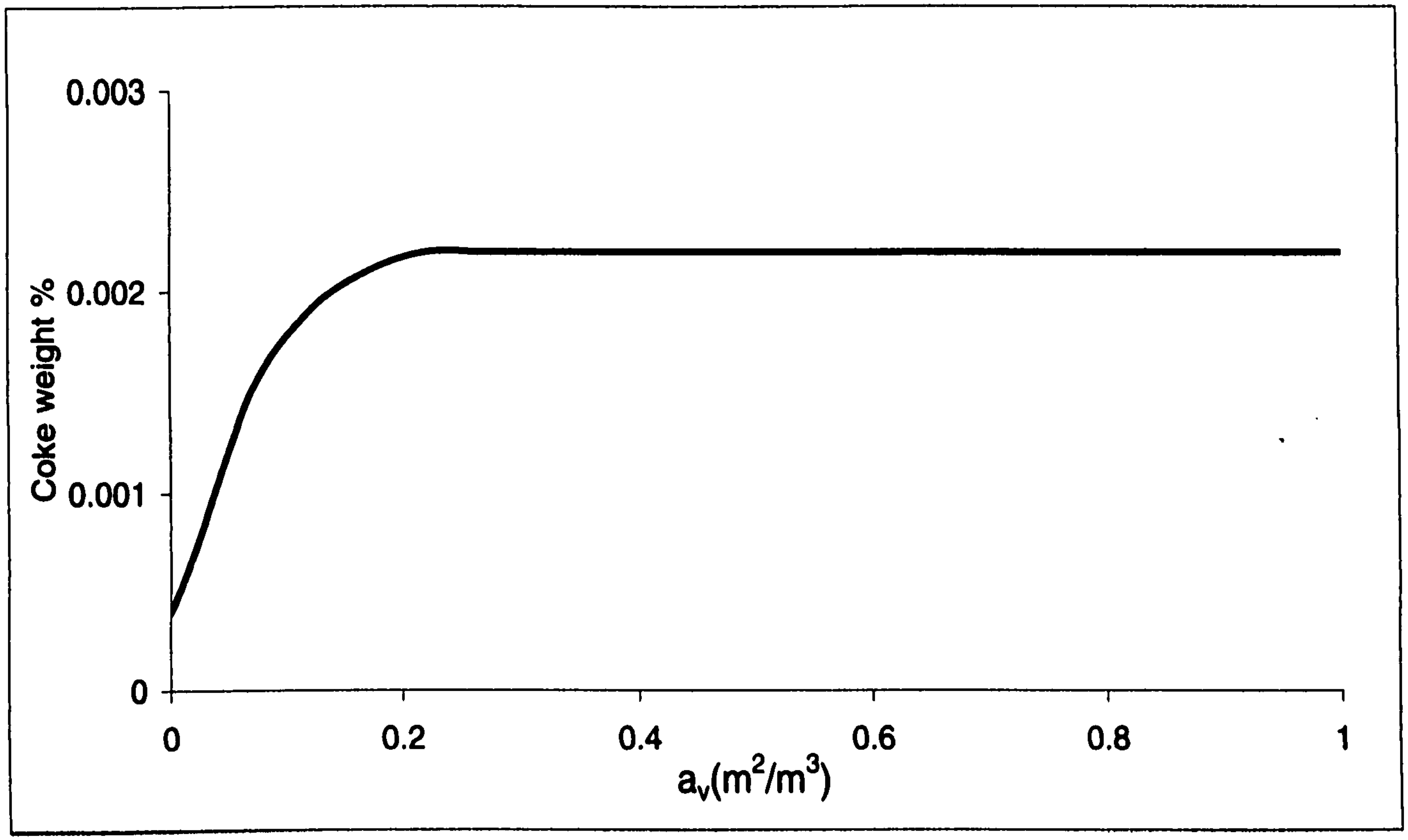

Fig. 4.47: Sensitivity of coke on regenerated catalyst to a_v

CHAPTER 5

CONCLUSIONS AND RECOMMENDATIONS

The primary objectives mentioned in Chapter 1 were fulfilled to a great extent. The research work gave good outputs and results throughout its period. Here are some conclusions and recommendations.

a) The research work resulted in the development of a new model for FCC-downer unit. The model is the first of its kind because it relates the downer with the regenerator to represent the actual performance of the whole unit. However, the previous models present in literature lack this feature. They deal only with the downer reactor without considering the role of the regenerator in the operation process. Furthermore, our model considers non-isothermal behavior in the downer while pervious models worked with isothermal assumptions inside the downer.

b) The model was verified against pilot plant data and showed good agreement. The deviations between the model results and the pilot plant data reflect that the assumptions made in deriving the model equations are reasonable.

c) The model uses four-lumped scheme for FCC cracking reaction accommodating the new researches which consider four-lumped scheme instead of three-lumped scheme as in the past.

d) The literature review reveals that more work should be done on hydrodynamics of the downer to understand some aspects which are not clear till now. For example, there is no extensive study to show the change of voidage of solids and gases versus the length of the downer.

e) The pilot plant should be operated at lower DOT such as 550°C to get more gasoline yields.

f) The pilot plant should be operated at higher DOT like 650°C if the objective is to get more olefins since operating at higher DOT gives more gases yield..

g) There are optimum designs of downer to improve gasoline yield since it is an intermediate product. For instance, at L_D of 1 m, the cross sectional area should be about 0.820 cm^2 at DOT of 600°C and 0.5 cm^2 at L_D of 2 m.

h) If the objective is to obtain olefins, it is advised to choose the downer with larger diameters and larger lengths.

i) Changing flow of air in the regenerator does not affect the performance of the unit when it is operated in complete combustion mode or in other words the air is fed in excess amount.

j) It is recommended to do more research work on the kinetics of FCC reaction to get more dependable kinetic parameters obtained under conditions similar to the operation of the FCC unit.

k) It is recommended to study the heats of cracking and coke burning reactions either theoretically by available computer packages or experimentally through thermodynamic techniques such as calorimetry.

l) It is recommended to do more investigation of computing h, k_g and a_v since they are important parameters in modeling the regenerator, and subsequently the performance of whole unit.

m) It is recommended to develop a model for FCC-riser unit and making a comparison between it and our model to prove the advantages of downer over risers claimed in the literature.

NOMENCLATURE

A		Gas oil
A_D, A_G	[m^2]	Area of the downer and the regenerator, respectively
a_v	[m^2/m^3]	Heat transfer surface area between the bubble and emulsion phases
a_b	[m^{-1}]	Bubble-emulsion interfacial area per bed volume
B		Gasoline
C		Coke
$C_{O_2,f}$	[kmol O_2/m^3]	Oxygen feed concentration
C_{ij}	[kmol/m^3]	Concentration of component i in the j phase (i = CO, CO_2, H_2O, and O_2) and j = bubble and emulsion
Cp_s	[kJ/kg.K]	Heat capacity of catalyst
Cp_a	[kJ/kg.K]	Heat capacity of air
Cp_{gD}	[kJ/kg.K]	Heat capacity of gases in the downer
Cp_{gG}	[kJ/kg.K]	Heat capacity of gases in the regenerator
D		Light hydrocarbon gases
d_p	[m]	Catalyst average particle size
d_b	[m]	Effective bubble diameter
d^*	[-]	Dimensionless measure of particle diameter
d_t	[m]	Bed or tube diameter
F_{gD}	[kg/s]	Hydrocarbon gases mass flow rate in the downer
F_{sG}	[kg/s]	Catalyst mass flow rate from in the regenerator

F_{sD}	[kg/s]	Catalyst mass flow rate in the downer
G_{IG}	[m^3/s]	Gas Flow rate in the regenerator emulsion phase
G_{CG}	[m^3/s]	Gas Flow rate in the regenerator bubble phase
g	[m/s^2]	Gravitational constant
H_{lD}	[-]	Dimensionless heat losses from the downer
H_{lG}	[-]	Dimensionless heat losses from the regenerator
h	[kJ/m^2s K]	Bubble and emulsion phases heat transfer coefficient
k_g	[s^{-1}]	Bubble and emulsion phases overall mass transfer coefficient
k_{AB}	[s^{-1}]	Reaction rate constant for cracking reaction of lump A to lump B
k_{be}	[m/s]	Mass transfer coefficient
k_c	[m^3/kmol O_2 s]	Reaction rate constant for coke burning
k_{coe}	[$(m^3)^{1.5}$/kmol $O_2{}^{0.5}$ kg of solids s]	Reaction rate constant for the catalytic CO combustion
K_{be}	[s^{-1}]	Overall coefficient of gas interchange between bubble and emulsion phase
L_D	[m]	Downer length
L_G	[m]	Regenerator bed height
M_{SG}	[kg]	Catalyst holdup in the regenerator
$M\ W_C$	[kg/kmol]	Carbon molecular weight
r_c	[kmol coke/kg cat s]	Rate of coke combustion in the regenerator bed
$r_{co,e}$	[kmol CO/kg cat s]	Rate of catalytic CO combustion in the regenerator bed

T	[-]	Dimensionless temperature
$\overline{T}_{air,f}$	[K]	Air feed temperature
$\overline{T}_f$	[K]	Fresh oil feed temperature
T_j	[-]	Dimensionless temperature of the phase j (j = bubble and emulsion) in regenerator
$\overline{T}_{ref,D}$	[K]	Reference temperature for the downer
$\overline{T}_{ref,G}$	[K]	Reference temperature for the regenerator
τ_c	[s]	Residence time in the downer; $\varepsilon_{gD} V_D/V_{gD}$
t_a	[s]	Air space time in the regenerator
U_a	[m/s]	Air velocity
U_{mf}	[m/s]	Minimum fluidization velocity
U_{br}	[m/s]	Rise velocity of a bubble with respect to the emulsion phase
U_b	[m/s]	Velocity of the bubble rising through a bed
U_o	[m/s]	Superfacial gas velocity
u^*	[-]	Dimensionless measure of particle velocity
V_D	[m^3]	Volume of the downer
V_{gD}	[m^3/s]	Volumetric flow rate of gases in the downer
W_{CG}	[kg coke/kg catalyst]	Coke mass fraction from the regenerator
W_{CD}	[kg coke/kg catalyst]	Coke mass fraction in the downer
y_j	[-]	Dimensionless weight percent of hydrocarbons in the downer, where j = A, B, C, and D

y_{ij}	[-]	Dimensionless concentration of component i in the j phase, where i = CO, CO_2, H_2O, and O_2 and j = bubble and emulsion
Z	[-]	Dimensionless axial distance in the downer, Z_D/L_D
Z_D	[m]	Axial distance in the downer
Z_G	[m]	Axial distance in the regenerator bed
z	[-]	Dimensionless axial distance in the regenerator, Z_G/L_G

Greek symbols

α	[-]	Catalyst decay coefficient
α_l		$(A_G.\varepsilon_{eG}\ (1 - \varepsilon_{bG}).L_G.k_g/G_{CG})$, see Eq. (28)
α_h		$(A_G\ .\ (1 - \varepsilon_{bG}).a_v h.L_G)/(G_{CG}\ .\ \rho_{gG}\ .\ cp_{gG})$, see Eq. (34)
σ	[kmol CO_2/kmol CO]	Instrinsic molar ratio of CO_2 to CO
δ		Bubble fraction
ΔH_{RAB}	[kJ/kg]	Heat of reaction for cracking of lump A to lump B
ΔH_{RAC}	[kJ/kg]	Heat of reaction for cracking of lump A to Lump C
ΔH_{RAD}	[kJ/kg]	Heat of reaction for cracking of lump A to lump D
ΔH_{RBC}	[kJ/kg]	Heat of reaction for cracking of lump B to lump C
ΔH_{RBD}	[kJ/kg]	Heat of reaction for cracking of lump B to lump D
ΔH_{R_c}	[kJ/kmol]	Heat of Reaction for coke burning
$\Delta H_{R_{coj}}$	[kJ/kmol]	Heat of reaction of CO combustion in the j phase, j = b refers to bubble phase and j = e refers to emulsion phase
ΔH_{vap}	[kJ/kg]	Heat of vaporization of gas oil

ε_{gD}		Hydrocarbon gases void fraction in the downer
ε_{bG}		Bubble void fraction in the regenerator bed
ε_{eD}		Emulsion phase void fraction in the regenerator
μ	[kg/(m s)]	Air viscosity
ϕ_D		Catalyst decay function
ρ_a	[kg/m^3]	Air density
ρ_b	[kg/m^3]	Catalyst bulk density
ρ_{gD}	[kg/m^3]	Density of gas phase in the downer
ρ_{gG}	[kg/m^3]	Density of gas phase in the regenerator
ρ_s	[kg/m^3]	Density of catalyst particles
θ_s		Catalyst particle sphericity

Subscripts

A	Gas oil
B	Gasoline
b	Bubble phase in regenerator
C	Coke
iD	Light gases
D	Downer
e	Emulsion phase in the regenerator
F	Feed
G	Regenerator
s	Catalyst solid particles

LITERATURE CITED

Al-Khattaf, S. and de Lasa, H., "Activity and Selectivity of Fluidized Catalytic Cracking Catalysts in a Riser Simulator: The Role of Y-Zeolite Crystal Size", Industrial Engineering & Chemistry Research, 38, 1350 (1999).

Ali, H., "Dynamic Modeling and Control of a Riser-Type Fluid Catalytic Cracking Unit", Ph.D. Thesis, University of Saskatchewan, Canada, (1995).

Ali, H. and Rohani, S., "Effect of Cracking Reactions Kinetics on the Model Predictions of an Industrial Fluid Catalytic Cracking Unit", Chemical Engineering Communications , 146, 163 (1996).

Ali, H. and Rohani, S., "Dynamic Modeling and Simulation of a Riser-Type Fluid Cataytic Cracking Unit", Chemical Engineering Technology, 20, 118 (1997).

Ali, H. and Rohani, S. and Corriou, J., "Modeling and Control of A Riser Type Fluid Catalytic Cracking (FCC) Unit", Chemical Engineering Research & Design, 75, 401 (1997).

Anameons, "Simulation and Optimization of Industrial FCC Units Using a Four-Lumped Kinetic Model", Submitted to KSU Journal;Engineering & Science (1998).

Arbel, A., Huang, Z., Rinard, I. and Shinnar, R., "Dynamic and Control of Fluidized Catalytic Crackers: 1. Mode of the Current Generation of FCC's", Industrial & Engineering Chemistry Research, 34, 1228 (1995).

Arbel, A., Huang, Z., Rinard, I. and Shinnar, R., "Dynamics and Control of Fluidized Catalytic Crackers – 2. Multiple Steady States and Instabilities", Industrial & Engineering Chemistry Research, 34, 3014 (1995).

Arbel, A., Huang, Z., Rinard, I. and Shinnar, R., "Dynamics and Control of Fluidized Catalytic Crackers – 4. The Impact of Design on Partial Control", Industrial & Engineering Chemistry Research, 36, 747 (1997).

Avidan, A. and Shinnar, R., "Development of Catalytic Cracking Technology A Lesson in Chemical Reactor Design", Industrial & Engineering Chemistry Research, 29, 931 (1990).

Blasetti, A. and de Lasa, H., "FCC Riser Unit Operated in the Heat Transfer Mode : Kinetic Modeling", Industrial & Engineering Chemistry Research, 36, 3223 (1997).

Bai, D., Zhu, J., Jin, Y., and Yu, Z., "Simulation of FCC Catalyst Regeneration in a Riser Regenerator", Chemical Engineering Journal, 71, 97 (1998).

Bai, D., Zhu, J., Jin, Y., and Yu, Z., "Novel Designs and Simulations of FCC Riser Regeneration", Industrial & Engineering Chemistry Research, 36, 4543 (1997).

Bai, D., Jin, Y., and Yu, Z. and Gan, N., "Gas-Solids Flow Patterns in a Concurrent Down Flow Fast Fluidized Bed (CDFFB)", Journal of Chemical Industry and Engineering (China), 6, 171 (1991).

Bai, D., Jin, Y., and Yu, Z. and Gan, N., "Radial Profiles of Local Concentration and Velocity in a Concurrent Down Flow Fast Fluidized Bed", in Circulating Fluidized Bed Technology III, TORONTO, 157 (1991)

Bolkan-Kenny, Y., Pugsley, T. and Berruti, F., "Computer Simulation of the Performance of Fluid Catalytic Cracking Risers and Downers", Industrial Engineering & Chemistry Research, 33, 3043 (1994).

Castiglioni, B., "How to Predict FCC Yields", Hydrocarbon Processing, 35 (1983)

Corella, J. & Frances,E. , "Modeling Some Revampings of the Riser Reactors of the FCCU's", AIChE Annual Meeting, Washington, U.S.A., (1990).

de Lasa, H., Errazu, A., Barreiro, E. and Solioz, S., "Analysis of Fluidized Bed Catalytic Cracking Regenerator Models in an Industrial Scale Unit", Canadian Journal of Chemical Engineering, 59, 549 (1981).

Ellis, R., Li, X. and Riggs, J., "Modeling and Optimization of a Model IV Fluidized Catalytic Cracking Unit", AIChE Journal, 44, 2068 (1998).

Elshishini, S., Elnashaie, S. and Alzahrani, S., "Digital Simulation of Industrial Fluid Catalytic Cracking Units-III, Effect of Hydrodynamics", Chemical Engineering Science, 47, 3152 (1992).

Elshishini, S. and Elnashaie, S., "Digital Simulation of Industrial Fluid Catalytic Cracking Units: Bifurcation and its Implications", Chemical Engineering Science, 45, 553 (1990).

Elnashaie, S. and Elshishini, S., "Comparison Between Different Mathematical Models for the Simulation of Industrial Fluid Catalytic Cracking (FCC) Units", Mathematical Computation Modeling, 18, 91 (1993).

Faltsi-Saravelou, O. and Vasalos, I., " FBSim: A Model for Fluidized Bed Simulation-I. Dynamic Modeling of an Adiabatic Reacting System of Small Gas Fluidized Particles", Computers & Chemical Engineering, 15, 639 (1991).

Faltsi-Saravelou, O., Vasalos, I. and Dinogiorgas, G. "FBSim: A Model for Fluidized Bed Simulation – II Simulation of an Industrial Fluidized Catalytic Cracking Regenerator", Computers & Chemical Engineering, 15, 647 (1991).

Filho, R., Batista, L. and Fusco, M., "A Fast Fluidized Bed Reactor for Industrial FCC Regenerator", Chemical Engineering Science, 51, 1807 (1996).

Fei, W., Xing, R., Rujin, Z., Guohua, L. and Yong, J., "A Dispersion Model for Fluid Catalytic Cracking Riser and Downer Reactors", Industrial & Engineering Chemistry Research, 36, 5049 (1997).

Forment, G. and Bischoff, K., "Chemical Reactor Analysis and Design", Wiley, New York (1990).

Gianetto, A., Farag, H., Blasetti, A. and de Lasa, H., "Fluid Catalytic Cracking Catalyst for Reformulated Gasoline Kinetic Modeling", Industrial & Engineering Chemistry Research, 33, 3053 (1994).

Grosdidier, P., Mason, A., Aitolahanti, A., Heinonen, P. and Vanhamaki, V., "FCC Unit Reactor Regenerator Control", Computers & Chemical Engineering, 17, 165 (1993).

Gross, B. and Ramage, M., "FCC Reactor With a Downflow Reactor Riser", U.S. Patent No. 4385985, (1983).

HS-FCC Project Team, "Third Progress Report", (1998).

Isnuza, F. and Martinez, R., “Dynamic Modeling of a Fluid Catalytic Cracking Unit, AIChE Annual Meeting, (1991).

Jacob, S., Gross, B., Voltz, S. and Weekman, V., “A Lumping and Reaction Scheme for Catalytic Cracking”, AIChE Journal, 22, 701 (1976).

Juraez, J., Isnuza, F., Rodriguez, E. and Sharma, R., “A Strategy for Kinetic Parameter Estimation in the Fluid Catalytic Cracking Process”, Industrial & Engineering Chemistry Research, 36, 5170 (1997).

Kumar, S., Chadha, A., Gupta, R. and Sharma, R., “CATCRACK: A process Simulator for an Integrated FCC-Regenerator System”, Industrial & Engineering Chemistry Research, 34, 3737 (1995).

Krishna, A., “Modeling the Regenerator in Commercial Fluid Catalytic Cracking Units”, Industrial Engineering & Chemistry Research, 57 (April 1985).

Kim, Y., Bangi, J. and Kim, S., “Bed-to-Wall Heat Transfer in a Downer Reactor”, Chemical Engineering Journal 77, 207 (1999).

Kim, N., Forcinito, M. and Berruti, F., “Hydrodynamic Aspects of Down Flow Gas-Solids Reactors”, AIChE Symposium Series , 93, 61(1996)

Kimm, N., Berruti, F. and Pugsley, T., “Modeling the Hydrodynamics of Downflow Gas-Solids Reactors”, Chemical Engineering Science, 51, 2661 (1996).

Kunii, D. and Levenspiel, O., “Fluidization Engineering”, Butterworth, Stoneham (1992).

Lee, E. and Groves, F., “Mathematical Model of the Fluidized Bed Catalytic Cracking Plant”, Transaction, 2, 219 (1985).

Lee, L., Chen, Y. And Huang, T., “Four Lump Kinetic Model for Fluid Catalytic Cracking Process”, Canadian Journal of Chemical Engineering, 67, 615, (1989).

Leiby, “FCC Catalyst Technologies Expand Limits of Process Capabilities”, Oil and Gas Journal, March 23, 49 (1992).

Larocca, M., Ng, S., and de Lasa, H., "Fast Catalytic Cracking of Heavy Gas Oils: Modeling Coke Deactivation", Industrial & Engineering Chemistry Research, 29, 171 (1990).

McFarlane, R., Reineman, R., Bartee, J. and Georgakis, C., "Dynamic Simulator for a Model IV Fluid Catalytic Cracking Unit", Computers & Chemical. Engineering, 17, 275 (1993).

Moorley, K. and de Lasa, H., "Regeneration of Cracking Catalyst Influence of the Homogeneous CO Post Combustion Reaction", Canadian Journal of Chemical Engineering, 66, 428 (1988).

Moorley, K. and de Lasa, H., "On the Determination of Kinetic Parameters for the Regeneration of Cracking Catalyst", Canadian Journal of Chemical Engineering, 65, 773 (1987).

Molerus, O. and Mattmann, W., "Heat Transfer Mechanisms in Gas Fluidized Beds. Part 3: Heat Transfer in Circulating Fluidized Beds", Chemical Engineering & Technology, 15, 291 (1992).

Mauleon, J. and Courcelle, J., "FCC Heat Balance Critical for Heavy Fuels", Oil and Gas Journal, October 21,64 (1985).

Ma, Y. and Zhu, J., "Characterizing Gas and Solids Distributors with Heat transfer Study in a Gas-Solids Downer Reactor", Chemical Engineering Journal, 72, 235 (1999).

Murphy, "Evolution Design Changes Mark FCC Process", Oil and Gas Journal, May 18, 49-58 (1992).

Muldowney, G., "FCC Process with Upflow and Downflow Reactor", U.S. Patent No. 5468369, (1995).

Nieuwland, J., Annaland, M., Kuipers, J., and Swaaij, W., "Hydrodynamic Modeling of Gas/Particle Flows in Riser Reactors", AIChE Journal, 42, 1569 (1996).

Pruski, J., Pekediz, A. and de Lasa, H., "Catalytic Cracking of Hydrocarbons in a novel Riser Simulator: Lump Adsorption Parameters Under Reaction Conditions", Chemical Engineering Science, 51, 1799 (1996).

Pekediz, A., Kraemer, D., Blasetti, A. and de Lasa, H., "Heats of Catalytic Cracking Determination in a Riser Simulator Reactor", Industrial & Engineering Chemistry Research, 36, 4516 (1997).

Puchyr, D., Mehrotra, A. and Behie, L., "Modeling a Circulation Fluidized Bed Riser Reactor with Gas-Solids Down Flow at the Wall", Canadian Journal of Chemical Engineering, 75, 317 (1997).

Pontier, R., Hoffman, F. and Galder, D., "Downflow Fluid Catalytic Cracking Process and Apparatus", U.S. Patent No. 5344554 (1994).

Reichle, "Fluid Catalytic Cracking Hits 50 Year Mark on the Run", Oil and Gas Journal, 20, 41 (1992).

Shaikh, A. and Carberry, J., "Model of Isothermal Transport-Line (Riser) and Moving-Bed Catalytic Reactor", Chemical Engineering Research & Design, 62, 387 (1984).

Sapre, A., Leibi, T. and Anderson, D., "FCC Regenerator Flow Model", Chemical Engineering Science, 45, 2203 (1990).

Samulesberg, A. and Hjertager, B., "Computational Modeling of Gas/Particle Flow in a Riser", AIChE Journal, 42, 1536 (1996).

Takatsuka, T. and Minami, H., " Fluid Catalytic Cracking", CH. 5 in Chemical Reaction and Design, Wiley, New York, (1998).

Takatsuka, T., Sato, S., Morimoto, Y. And Hashimoto, H., "A Reaction Model for Fluidized Bed Catalytic Cracking of Residual Oil", International Chemical Engineering, 27, 107 (1987).

Theologos, K., Nikou, A., Lygeros, A. and Markatos, N., "Simulation and Design of Fluid Catalytic – Cracking Riser– Type Reactors", AIChE Journal, 43, 486 (1997).

Thelogos, K. and Marktos, N., "Advanced Modeling of Fluid Catalytic Cracking Riser-Type Reactors", AIChE Journal, 39, 1007 (1993)

Tatrai, F., Lant, P., Lee, P., Cameron, I. and Nemell, R., "A Lumped Parameter Model for Model IV Fluid Catalytic Cracking Units", Computers & Chemical Engineering, 18, S177 (1994).

Thanamani, G., Narendran, T. and Subramanian, R., "Assessment of Availability of a Fluid Catalytic Cracking unit Through Simulation", Reliability Engineering and System Society, 47, 207 (1995).

Wang, G., Lin, S., Moi, W., Peng, C. and Yang, G., "Kinetic of Combustion of Carbon on Hydrogen in Carbonaceous Deposits on Zeolite-Type Cracking Catalysts", Industrial & Engineering Chemistry Product Research & Development, 25, 626 (1986).

Wang, Z., Bai, D. and Jin, Y., "Hydrodynamics of Cocurrent Downflow Circulating Fluidized Bed (CDCFB)", Powder Technology, 70, 271 (1992).

Wong, R., Pugsley, T. and Berruti, F., "Modeling the Axial Voidage Profile and Flow Structure in Risers of Circulating Fluidized Beds", Chemical Engineering Science, 47, 2301 (1992).

Weekman, V., "Lumps, Models and Kinetic in Practice", AIChE Monograph Series II, 75, 1 (1979).

Weekman, V. and Nace, D., "Kinetics of Catalytic Cracking Selectivity in Fixed, Moving, and Fluid Bed Reactors", AIChE Journal, 16, 396 (1970).

Wallenstein, D. and Alkemade, U., "Modeling of Selectivity Data Obtained from Microactivity Testing of FCC Catalysts", Applied Catalysis A, 137, 37 (1996).

Wei, F., Wang, Z., Jin, Y., Yu, Z. and Chen, W., "Dispersion of Lateral and Axial Solids in a Cocurrent Down Flow Circulating Fluidized Bed", Powder Technology, 81, 25 (1994).

Wei, F., Jin, Y., Yu, Z. and Liu, J., "Gas Mixing in the Cocurrent Down Flow Circulating Fluidized Bed", Chemical Engineering & Technology, 18, 59 (1995).

Wilson, J., "Fluid Catalytic Cracking Technology and Operation", PenWell, Tulsa, (1997).

Yen, L., Wrench, R. and Ong, A., "Reaction Kinetic Correlation Equation Predicts Fluid Catalytic Cracking Coke Yields", Oil and Gas Journal, January 11, 67 (1988).

Yates et al., "Experimental Observations of Voidage Distribution Around Bubbles in a Fluidized Bed", Chemical Engineering Science, 49, 1885 (1994).

Yang, Y., Jin, Y., Yu, Z. and Wang, Z., "Particle Flow Patterns in a Dilute Concurrent Up Flow and Down Flow Circulating Fluidized Bed", Fluidization VII, 66.

Zheng, Y., "Dynamic Modeling and Simulation of a Catalytic Cracking Unit, Computers & Chemical Engineering., 18, 39 (1993).

Zhu, J., Ma, Y. and Zhang, H., "Gas-Solids Contact Efficiency in the Entrance Region of A Co-Current Down Flow Fluidized Bed (Downer)", Chemical Engineering Research & Design, 77, 151 (1999).

Zhu, J., Yu, Z., Jin, Y., Grace, J. and Issangya, A., "Cocurrent Downflow Circualting Fluidized Bed (Downer) Reactors – A State of the Art Review", Canadian Journal of Chemical Engineering, 73, 662 (1995).

Zhu, J. and Wei, F., "Recent Developments of Downer Reactor and Other Types of Short Contact Time Reactors", Fluidization VIII, 501.

Zhang H., Zhu, J. ad BerGougnou, M., "Flow Development in a Gas Solids Downer Fluidized Bed", The Canadian Journal of Chemical Engineering, 77, 194 (1999).

APPENDIX A

DETAILED DERIVATION OF THE DOWNER MODEL EQUATIONS

A.1 Downer Material Balance

Gas Oil (A)

$$F_{gD}\; y_A \Big|_{Z_D} - F_{gD}\; y_A \Big|_{Z_D + \Delta Z_D} = \left[(A_D\; \Delta Z_D)\,\varepsilon_{gD}\right]\rho_{gD}\,\left[\phi_D\,(-r_D)\right] \qquad \text{(A.1.1)}$$

Divide by ΔZ_D

$$\frac{F_{gD}\left[y_A \big|_{Z_D} - y_A \big|_{Z_D + \Delta Z_D}\right]}{\Delta Z_D} = A_D\;\; F_{gD}\; \rho_{gD}\,\phi_D\,(-r_A) \qquad \text{(A.1.2)}$$

Taking the limit at ΔZ approaches zero

$$-F_{gD}\frac{dy_A}{dZ_D} = A_D\;\; \varepsilon_{gD}\,\rho_{gD}\,\phi_D\,(-r_A) \qquad \text{(A.1.3)}$$

Normalizing Z_D by length of the downer L_D to obtain the dimensionless form:

$$\frac{F_{gD}}{L_D}\;\frac{dy_A}{d(Z_D/L_D)} = A_D\,\varepsilon_{gD}\,\rho_{gD}\,\phi_D\,(-r_A)$$

or $$-F_{gD}\frac{dy_A}{dZ} = A_D\,L_D\,\varepsilon_{gD}\,\rho_{gD}\,\phi_D\,(-r_A) \qquad \text{(A.1.4)}$$

Substitute for the gas oil reaction term ($-r_A$),

$$-F_{gD}\frac{dy_A}{dZ} = A_D\,\varepsilon_{gD}\,\rho_{gD}\,\phi_D\left[k_{AB}+k_{AC}+k_{AD}\right]y_A^2 \tag{A.1.5}$$

So, the mass balance of gas in the downer in its final form is:

$$\frac{dy_A}{dZ} = -\frac{A_D\,L_D\,\varepsilon_{gD}\,\rho_D\,\phi_D}{F_{gD}}\left[k_{AB}+k_{AC}+k_{AD}\right]y_A^2 \tag{A.1.6}$$

Gasoline (B)

$$F_{gD}\,y_B\Big|_{Z_D} - F_{gD}\,y_B\Big|_{Z_D+\Delta Z_D} = \left[A_D\;\Delta_{Z_D}\;\varepsilon_{gD}\right]\rho_{gD}\left[\phi_D(-r_A)\right] \tag{A.1.7}$$

Dividing by Δ_{Z_D} and taking the limit giving :

$$-F_{gD}\frac{dy_B}{dZ_D} = A_D\,\varepsilon_{gD}\,\phi_D\,(-r_B) \tag{A.1.8}$$

Normalizing Z_D by L_D to give the dimensionless form:

$$\frac{-F_{gD}}{L_D}\frac{dy_B}{dZ} = A_D\,\varepsilon_{gD}\,\rho_{gD}\,\phi_D\,(-r_B) \tag{A.1.9}$$

rearranging

$$F_{gD}\frac{dy_B}{dZ} = A_D\,L_D\,\varepsilon_{gD}\,\rho_{gD}\,\phi_D\,(-r_B) \tag{A.1.10}$$

or

$$\frac{dy_B}{dZ} = -\frac{A_D\,L_D\,\varepsilon_{gD}\,\rho_{gD}\,\phi_D}{F_{gD}}(-r_B) \tag{A.1.11}$$

Substitute for the gasoline reaction term ($-r_B$) to give the final form of gasoline mass balance:

$$\frac{dy_B}{dZ} = \frac{-A_D L_D \varepsilon_{gD} \rho_{gD} \phi_D}{F_{gD}} \left[k_{AB} y_A^2 - (k_{BC} + k_{BD}) y_B\right]$$

Coke (C)

Doing the similar deviation as gas oil and gasoline, the coke mass balance in the downer is :

$$\frac{dy_C}{dZ} = \frac{-A_D L_D \varepsilon_{gD} \rho_{gD} \phi_D}{F_{gD}} (-r_C) \qquad \text{(A.1.13)}$$

The final form after substituting ($-r_C$) is:

$$\frac{dy_C}{dZ} = \frac{A_D L_D \varepsilon_{gD} \rho_{gD} \phi_D}{F_{gD}} \left[k_{AC} y_A^2 + k_{BC} y_B\right] \qquad \text{(A.1.14)}$$

Gases (D)

Similarly as before:

$$\frac{dy_D}{dZ} = \frac{-A_D L_D \varepsilon_{gD} \rho_{gD} \phi_D}{F_{gD}} (-r_D) \qquad \text{(A.1.15)}$$

or in final form as:

$$\frac{dy_D}{dZ} = \frac{A_D L_D \varepsilon_{gD} \rho_{gD} \phi_D}{F_{gD}} \left(+ k_{AD} y_A^2 + k_{BD} y_B\right) \qquad \text{(A.1.16)}$$

A.2 Downer Energy Balance

For plug flow assumption, the heat balance is:

$$U_o \rho C_p \frac{d\bar{T}}{dZ} = -(\pm \Delta H)(-r_A) \tag{A.2.1}$$

when it is applied to the FCC reaction in the downer:

$$\begin{aligned} &\left(F_{gD} C_{P_{gD}} + C_{P_S}\right)\frac{d\bar{T}}{dZ_D} \\ &= -\Sigma \phi_D (+\Delta H_i)(-r_A)_i * A_D \varepsilon_{gD} \rho_{gD} - H_{\ell D} \end{aligned} \tag{A.2.2}$$

Normalize T by T_{ref_D} and Z by L_D to give:

$$\left(F_{gD} C_{P_{gD}} + F_{S_D} C_{P_S}\right)\frac{T_{ref_D}}{L_D}\frac{dT}{d_Z} = -A_D \varepsilon_{gD} \rho_{gD} \phi_D \, \Sigma(\Delta H_i)(-r_i) - H_{\ell D}$$

or in other form

$$\begin{aligned} \frac{dT_D}{dZ} = &\frac{-A_D L_D \varepsilon_{gD} \rho_{gD} \phi_D}{\left(F_{gD} C_{P_{gD}} + F_{gD} C_{P_S}\right)T_{ref_D}} \Sigma(\Delta H_i)(-r_i) \\ &- \frac{H_{lD} L_D}{\left(F_{gD} C_{P_{gD}} + F_{gD}\right)T_{ref_D}} \end{aligned} \tag{A.2.3}$$

where :

$$\begin{aligned} \Sigma(\Delta H_i)(-r_i) = &\left(\Delta H_{AB} k_{AB} + \Delta H_{AC} k_{AC} + \Delta H_{AD} k_{AD}\right) y_A^2 \\ &+ \left(\Delta H_{BC} k_{BC} + \Delta H_{BD} k_{BD}\right) y_B^2 \end{aligned}$$

So, the heat balance in the downer in its final forms is:

$$\frac{dT_D}{dZ} = \frac{-A_D L_D \varepsilon_{gD} \rho_{gD} \phi_D}{\left[F_{gD} C_{P_{gD}} + F_{gD} C_{P_S}\right] T_{ref_D}} \begin{bmatrix} (\Delta H_{AB} k_{AB} + \Delta H_{AC} k_{AC} + \Delta H_{AD} k_{AD})y_A^2 \\ +(\Delta H_{BC} k_{BC} + \Delta H_{BD} k_{BD})y_B^2 \end{bmatrix} - \frac{H_{lD} L_D}{\left(F_{gD} C_{P_{gD}} + F_{gD}\right) T_{ref_D}} \tag{A.2.4}$$

APPENDIX B

DETAILED DERIVATION OF THE REGENERATOR MODEL EQUATIONS

B.1 Material Balances in Bubble Phase

B.1.1 CO Material Balance

$$L_G\left[+(U_a-U_{mf})A_G\frac{d\,C_{CO,b}}{d_{Z_G}}\right]=V_{gas}\,k_g\left(C_{CO,e}-C_{CO,b}\right) \tag{B.1.1}$$

Normalizing as follows:

$$z\equiv\frac{Z_G}{L_G}\ \&\ y_{CO}=\frac{C_{CO}}{C_{O_2,f}}$$

Equation (B.1.1) becomes :

$$\left(U_a-U_{mf}\right)A_G\ \frac{dy_{O_2,b}}{dZ}=V_{gas}\,k_g\left(y_{CO,e}-C_{CO,b}\right) \tag{B.1.2}$$

Where $V_{gas}=\frac{V_{gas}}{V_e}\frac{V_e}{V_G}V_G=\varepsilon_{eg}\ (1-\varepsilon_{bG})(A_G\,L_G)$

Substituting in equation (B.1.2) to give:

$$\underbrace{\left(U_a - U_{mf}\right)}_{G_{CG}} \frac{dy_{CO,b}}{dZ} = \varepsilon_{eG}\left(1 - t_{bG}\right) A_G\, L_G\, k_g \left(y_{CO,e} - y_{CO,b}\right) \quad \text{(B.1.3)}$$

Rearranging

$$\frac{dy_{COb}}{dz} = \frac{A_G\, L_G\, \varepsilon_{eG}\left(1-\varepsilon_{bG}\right)}{G_{CG}}\, k_g \left(y_{COe} - y_{COb}\right) \quad \text{(B.1.4)}$$

Integrating :

$$\int_{y_{CO,f}}^{y_{CO,b}} \frac{dy_{CO,b}}{\left(y_{CO,e} - y_{CO,b}\right)} = + \underbrace{\frac{A_G\, L_G\, \varepsilon_{eG}\left(1-\varepsilon_{bG}\right) k_g}{G_{CG}}}_{\alpha_1} \int_{O}^{Z} dZ$$

its solution:

$$\ell n\left(y_{COb} - y_{COe}\right) \Bigg|_{y_{COf}}^{y_{COb}} = + \alpha_1\, z \quad \text{(B.1.5)}$$

or :

$$\ell n\, \frac{\left(y_{CO,b} - y_{CO,e}\right)}{\left(y_{CO,f} - y_{CO,e}\right)} = \alpha_1\, z \quad \text{(B.1.6)}$$

The final form of CO material balance in the bubble phase is:

$$y_{CO,b} = y_{CO,e} + \left(y_{CO,f} - y_{CO,e}\right) \bar{e}^{\alpha_1 z} \quad \text{(B.1.7)}$$

B.1.2 O_2 Material Balance

$$L_G\left[-(U_a-U_{mf})A_G\,\frac{dC_{O_2,b}}{dZ_G}\right]=V_{gas}\;k_g\left(C_{O_2,b}-C_{O_2,e}\right)\qquad\text{(B.1.8)}$$

Normalizing as follows:

$$z\equiv\frac{Z_G}{L_G}\;\; and \;\; y_{O_2}\equiv\frac{C_{O2}}{C_{O2},f}$$

to give the dimensionless form:

$$\underbrace{-\left(U_a-U_{mf}\right)A_G}_{G_{CG}}\;\frac{d_{y_{O_2,b}}}{d_z}=V_{gas}\;kg\left(y_{O_2,b}-y_{O_2,e}\right)\qquad\text{(B.1.9)}$$

or

$$\frac{-dy_{O_2,b}}{dz}=\frac{A_G\,L_G\,\varepsilon_{eG}\left(1-\varepsilon_{bG}\right)}{G_{CG}}\left(y_{O_2,b}-y_{O_2,e}\right)\qquad\text{(B.1.10)}$$

Integrating to give the final form of O_2 mass balance in the bubble phase:

$$y_{O_2,b}=y_{O_2,e}+\bar{e}^{\alpha_1 z}\left(y_{O_2,f}-y_{O_2,e}\right)\qquad\text{(B.1.11)}$$

B.2 Material Balances in Emulsion Phase

B.2.1 Carbon Balance

Coke enters with weight %, W_{CD}, and leaves regenerator with W_{CG} while its reaction rate is

$$-r_C = k_C \, W_{CG} \, C_{O_2,e} \tag{B.2.1}$$

The mass balance on coke on the catalyst in the regenerator is:

$$F_{SG} \, W_{CD} - F_{SG} \, W_{CG} = V_{SG} \, \rho_S \, (-r_C) \tag{B.2.2}$$

where V_{SG} = volume of solid catalyst in regenerator

$$= V_G \left[\frac{V_e}{V_G} - \frac{V_s}{V_e} \right] =$$

$$= V_G \, (1 - \varepsilon_{bG}) \, (1 - \varepsilon_{eG}) \tag{B.2.3}$$

Substituting in B.2.2 to give:

$$\begin{aligned} F_{SG} \, (W_{CD} - W_{CG}) &= V_G \, (1 - \varepsilon_{bG})(1 - \varepsilon_{eG}) \rho_S \, (-r_C) \\ &= A_G \, L_G \, (1 - \varepsilon_{bG})(1 - \varepsilon_{eG}) \rho_S \left(k_C \, W_{CG} \, C_{O_2,e} \right) \end{aligned} \tag{B.2.4}$$

Normalizing $C_{O_2,e}$ by oxygen feed concentration $C_{O_2,f}$ as:

$$y_{O_2,e} = \frac{C_{O_2,e}}{C_{O_2,f}}$$

So carbon balance in emulsion phase is:

$$F_{SG} \, (W_{CD} - W_{CG}) = A_G \, L_G \, (1 - \varepsilon_{bG})(1 - \varepsilon_{eG}) \rho_S \, C_{O_2,f} \, k_C \, W_{CG} \, y_{O_2,e} \tag{B.2.5}$$

B.2.2 CO Balance

The sources of CO to emulsion phase as by flow and as a product from burning reactions, mathematically as:

$$
\begin{aligned}
C_{CO,f} + [& k_{CO,e}\, C_{CO,e}\, C_{O_2,e}^{.5}\, A_G\, L_G\, (1-\varepsilon_{bG})\varepsilon_{eG}\,\rho_b \\
& - k_C \left(\frac{1}{1+\sigma}\right) W_{CG}\, C_{O_2,e}\, A_G\, L_G\, (1-\varepsilon_{bG})(1-\varepsilon_{eG})\rho_S]
\end{aligned}
$$

and CO out from the emulsion phase by flow and by mass transfer to the bubble phase, mathematically as:

$$
(U_{mf}\, A_G) C_{CO,e} + A_G\, (1-\varepsilon_{bG})\varepsilon_{eG} \int_O^{L_G} k_g\, (C_{CO,e} - C_{CO,b})\, dz_G
$$

So In = Out gives:

$$
(U_{mf}\, A_G) C_{CO,f} + A_G\, L_G (1-\varepsilon_{bG}) \begin{bmatrix} \varepsilon_{eG}\, \rho_b\, k_{CO,e}\, C_{CO,e}\, C_{CO,e}^{.5} \\ -(1-\varepsilon_{eG})\rho_S\, k_C \left(\dfrac{1}{1+\sigma}\right) W_{CG}\, C_{O_2,e} \end{bmatrix}
$$

$$
= (U_{mf}\, A_G) C_{CO,e} + A_G (1-\varepsilon_{bG})\varepsilon_{eG} \int_O^{L_G} k_g\, (C_{CO,e} - C_{CO,b})\, dz_G \qquad \text{(B.2.6)}
$$

Normalize Z_G by L_G and concentrations by $C_{O_2,f}$ as

$$
z = \frac{Z_G}{L_G} \; ; \; y \equiv \frac{C}{C_{O_2,f}}
$$

$$C_{O_2,f}\ U_{mf}\ y_{CO,f} + L_G\ (1-\varepsilon_{bG})\begin{bmatrix}\varepsilon_{eG}\,\rho_b\,k_{CO,e}\,C_{CO,e}\,C_{O_2,f}^{1.5}\ y_{CO,e}\ y_{O_2,e}^{.5} \\ -(1-\varepsilon_{eG})\rho_S\,k_C\,C_{O_2,f}\left(\dfrac{1}{1+\sigma}\right)W_{CG}\,y_{O_2,e}\end{bmatrix}$$

$$= C_{O_2,f}\ U_{mf}\ y_{CO,e} + (1-\varepsilon_{bG})(\varepsilon_{eG})C_{O_2,f}\ L_G \int_O^1 k_g\ \left(y_{CO,e} - y_{CO,b}\right)dZ \qquad \text{(B.2.7)}$$

Solving The Integral is solved as follows:

$$\int_O^1 k_g\left(y_{CO,e} - y_{CO,b}\right)dZ$$

$$= k_g \int_O^1 \left[y_{CO,e} - y_{CO,e}\left(y_{CO,f} + y_{CO,e}\right)\bar{e}^{\alpha_1 Z}\right]dZ$$

$$= -k_g \int_O^1 \left(y_{CO,f} - y_{CO,e}\right)\bar{e}^{\alpha_1 Z}\ dZ$$

$$= \frac{-k_g\ \left(y_{CO,f}\ -\ y_{CO,e}\right)}{-\alpha_1}\ \bar{e}^{\alpha_1 Z}\ \Big|_O^1$$

$$= \frac{k_g\ \left(y_{CO,f}\ - y_{CO,e}\right)}{\alpha_1}\ \left(e^{-\alpha_1} - 1\right)$$

Equation B.2.7 becomes:

$$U_{mf}\ \left(y_{CO,f} - y_{CO,e}\right) + L_G\ (1-\varepsilon_{bG})\varepsilon_{eG}\,\rho_b\ k_{CO,e}\,C_{O_2,f}^{.5}\ y_{CO,e}\ y_{O_2,e}^{.5}$$

$$-\ L_G(1-\varepsilon_{bG})(1-\varepsilon_{eG})\,\rho_S\quad k_C\left(\frac{1}{1+\sigma}\right)W_{CG}\ \ y_{O_2,e}$$

$$= \frac{G_{CG}}{A_G}\left(y_{CO,f} - y_{CO,e}\right)\left(\bar{e}^{\alpha_1} - 1\right) \tag{B.2.8}$$

After rearrangement:

$$\left(y_{CO,f} - y_{CO,e}\right)\left[U_{mf} - \frac{\left(U_{mf} - U_a\right)A_G}{A_G}\left(\bar{e}^{\alpha_1} - 1\right)\right]$$

$$+ L_G\left(1 - \varepsilon_{bG}\right)\varepsilon_{eG}\,\rho_b\,k_{CO,e}\,C_{O_2,f}^{.5}\;y_{CO,e}\,y_{O_2,e}^{.5}$$

$$- L_G\left(1 - \varepsilon_{bG}\right)\left(1 - \varepsilon_{eG}\right)\rho_S\;k_C\left(\frac{1}{1+\sigma}\right)W_{CG}\;y_{O_2,e} = 0 \tag{B.2.9}$$

or:

$$+ A_G L_G\left(1 - \varepsilon_{bG}\right)\varepsilon_{eG}\,\rho_b\,k_{CO,e}\,C_{O_2,f}^{.5}\;y_{CO,e}\,y_{O_2,e}^{.5}$$

$$- A_G\,L_G\left(1 - \varepsilon_{bG}\right)\left(1 - \varepsilon_{eG}\right)\rho_S\;k_C\left(\frac{1}{1+\sigma}\right)W_{CG}\;y_{O_2,e} = 0 \tag{B.2.10}$$

as substituting G_{IG} *and* G_{CS} : $G_{IG} = U_{mf}\;A_G$ *and* $G_{CG} = \left(U_a - U_{mf}\right)A_G$

to give the final equation of CO balance in emulsion phase is :

$$\frac{\left[G_{IG} + G_{CG}\left(1 - \bar{e}^{\alpha_1}\right)\right]}{A_G\;L_G\left(1 - \varepsilon_{bG}\right)\varepsilon_{eG}}\left(y_{CO,f} - y_{CO,e}\right)$$

$$- L_G\,\frac{\left(1 - \varepsilon_{eG}\right)}{\varepsilon_{eG}}\,\rho_S\;k_C\left(\frac{1}{1+\sigma}\right)W_{CG}\;y_{O_2,e}$$

$$+ L_G\;\rho_b\,k_{CO,e}\;C_{O_2,f}^{.5}\;y_{CO,e}\;y_{O_2,e}^{.5} \tag{B.2.11}$$

B.2.3 O_2 Balance

Derivation is similar to CO, but here:

$$(-r_{O_2}) = k_C\left(\frac{2\alpha + 1}{2\alpha + 2}\right)W_{CG}\, C_{O_2,e} + \frac{k_{CO,e}\, C_{CO,e}\, C^{.5}_{O_2,e}}{2} \qquad \text{(B.2.12)}$$

Mass transfer is vise versa (i.e., from bubble phase to emulsion phase). The final from of O_2 materials balance in emulsion phase will be:

$$\frac{\left[G_{IG} + G_{CG}\left(1 - \bar{e}^{\alpha_1}\right)\right]}{A_G\, L_G\, (1 - \varepsilon_{bG})\varepsilon_{eG}}\left(y_{CO,f} - y_{CO,e}\right) =$$

$$\frac{L_G\, \rho_b\, \left(k_{CO,e}\;\; C^{.5}_{O_2,f}\right) y_{CO,e}\;\; y^{.5}_{O_2,e}}{2}$$

$$+ \; L_G\, \frac{(1 - \varepsilon_{eG})}{\varepsilon_{eG}}\, \rho_S\; k_C\left(\frac{2}{2 + \sigma}\right)W_{CG}\;\; y_{O_2,e} \qquad \text{(B.2.13)}$$

B.3 Energy Balance

B.3.1 Energy Balances in Bubble Phase

$$\left[(U_a - U_{mf})L_G\, A_G\right]\rho_{gG}\, C_{p_{gG}}\, \frac{d\bar{T}_e}{dz} = V_e\, a_v\, h\left(\bar{T}_e - \bar{T}_b\right) \qquad \text{(B.3.1)}$$

Normalizing Z_G by Z and temperature by $\bar{T}_{refG}$ to give:

$$G_{CG}\;\rho_{gG}\;C_{p_{gG}}\,\frac{dT_b}{dz} = (1 - \varepsilon_{bG})\, L_G\, A_G\, a_v h(T_e - T_b) \qquad \text{(B.3.2)}$$

rearranging:

$$\frac{d\,T_b}{d_Z} = \frac{(1-\varepsilon_{bG})\,L_G\,A_G\,a_v h}{G_{CG}\;\rho_{gG}\;C_{P_{gG}}}\,(T_e - T_b) \tag{B.3.3}$$

$$Let\;\alpha_h = \frac{(1-\varepsilon_{bG})\,L_G\,A_G\,a_v h}{G_{CG}\;\rho_{gG}\;C_{P_{gG}}}$$

Equation (B.3.3) becomes:

$$\frac{d\,T_b}{d_Z} = \alpha_h\;(T_e - T_b) \tag{B.3.4.}$$

Integrating:

$$\int_{T_{airf}}^{T_b} \frac{d\,T_b}{(T_e - T_b)} = \int_O^1 \alpha_h\,d_Z$$

is

$$-\left[\ell n\,\frac{T_e - T_b}{T_e - T_{airf}}\right] = \alpha_h\;z$$

or

$$T_e - T_b = \bar{e}^{\alpha_h Z}\;\left[T_e - T_{airf}\right]$$

or

$$T_b = T_e - \;\bar{e}^{\alpha_h Z}\;\left[T_e - T_{airf}\right]$$

or

$$T_b = T_e + \;\bar{e}^{\alpha_h Z}\;\left[T_{airf} - T_e\right] \tag{B.3.5}$$

noting that $T_{airf} = 1$, energy balance in the bubble in its final form:

$$T_b = T_e + \bar{e}^{\alpha_h Z} \left[1 - T_e\right] \qquad \text{(B.3.6)}$$

B.3.2 Energy Balance in Emulsion Phase

In emulsion phase:

Heat in are - by air flow
- by reactions
- by solid flow

Heat out are - by air flow
- by heat transfer to bubble phase
- by solid flow
- by losses to surroundings

$$\text{In} = \begin{array}{l} G_{IG}\, \rho_{gG}\, C_{P_{gG}}\, \overline{T}_{airf} + \left\{L_G\, A_G\, (1-\varepsilon_{bG})\varepsilon_{bG}\, \rho_b\, (-r_{CO,e})(-\Delta H_{R,CO}) + M_{SG}\, (-r_C) - (\Delta H_{RO})\right\} \\ \qquad + F_{SG}\, C_{P_S}\, \overline{T}_D \end{array}$$

$$\text{Out} = G_{IG}\, \rho_{gG}\, \overline{T}_e + A_G\, (1-\varepsilon_{bG}) \int_O^{L_G} a_v h\, \left(\overline{T}_e - \overline{T}_b\right) d_{Z_G} + F_{SG}\, C_{P_S}\, \overline{T}_e\, \overline{H}_{\ell G}$$

In = Out $\Rightarrow$

with $T = \dfrac{\overline{T}_j}{\overline{T}_{refG}}$ *and* $z \equiv \dfrac{Z_G}{L_G}$

$$\Rightarrow G_{IG}\, \rho_{gG}\, C_{P_{gG}}\, \overline{T}_{refG}\, \left(T_{airf} - T_e\right) + \left\{R_{xns}\right\}$$

$$+ F_{SG}\, C_{P_S}\, \overline{T}_{refG}\, \left(T_D - T_e\right)$$

$$= A_G\,(1-\varepsilon_{bG})\int_o^1 L_G\, a_v h\ \overline{T}_{refG}\,(T_e - T_b)\,d_Z \qquad \text{(B.3.7)}$$
$$+\ \overline{H}_{\ell G}$$

Solving the integral:

$$\int_o^1 (T_e - T_b)d_Z = -\int_o^1 e^{-\alpha_h Z}\left[T_{airf} - T_e\right]d_Z$$

$$= \frac{(T_{airf} - T_e)}{\alpha_h}\left(e^{-\alpha_h} - 1\right)$$

$$= \frac{(T_{airf} - T_e)G_{CG}\,\rho_{gG}\,C_{P_{gG}}}{(1-\varepsilon_{bG})L_G\,A_G\,a_v h}\left(e^{-\alpha_h} - 1\right)$$

Equation (B.3.7) will be :

$$G_{IG}\,\rho_b\,C_{P_{gG}}\,(T_{airf} - T_e) + F_{SG}\,C_{P_S}\,(T_D - T_e)$$

$$+\ \frac{1}{\overline{\overline{T}}_{refG}}\left\{\begin{matrix} L_G\,A_G\,(1-\varepsilon_{bG})\varepsilon_{eG}\,\rho_b\,k_{CO,e}\,C^{1.5}_{O_2,f}\ y_{CO,e}\ y^{.5}_{O_2,e}\left(-\Delta H_{R,CO}\right) \\ +\,M_{SG}\left[k_C\,W_{CG}\,(C_{O_2,f})y_{O_2,e}\right]\left(-\Delta H_{R_C}\right) \end{matrix}\right\}$$

$$= G_{CG}\,\rho_{gG}\,C_{P_{gG}}\,(T_{airf} - T_e)\left(e^{-\alpha_h} - 1\right) + \frac{\overline{H}_{\ell_G}}{\overline{\overline{T}}_{refG}} \qquad \text{(B.3.8)}$$

or

$$\frac{\left[G_{IG} - G_{CG}\left(e^{-\alpha_h} - 1\right)\right]\rho_{gG}\,C_{P_{gG}}}{F_{SG}\,C_{P_S}}\,(T_{airf} - T_e)$$

$$+\ (T_D - T_e) + \frac{1}{\overline{\overline{T}}_{refG}\,F_G\,C_{P_S}}\left\{\begin{matrix} L_G\,A_G\,(1-\varepsilon_{bG})\varepsilon_{eG}\,\rho_b\,k_{CO,e}\,C^{1.5}_{O_2,f}\ y_{CO,e}\ y^{.5}_{O_2,e}\left(-\Delta H_{R,CO}\right) \\ +\,M_{SG}\,k^*_C\,W_{CG}\,C_{O_2,f}\ y_{O_2,e}\left(-\Delta H_{R,C}\right) \end{matrix}\right\}$$

$$- \frac{\overline{H}_{\ell G}}{\overline{T}_{refG} \; F_{SG} \, C_{P_S}} \tag{B.3.9}$$

Since $\overline{T}_{refG} = \overline{T}_{airf}$

$\therefore T_{airf} = 1$

The final form will be :

$$\begin{aligned} &\frac{\left[G_{IG} - G_{CG}\left(\overline{e}^{\alpha_h} - 1\right)\right]\rho_{gG} \, C_{P_{gG}}}{F_{SG} \; C_{P_S}} (1 - T_e) + (T_D - T_e) \\ &+ \frac{L_G \, A_G \, (1 - \varepsilon_{bG})\varepsilon_{bG} \, \rho_b}{\overline{T}_{refG} \; F_{SG} \, C_{P_S}} \left[k_{CO,e} \, C_{O_2,f}^{1.5} \; y_{CO,e} \, y_{O_2,e}^{.5}\right]\left(-\Delta H_{R,CO}\right) \\ &+ \frac{M_{SG}}{\overline{T}_{refG} \; F_{SG} \, C_{P_S}} \left[k_C^{*} \, W_{CG} \, C_{O_2,f} \; y_{O_2,e}\right]\left(-\Delta H_{R,C}\right) - H_{\ell G} = O \end{aligned} \tag{B.3.10}$$

APPENDIX C

COMPUTER CODES DEVELOPED TO ACHIEVE THE SIMULATION

C-1: PROGRAM FOR SOLVING THE DOWNER-REGENERATOR MODEL (FIVE ODE'S IN DOWNER AND SEVEN NON-LINEAR EQUATIONS IN REGENERATOR):

```
**********************************************
```

MAIN PROGRAM

```
**********************************************
 USE  MSIMSL

INTEGER    MXPARM, M
PARAMETER  (MXPARM=50, M=4 , J=5,JJ=3)
!                   SPECIFICATIONS FOR LOCAL VARIABLES
 INTEGER   IDO, ISTEP, NOUT
 COMMON/GEN/TF,TAIRF,TREFD,TREFG
 COMMON/REG/YY,DG,LG,AG,WCD,MSG,UA,UMF,MMM,KK
COMMON/DOWN/FSD,FGD,LD,DD,AD
  REAL       PARAM(MXPARM), TIME, TEND, TOL,FSTEP,Z,Y(J),X(M),S(JJ)
  REAL       MSG,XGUESS(M),F(M),KC,MWC,KCOD,UP,DOWN,TD1,TREFD,TREFG
  REAL       FGD,FSD,LD,DD,AD,WCD
 REAL      LG,DG,AG,UMF
DATA CPL,TBOIL,HVAP/2.1,673.,270./
DATA CPS,CPGD/1.108,2.04/

EXTERNAL  FUN,FCC,FCN
TF=523.
TAIRF=298.15
UA = .057
UMF = 13.6E-4
FGD=2.778E-4
MSG = 2.46
```

```
LD = 1.0
DD = 10.9E-3
DG = .0739

LG = 1.037
!                       REFERENCES
TREFD= TF
TREFG= TAIRF
OPEN (UNIT=600,FILE='TOTAL#62.NUT',STATUS='UNKNOWN')
OPEN (UNIT=400,FILE='DN#62.NUT',STATUS='UNKNOWN')
OPEN (UNIT=800,FILE='RG#62.NUT',STATUS='UNKNOWN')

MMM=30

XGUESS(4)=950./TREFG
FSD=6.94E-3*29.2/25.
NNN = 1

IF(NNN.EQ.1) THEN

XGUESS(1)=.00045
XGUESS(2)=.002
XGUESS(3)=.006

ENDIF
X(4)=XGUESS(4)

DO 777 KK=1,10
!               Set initial conditions
TIME = 0.0

!               Set error tolerance
 TOL = 0.005
!               Set PARAM to default
 CALL SSET (MXPARM, 0.0, PARAM, 1)
!               Select absolute error control
 PARAM(10) = 1.0

PARAM(4)=100000
Z = 0.0
 Y(1) = 1.0
 Y(2) = 0.0
Y(3) = 0.0
Y(4) = 0.0
 TS=X(4)*TREFG

 UP = FSD*CPS*TS-FGD*(CPL*(TF-TBOIL)+HVAP-CPGD*TBOIL)
 DOWN = FGD*CPGD+FSD*CPS
 TD1 = UP/DOWN
```

```
Y(5) = TD1/TREFD
IDO=1

DO 20 FSTEP=0,1.,.01
    TENP = FSTEP
  CALL IVPRK (IDO, J, FCC, Z, TENP, TOL, PARAM, Y)

WRITE (NOUT,'(F6.3,5F12.5)') Z,  Y(1),Y(2),Y(3),Y(4),Y(5)*TREFD
WRITE (400,'(F6.3,5F12.5)') Z, Y(1),Y(2),Y(3),Y(4),Y(5)*TREFD

YY=Y(5)
WCD=Y(3)/MMM

20 CONTINUE

!                Final call to release workspace
IDO = 3

CALL IVPRK (IDO, J, FCC, Z, TENP, TOL, PARAM, Y)

WRITE (NOUT,99999) PARAM(35)
99998 FORMAT (4X, 'FSTEP', 5X, 'LENGTH', 9X, 'Y1', 11X, 'Y2',9X, 'Y3', 11X, 'Y4)
99999 FORMAT (4X, 'Number of fcn calls with IVPRK =', F6.0)
ERRREL = 0.001
ITMAX  = 100
CALL UMACH (2, NOUT(
!                Find the solution
CALL NEQNF (FUN, ERRREL, M, ITMAX, XGUESS, X, FNORM)
!                Output

WRITE (800,'(3F8.6,F9.3)') X(1),X(2),X(3),X(4)*TREFG
DO I=1,4
XGUESS(I)=X(I)
ENDDO

NNN = NNN+1
WRITE(600,*)'MMM = ',MMM,'     KK=',KK
WRITE (600,'(F6.3,5F12.5)') Z,  Y(1),Y(2),Y(3),Y(4),Y(5)*TREFD
WRITE (600,'(3F8.6,F9.3)') X(1),X(2),X(3),X(4)*TREFG
WRITE(600,*)'==================================================='
777  CONTINUE
WRITE(600,*)'MMM = ',MMM
WRITE (600,'(F6.3,5F12.5)') Z,  Y(1),Y(2),Y(3),Y(4),Y(5)*TREFD
 WRITE (600,'(3F8.6,F9.3)') X(1),X(2),X(3),X(4)*TREFG
WRITE(600,*)'==================================================='
ENDDO

END
```

```
**********************************************
!        SUBROUTINE FUN TO SOLVE NON-LINEAR EQUATIONS
**********************************************
SUBROUTINE FUN (X, F, M)
USE MSIMSL
PARAMETER  (JJ=3)
EXTERNAL FCN
COMMON/ENV/ALPHA1,ALPHAH,XX
COMMON/GEN/TF,TAIRF,TREFD,TREFG
COMMON/REG/YY,DG,LG,AG,WCD,MSG,UA,UMF,MMM,KK
COMMON/DOWN/FSD,FGD,LD,DD;AD
INTEGER   M,JJ
REAL      ALPHA1,ALPHAH,X(M),XGUESS(M),
F(M),KCOD,KCODP,KC,KG,MWC,S(JJ),MSG
REAL  XX(4),PARAM(50),FEED(5),TREFD,TREFG
REAL DG,LG,LD,UMF


DATA EPSDG,KG,R/.51,3.37,8.314/
DATA AV,H,RHOGG,CPGG/5.45,2.34,.71,1.149/
DATA CPS,CPGD/1.108,2.04/
DATA FEED/0.002,0.001,1.0,1.0,.01374/
DATA EPSBG,RHOB,MWC/.571,820.,12./
DATA HRC,HRCOD/450.0E3,566.00E3/
FSG=FSD
KG = .51
AV = .08
AG = 3.141*DG**2./4.
GIG = UMF*AG
GCG = AG*(UA-UMF)
DO I=1,M
XX(I)=X(I)
ENDDO
TD = YY*TREFD/TREFG
RHOS = 1500.
KC=1.4E8*EXP(-125.E3/(R*X(4)*TREFG))
KCOD=247.75*EXP(-70.47E3/(R*X(4)*TREFG))
KCODP=FEED(5)**.5*KCOD
I = 0
ALPHA1=AG*EPSDG*(1.-EPSBG)*LG*KG/GCG
MWC=12.0
DO I=1,4
X(I)=ABS(X(I))
ENDDO
GG=GIG+GCG*(1-EXP(-ALPHA1))
AA=AG*(1-EPSBG)*RHOB*LG*(1-EPSDG)
RL=+KCODP*X(2)*X(3)**.5-KC*X(1)*X(3)/MWC
RM=+KCODP*X(2)*X(3)**.5/2.+KC*X(1)*X(3)/MWC
```

```
ALPHAH=AG*(1-EPSBG)*AV*H*LG/(GCG*RHOGG*CPGG)
AW= AG*(1-EPSBG)*(1-EPSDG)*LG*RHOS*FEED(5)*KC*X(1)*X(3)
GGS=GG/(AG*(1-EPSBG)*EPSDG)
AAS=LG*RHOB*KCODP
RLS=LG*(1-EPSDG)*RHOS*KC/(EPSDG*MWC)
ATD=(GIG+GCG*(EXP(-ALPHAH)-1.))*RHOGG*CPGG
BTD=FSG*CPS
CTD=AG*(1-EPSBG)*(1-EPSDG)*RHOB*LG*FEED(5)/TREFG
DTD=KC*X(1)*X(3)*HRC/MWC+KCODP*X(2)*X(3)**.5*HRCOD
GAMA=ATD/(FSG*CPS)
SETA=AG*(1-
EPSBG)*LG*EPSDG*RHOB*FEED(5)**1.5*KCOD*HRCOD*X(2)*X(3)**.5/(FSG*CPS*TR
EFG)
THETA=MSG*FEED(5)*KC*HRC*X(3)/(FSG*CPS*TREFG)
ATS=ATD/(FSG*CPS)
BTS=AG*(1-
EPSBG)*LG*EPSDG*RHOB*FEED(5)**1.5*KCOD*HRCOD/(FSG*CPS*TREFG)
CTS=MSG*FEED(5)*KC*HRC/(FSG*CPS*TREFG*MWC)
F(1) = FSG*(WCD-X(1))-AW
F(2) = GGS*(FEED(1)-X(2))-AAS*X(2)*X(3)**.5+RLS*X(1)*X(3)
F(3) = GGS*(FEED(3)-X(3))-AAS/2.*X(2)*X(3)**.5-RLS*X(1)*X(3)
F(4) = ATS*(FEED(4)-X(4))+(TD-X(4))+BTS*X(2)*X(3)**.5+CTS*X(1)*X(3)-.00

TIME=0.0
TOL=.005
PARAM(10)=1.0
PARAM(4)=100000
ZEE=0.0
S(1)=0.00
S(2)=1.0
S(3)=TAIRF/TREFG
IDO=1
DO 20 FSTEP=0,1.,.01
TENP = FSTEP
CALL IVPRK (IDO, JJ, FCN, ZEE, TENP, TOL, PARAM, S)
IF(KK.EQ.50) WRITE (800,'(F6.3,5F12.5)') ZEE, S(1),S(2),S(3)*TREFG
 WRITE (800,'(F6.3,5F12.5)') ZEE, S(1),S(2),S(3)*TREFG
WRITE (NOUT,'(F6.3,5F12.5)') ZEE,  S(1),S(2),S(3)
20 CONTINUE
!                 Final call to release workspace

IDO = 3
CALL IVPRK (IDO, JJ, FCN, ZEE, TENP, TOL, PARAM, S)

!                 Show number of function calls.
WRITE (NOUT,99999) PARAM(35)
99998  FORMAT (4X, 'FSTEP', 5X, 'LENGTH', 9X, 'S1', 11X, 'S2',9X, 'S3')
99999  FORMAT (4X, 'Number of fcn calls with IVPRK =', F6.0)
RETURN
```

```
END


SUBROUTINE FCN(JJ,ZEE,S,SPRIME)
COMMON/ENV/ALPHA1,ALPHAH,XX
REAL S(JJ),SPRIME(JJ),ZEE,XX(4)

SPRIME(1)= ALPHA1*(XX(2)-S(1) )
SPRIME(2)= ALPHA1*(XX(3)-S(2))
SPRIME(3)= ALPHAH*(XX(4)-S(3))
RETURN
END

************************************************
!              THE SUBROUTINE SOLVING DOWNER'S ODES
************************************************

SUBROUTINE FCC (N, Z, Y, YPRIME)
COMMON/GEN/TF,TAIRF,TREFD,TREFG
COMMON/DOWN/FSD,FGD,LD,DD,AD
INTEGER   N
REAL      Z, Y(N), YPRIME(N),KAB,KAC,KBC,KAD,KBD,NEMO,MSG
REAL      LD,DD,AD
DATA R,HAB,HAC,HAD,HBC,HBD/8.314,.5e3,-3.0e3,3.5e3,-3.35E3,2.20e3/
DATA CPS,CPGD/.98,2.04/
DATA EPSD,RHOGD/.997,8.4/
AD = 3.141*DD**2./4.0
KD=2.4*EXP(-32.782E3/(R*Y(5)*TREFD))
PHID=EXP(-KD*1.36)
MMM=1
CONST = PHID*AD*EPSD*LD*RHOGD/FGD
DEMO  = (FSD*CPS+FGD*CPGD)*TREFD
KAB= 31.0*20*EXP(-47.626e3/(R*Y(5)*TREFD))
KAC= 4.4*20*EXP(-60.275e3/(R*Y(5)*TREFD))
 KAD= 3.0*20*EXP(-39.781e3/(R*Y(5)*TREFD))
KBC=0.0
KBD= 1.7E2*20*EXP(-76.366e3/(R*Y(5)*TREFD) )

YPRIME(1) = -CONST*(KAB+KAC+KAD)*Y(1)**2
YPRIME(2) = -CONST*((KBC+KBD)*Y(2)-KAB*Y(1)**2)
 YPRIME(3) = +CONST*(KBC*Y(2)+KAC*Y(1)**2)
YPRIME(4) = +CONST*(KBD*Y(2)+KAD*Y(1)**2)
YPRIME(5) = -
CONST*FGD/DEMO*(Y(1)**2*(KAB*HAB+KAC*HAC+KAD*HAD)+Y(2)*(KBC*HBC+K
BD*HBD))-.02
MMM=MMM+1
RETURN
 END
```

C-2: PROGRAM FOR TO DEMONSTRATE THE EFFECT OF CHANGING CATALYST TO OIL RATIO ON DIFFERENT PARAMETERS IN THE FCC-DOWNER UNIT

```
***********************************************
```

MAIN PROGRAM

```
***********************************************************************
USE MSIMSL
INTEGER    MXPARM, M
PARAMETER  (MXPARM=50, M=4 , J=5,JJ=3)

INTEGER   IDO, ISTEP, NOUT
 COMMON/GEN/TF,TAIRF,TREFD,TREFG
COMMON/REG/YY,DG,LG,AG,WCD,MSG,UA,UMF,MMM,LOSS
COMMON/DOWN/FSD,FGD,LD,DD,AD
REAL      PARAM(MXPARM), TIME, TEND, TOL,FSTEP,Z,Y(J),X(M),S(JJ)
 REAL MSG,XGUESS(M),F(M),KC,MWC,KCOD,UP,DOWN,TD1,TREFD,TREFG
REAL      FGD,FSD,LD,DD,AD,WCD
REAL      LG,DG,AG,UMF,LOSS
DATA CPL,TBOIL,HVAP/2.1,673.,270./
DATA CPS,CPGD/1.108,2.04/

EXTERNAL  FUN,FCC,FCN

 TF=523.
TAIRF=298.15
UA = .057
UMF = 13.6E-4
FGD=  2.778E-4
MSG = 2.46
LD = 1.0
DD = 10.9E-3
DG = .0739
LG = 1.037
!
!                        REFERENCES

TREFD= TF
TREFG= TAIRF

OPEN (UNIT=600,FILE='T-CO-DOT600.NUT',STATUS='UNKNOWN')
OPEN (UNIT=1000,FILE='SUM-CO-DOT600.NUT',STATUS='UNKNOWN')
OPEN (UNIT=2000,FILE='SUM+-CO-DOT600.NUT',STATUS='UNKNOWN')
DO MMM=10,30,5
IF(MMM.EQ.10)THEN
```

```
OPEN (UNIT=400,FILE='DN-10-DOT600.NUT',STATUS='UNKNOWN')
OPEN (UNIT=800,FILE='RG-10-DOT600.NUT',STATUS='UNKNOWN')
XGUESS(4)=950./TREFG
LOSS=.33
ELSEIF(MMM.EQ.15)THEN

OPEN (UNIT=400,FILE='DN-15-DOT600.NUT',STATUS='UNKNOWN')
OPEN (UNIT=800,FILE='RG-15-DOT600.NUT',STATUS='UNKNOWN')
XGUESS(4)=950./TREFG
LOSS=.25
ELSEIF(MMM.EQ.20)THEN
OPEN (UNIT=400,FILE='DN-20-DOT600.NUT',STATUS='UNKNOWN')
OPEN (UNIT=800,FILE='RG-20-DOT600.NUT',STATUS='UNKNOWN')
XGUESS(4)=970./TREFG
LOSS=.21
ELSEIF(MMM.EQ.25)THEN
OPEN (UNIT=400,FILE='DN-25-DOT600.NUT',STATUS='UNKNOWN')
OPEN (UNIT=800,FILE='RG-25-DOT600.NUT',STATUS='UNKNOWN')
XGUESS(4)=950./TREFG
LOSS=.19
ELSE
OPEN (UNIT=400,FILE='DN-30-DOT600.NUT',STATUS='UNKNOWN')
OPEN (UNIT=800,FILE='RG-30-DOT600.NUT',STATUS='UNKNOWN')
XGUESS(4)=950./TREFG
LOSS=.17

ENDIF

305     FSD=6.94E-3*MMM/25.

XGUESS(1)=.00008
XGUESS(2)=.002
XGUESS(3)=.06
XGUESS(4)=970./TREFG
X(4)=XGUESS(4)

DO 777 KK=1,200
!                    Set initial conditions
TIME = 0.0


!                    Set error tolerance
TOL = 0.005
!                    Set PARAM to default

CALL SSET (MXPARM, 0.0, PARAM, 1)
!                    Select absolute error control
PARAM(10) = 1.0
PARAM(4)=100000
```

```
Z = 0.0
Y(1) = 1.0
Y(2) = 0.0
Y(3) = 0.0
Y(4) = 0.0
TS=X(4)*TREFG
UP = FSD*CPS*TS-FGD*(CPL*(TF-TBOIL)+HVAP-CPGD*TBOIL)
DOWN = FGD*CPGD+FSD*CPS
TD1 = UP/DOWN
Y(5) = TD1/TREFD
IDO=1
DO  20 FSTEP=0,1.,.01
TENP = FSTEP
CALL IVPRK (IDO, J, FCC, Z, TENP, TOL, PARAM, Y)
WRITE (NOUT,'(F6.3,5F12.5)') Z,  Y(1),Y(2),Y(3),Y(4),Y(5)*TREFD
WRITE (400,'(F6.3,5F12.5)') Z, Y(1),Y(2),Y(3),Y(4),Y(5)*TREFD
YY=Y(5)
WCD=Y(3)/MMM

20 CONTINUE
!                    Final call to release workspace

   IDO = 3

CALL IVPRK (IDO, J, FCC, Z, TENP, TOL, PARAM, Y)

WRITE (NOUT,99999) PARAM(35)
99998 FORMAT (4X, 'FSTEP', 5X, 'LENGTH', 9X, 'Y1', 11X, 'Y2',9X, 'Y3', 11X, 'Y4')
99999 FORMAT (4X, 'Number of fcn calls with IVPRK =', F6.0)
ERRREL = 0.0001
ITMAX  = 1000
CALL UMACH (2, NOUT)
!                    Find the solution

CALL NEQNF (FUN, ERRREL, M, ITMAX, XGUESS, X, FNORM)
WRITE (800,'(3F8.6,F9.3)') X(1),X(2),X(3),X(4)*TREFG

DO I=1,4
XGUESS(I)=X(I)
ENDDO

DOT = Y(5)*TREFD-273.15
WRITE(600,*)'MMM = ',MMM,'     KK=',KK,'     DOT = ',DOT
WRITE (600,'(F6.3,5F12.5)') Z,  Y(1),Y(2),Y(3),Y(4),Y(5)*TREFD
WRITE (600,'(3F8.6,F9.3)') X(1),X(2),X(3),X(4)*TREFG
WRITE(600,*)'============================================='

777      CONTINUE
```

```
WRITE(600,*)'MMM = ',MMM, '      LOSS = ',LOSS
WRITE (600,'(F6.3,6F12.5)') Z,  Y(1),Y(2),Y(3),Y(4),Y(5)*TREFD,WCD
WRITE (600,'(3F8.6,2F9.3)') X(1),X(2),X(3),X(4)*TREFG,FNORM
WRITE(600,*)'================================================'

WRITE(2000,'(I4,F7.5,9F10.4)')MMM,LOSS,(1.-
Y(1))*100,Y(2)*100,Y(3)*100,Y(4)*100,DOT,X(1)*100,X(2)*100,X(3)*100,X(4)*TREFG-
273.15
IF(DOT.LT.595) THEN
LOSS=LOSS+.003
GOTO 305
ENDIF
IF(DOT.GT.605) THEN
LOSS=LOSS-.003
GOTO 305
ENDIF
WRITE(1000,'(I4,F7.5,9F10.4)')MMM,LOSS,(1.-
Y(1))*100,Y(2)*100,Y(3)*100,Y(4)*100,DOT,X(1)*100,X(2)*100,X(3)*100,X(4)*TREFG-
273.15
ENDDO
END
SUBROUTINE FCN(JJ,ZEE,S,SPRIME)
COMMON/ENV/ALPHA1,ALPHAH,XX
REAL S(JJ),SPRIME(JJ),ZEE,XX(4)
SPRIME(1)= ALPHA1*(XX(2)-S(1))
SPRIME(2)= ALPHA1*(XX(3)-S(2))
SPRIME(3)= ALPHAH*(XX(4)-S(3))
RETURN
END


***************************************************
        SUBROUTINE FUN TO SOLVE NON-LINEAR EQUATIONS
! ***************************************************
SUBROUTINE FUN (X, F, M)
USE MSIMSL
PARAMETER  (JJ=3)
EXTERNAL FCN
COMMON/ENV/ALPHA1,ALPHAH,XX
COMMON/GEN/TF,TAIRF,TREFD,TREFG
COMMON/REG/YY,DG,LG,AG,WCD,MSG,UA,UMF,MMM,LOSS
COMMON/DOWN/FSD,FGD,LD,DD,AD
INTEGER    M,JJ
REAL       ALPHA1,ALPHAH,X(M),XGUESS(M),
F(M),KCOD,KCODP,KC,KG,MWC,S(JJ),MSG
REAL  XX(4),PARAM(50),FEED(5),TREFD,TREFG
REAL DG,LG,LD,UMF,LOSS
REAL KCP1,KCP3
```

```
DATA EPSDG,KG,R/.51,3.37,8.314/
DATA AV,H,RHOGG,CPGG/5.45,2.34,.71,1.149/
DATA CPS,CPGD/1.108,2.04/

DATA FEED/0.002,0.001,1.0,1.0,.01374/
DATA EPSBG,RHOB,MWC/.571,820.,12./
DATA HRC,HRCOD/251.540E3,282.0E3/

FSG=FSD
KG = .51
AV = .08
AG = 3.141*DG**2./4.
GIG = UMF*AG
GCG = AG*(UA-UMF)
DO I=1,M
XX(I)=X(I)
ENDDO
TD = YY*TREFD/TREFG
RHOS = 1500.
SEGMA=1.7
KC=1.4E8*EXP(-125.E3/(R*X(4)*TREFG))
KCP1=1.0/(SEGMA+1.0)*KC
KCP3=(SEGMA+.5)/(SEGMA+1.0)*KC
KCOD=247.75*EXP(-70.47E3/(R*X(4)*TREFG))
KCODP=FEED(5)**.5*KCOD

I = 0
ALPHA1=AG*EPSDG*(1.-EPSBG)*LG*KG/GCG
MWC=12.0

DO I=1,4
X(I)=ABS(X(I))
ENDDO
GG=GIG+GCG*(1-EXP(-ALPHA1))
AA=AG*(1-EPSBG)*RHOB*LG*(1-EPSDG)

RL=+KCODP*X(2)*X(3)**.5-KC*X(1)*X(3)/MWC
RM=+KCODP*X(2)*X(3)**.5+KC*X(1)*X(3)/MWC
ALPHAH=AG*(1-EPSBG)*AV*H*LG/(GCG*RHOGG*CPGG)
AW= AG*(1-EPSBG)*(1-EPSDG)*LG*RHOS*FEED(5)*KC*X(1)*X(3)
GGS=GG/(AG*(1-EPSBG)*EPSDG)
AAS=LG*RHOB*KCODP/2.0
RLS=LG*(1-EPSDG)*RHOS*KC/(EPSDG*MWC)
RLS1=LG*(1-EPSDG)*RHOS*KCP1/(EPSDG*MWC)
 RLS3=LG*(1-EPSDG)*RHOS*KCP3/(EPSDG*MWC)
ATD=(GIG-GCG*(EXP(-ALPHAH)-1.))*RHOGG*CPGG
BTD=FSG*CPS
CTD=AG*(1-EPSBG)*(1-EPSDG)*RHOB*LG*FEED(5)/TREFG
DTD=KC*X(1)*X(3)*HRC/MWC+KCODP*X(2)*X(3)**.5*HRCOD
```

```
GAMA=ATD/(FSG*CPS)
SETA=AG*(1-
EPSBG)*LG*EPSDG*RHOB*FEED(5)**1.5*KCOD*HRCOD*X(2)*X(3)**.5/(FSG*CPS*TR
EFG)
THETA=MSG*FEED(5)*KC*HRC*X(3)/(FSG*CPS*TREFG)
ATS=ATD/(FSG*CPS)
BTS=AG*(1-
EPSBG)*LG*EPSDG*RHOB*FEED(5)**1.5*KCOD*HRCOD/(FSG*CPS*TREFG)
CTS=MSG*FEED(5)*KC*HRC/(FSG*CPS*TREFG*MWC)
F(1) = FSG*(WCD-X(1))-AW
F(2) = GGS*(FEED(1)-X(2))-AAS*X(2)*X(3)**.5+RLS1*X(1)*X(3)
F(3) = GGS*(FEED(3)-X(3))-AAS*X(2)*X(3)**.5-RLS3*X(1)*X(3)
F(4) = ATS*(FEED(4)-X(4))+(TD-X(4))+BTS*X(2)*X(3)**.5+CTS*X(1)*X(3)+LOSS
TIME=0.0
TOL=.005
PARAM(10)=1.0
PARAM(4)=100000
ZEE=0.0
S(1)=0.00
S(2)=1.0
S(3)=TAIRF/TREFG
IDO=1
DO 20 FSTEP=0,1.,.01
TENP = FSTEP
CALL IVPRK (IDO, JJ, FCN, ZEE, TENP, TOL, PARAM, S)
WRITE (800,'(F6.3,5F12.5)') ZEE, S(1),S(2),S(3)*TREFG
WRITE (NOUT,'(F6.3,5F12.5)') ZEE,  S(1),S(2),S(3)
20 CONTINUE

!                    Final call to release workspace

IDO = 3
CALL IVPRK (IDO, JJ, FCN, ZEE, TENP, TOL, PARAM, S)

WRITE (NOUT,99999) PARAM(35)
99998 FORMAT (4X, 'FSTEP', 5X, 'LENGTH', 9X, 'S1', 11X, 'S2',9X, 'S3')
99999 FORMAT (4X, 'Number of fcn calls with IVPRK =', F6.0)
RETURN
END

**************************************************
          THE SUBROUTINE SOLVING DOWNER'S ODES
**************************************************
SUBROUTINE FCC (N, Z, Y, YPRIME)
COMMON/GEN/TF,TAIRF,TREFD,TREFG
COMMON/DOWN/FSD,FGD,LD,DD,AD
INTEGER   N
```

```
REAL    Z, Y(N), YPRIME(N),KAB,KAC,KBC,KAD,KBD,NEMO,MSG
REAL    LD,DD,AD
DATA R,HAB,HAC,HAD,HBC,HBD/8.314,.5e3,-3.0e3,3.5e3,-3.35E3,2.20e3/
DATA CPS,CPGD/.98,2.04/
DATA EPSD,RHOGD/.997,8.4/
AD = 3.141*DD**2./4.0
KD=2.4*EXP(-32.782E3/(R*Y(5)*TREFD))
PHID=EXP(-KD*1.36)
MMM=1
CONST = PHID*AD*EPSD*LD*RHOGD/FGD
DEMO  = (FSD*CPS+FGD*CPGD)*TREFD

KAB= 31.0*20*EXP(-47.626e3/(R*Y(5)*TREFD))
KAC= 4.4*20*EXP(-60.275e3/(R*Y(5)*TREFD))
KAD= 3.0*20*EXP(-39.781e3/(R*Y(5)*TREFD))
KBC=0.0
KBD= 1.7E2*20*EXP(-76.366e3/(R*Y(5)*TREFD))

YPRIME(1) = -CONST*(KAB+KAC+KAD)*Y(1)**2
YPRIME(2) = -CONST*((KBC+KBD)*Y(2)-KAB*Y(1)**2)
YPRIME(3) = +CONST*(KBC*Y(2)+KAC*Y(1)**2)
YPRIME(4) = +CONST*(KBD*Y(2)+KAD*Y(1)**2)
YPRIME(5) = -
CONST*FGD/DEMO*(Y(1)**2*(KAB*HAB+KAC*HAC+KAD*HAD)+Y(2)*(KBC*HBC+K
BD*HBD))-.02
MMM=MMM+1
RETURN
END
```

APPENDIX D

FCC- DOWNER UNIT OUTPUT SAMPLE

Run No.	DF031	DF032	DF033	DF034	DF035	DF036	DF037	DF038
Date	98/11/04	98/11/04	98/11/07	98/11/09	98/11/11	98/11/11	98/11/16	98/11/16
Feed Oil	VGO3	VGO3	VGO3	VGO3	VGO3	VGO3	VGO3	VGO3
Catalyst	Eqi4	Eqi4	Eqi3	Eqi3	Eqi3	Eqi3	NFC-97-7	NFC-97-7
RT(s)	1.39	1.42	1.38	0.83	1.36	0.79	1.38	1.38
ROT°C	600	597	600	600	600	600	600	600
Cat/Oil	65.7	38.4	54.1	53.8	52.7	53.4	59.7	48.3
Conv.(wt%	84.0	75.3	75.6	69.7	73.4	71.0	75.1	74.6
m.b.(%)	100.0	100.0	100.0	100.0	100.0	100.0	100.0	100.0
Yields(wt%)								
H2	0.11	0.08	0.16	0.15	0.17	0.14	0.06	0.07
C1	1.50	1.23	1.70	1.87	1.74	1.73	1.58	1.78
C2	0.83	0.77	1.01	1.14	1.06	1.04	1.15	1.35
C2=	2.00	1.69	2.12	2.42	2.17	2.24	1.89	2.17
C3	1.17	0.88	1.04	0.85	0.98	0.88	0.67	0.69
C3=	11.75	9.39	9.56	9.39	9.34	9.21	7.77	7.66
iC4	3.87	3.04	3.07	2.17	2.79	2.43	1.63	1.48
nC4	0.82	0.61	0.70	0.50	0.63	0.55	0.36	0.35
t2C4=	3.06	2.75	2.69	2.45	2.59	2.48	2.39	2.40
1C4=	2.66	2.38	2.36	2.27	2.31	2.26	2.12	2.16
iC4=	3.39	3.11	2.94	3.03	2.92	2.95	3.34	3.43
c2C4=	2.32	2.09	2.05	1.86	1.97	1.90	1.80	1.82
C4'(Liq.)	0.27	0.40	0.00	0.29	0.00	0.00	0.98	0.84
1,3-BD	0.05	0.06	0.06	0.09	0.07	0.08	0.08	0.09
total gase	33.74	28.42	29.40	28.38	28.67	27.81	25.74	26.20
Gasl.(C5+	40.34	42.60	39.82	36.18	38.57	37.83	46.66	46.27
LCO	9.77	12.35	11.91	13.39	12.85	12.26	13.97	13.69
HCO	6.25	12.30	12.45	16.89	13.77	16.72	10.97	11.70
Coke	9.85	4.27	6.36	5.01	6.08	5.30	2.58	2.06
Total	100.00	100.00	100.00	99.94	100.00	100.00	100.00	100.00

Run No.	DF039	DF040	DF031	DF032	DF033	DF034	DF035	DF036
Date	98/11/16	98/11/16	98/11/04	98/11/04	98/11/07	98/11/09	98/11/11	98/11/11
Feed Oil	VGO3	VGO3	VGO3	VGO3	VGO3	VGO3	VGO3	VGO3
Catalyst	NFC-97-7	NFC-97-7	Eqi4	Eqi4	Eqi3	Eqi3	Eqi3	Eqi3
RT(s)	1.38	1.41	1.39	1.42	1.38	0.83	1.36	0.79
ROT°C	600	575	600	597	600	600	600	600
Cat/Oil	32.4	16.6	65.7	38.4	54.1	53.8	52.7	53.4
Conv.(wt%	70.4	67.3	84.0	75.3	75.6	69.7	73.4	71.0
m.b.(%)	100.0	100.0	100.0	100.0	100.0	100.0	100.0	100.0
Yields(wt%)								
H2	0.07	0.05	0.11	0.08	0.16	0.15	0.17	0.14
C1	1.86	1.41	1.50	1.23	1.70	1.87	1.74	1.73
C2	1.48	1.20	0.83	0.77	1.01	1.14	1.06	1.04
C2=	2.44	1.97	2.00	1.69	2.12	2.42	2.17	2.24
C3	0.66	0.54	1.17	0.88	1.04	0.85	0.98	0.88
C3=	6.45	4.76	11.75	9.39	9.56	9.39	9.34	9.21
iC4	1.02	0.82	3.87	3.04	3.07	2.17	2.79	2.43
nC4	0.28	0.23	0.82	0.61	0.70	0.50	0.63	0.55
t2C4=	1.99	1.52	3.06	2.75	2.69	2.45	2.59	2.48
1C4=	1.82	1.41	2.66	2.38	2.36	2.27	2.31	2.26
iC4=	2.85	2.18	3.39	3.11	2.94	3.03	2.92	2.95
c2C4=	1.51	1.16	2.32	2.09	2.05	1.86	1.97	1.90
C4'(Liq.)	0.74	0.82	0.27	0.40	0.00	0.29	0.00	0.00
1,3-BD	0.11	0.09	0.05	0.06	0.06	0.09	0.07	0.08
total gase	23.17	18.05	33.74	28.42	29.40	28.38	28.67	27.81
Gasl.(C5+	45.60	48.34	40.34	42.60	39.82	36.18	38.57	37.83
LCO	15.03	16.59	9.77	12.35	11.91	13.39	12.85	12.26
HCO	14.56	16.07	6.25	12.30	12.45	16.89	13.77	16.72
Coke	1.47	0.79	9.85	4.27	6.36	5.01	6.08	5.30
Total	99.93	99.93	100.00	100.00	100.00	99.94	100.00	100.00

Run No.	DF037	DF038	DF039	DF040	DF041	DF038	DF042	DF043
Date	98/11/16	98/11/16	98/11/16	98/11/16	98/11/17	98/11/16	98/11/17	98/11/17
Feed Oil	VGO3	VGO3	VGO3	VGO3	VGO3	VGO3	VGO3	VGO3
Catalyst	NFC-97-7	NFC-97-7	NFC-97-7	NFC-97-7	NFC-97-7	NFC-97-7	NFC-97-7	NFC-97-7
RT(s)	1.38	1.38	1.38	1.41	1.28	1.38	1.43	1.53
ROT°C	600	600	600	575	650	600	549	501
Cat/Oil	59.7	48.3	32.4	16.6	51.0	48.3	55.0	51.1
Conv.(wt%	75.1	74.6	70.4	67.3	74.0	74.6	72.5	66.6
m.b.(%)	100.0	100.0	100.0	100.0	100.0	100.0	100.0	100.0
Yields(wt%)								
H2	0.06	0.07	0.07	0.05	0.15	0.07	0.05	0.05
C1	1.58	1.78	1.86	1.41	4.27	1.78	1.12	0.64
C2	1.15	1.35	1.48	1.20	2.74	1.35	0.80	0.49
C2=	1.89	2.17	2.44	1.97	5.61	2.17	1.34	0.66
C3	0.67	0.69	0.66	0.54	0.80	0.69	0.56	0.58
C3=	7.77	7.66	6.45	4.76	8.93	7.66	5.72	4.51
iC4	1.63	1.48	1.02	0.82	0.58	1.48	1.95	2.67
nC4	0.36	0.35	0.28	0.23	0.22	0.35	0.34	0.40
t2C4=	2.39	2.40	1.99	1.52	2.16	2.40	1.85	1.57
1C4=	2.12	2.16	1.82	1.41	2.12	2.16	1.61	1.25
iC4=	3.34	3.43	2.85	2.18	3.10	3.43	2.55	1.87
c2C4=	1.80	1.82	1.51	1.16	1.66	1.82	1.38	1.16
C4'(Liq.)	0.98	0.84	0.74	0.82	0.00	0.84	1.07	0.00
1,3-BD	0.08	0.09	0.11	0.09	0.27	0.09	0.06	0.03
total gase	25.74	26.20	23.17	18.05	32.60	26.29	20.40	15.87
Gasl.(C5+	46.66	46.27	45.60	48.34	38.64	46.27	49.78	48.08
LCO	13.97	13.69	15.03	16.59	13.88	13.69	15.06	16.35
HCO	10.97	11.70	14.56	16.07	12.09	11.70	12.43	17.09
Coke	2.58	2.06	1.47	0.79	2.73	2.06	2.39	2.61
Total	100.00	100.00	99.93	99.93	99.94	100.00	100.07	100.00

Run No.	DF044	DF045	DF046	DF047	DF048	DF049	DF050	DF051
Date	98/12/14	98/12/14	98/12/15	98/12/21	98/12/26	98/12/26	98/12/26	98/12/27
Feed Oil	VGO3	VGO3	VGO3	VGO3	VGO3	VGO3	VGO3	VGO3
Catalyst	Eqi4	Eqi4	Eqi4	Eqi4	NFC-97-7	NFC-97-7	NFC-97-7	NFC-97-7
RT(s)	1.46	1.04	1.05	1.44	1.23	1.11	1.34	1.20
ROT°C	550	550	550	549	550	550	550	550
Cat/Oil	40.0	42.5	42.5	44.7	24.5	51.4	73.6	58.2
Conv.(wt%	70.5	71.7	62.2	76.8	67.7	69.0	62.5	59.4
m.b.(%)	100.0	100.0	100.0	100.0	100.0	100.0	100.0	100.0
Yields(wt%)								
H2	0.06	0.06	0.07	0.06	0.05	0.05	0.05	0.04
C1	0.66	0.69	0.74	0.63	0.66	0.67	0.76	0.70
C2	0.46	0.48	0.59	0.41	0.49	0.52	0.56	0.55
C2=	0.72	0.78	0.80	0.76	0.74	0.75	0.92	0.85
C3	0.96	1.00	1.02	0.96	0.51	0.46	0.52	0.46
C3=	5.29	6.00	5.09	5.81	5.06	4.94	5.38	4.72
iC4	3.35	3.62	2.55	4.04	2.39	2.01	2.45	2.00
nC4	0.67	0.73	0.63	0.73	0.40	0.33	0.38	0.31
t2C4=	1.68	1.99	1.65	1.81	1.85	1.80	1.84	1.59
1C4=	1.35	1.59	1.36	1.44	1.44	1.45	1.45	1.31
iC4=	1.86	2.22	2.19	1.76	2.33	2.41	2.31	2.07
c2C4=	1.23	1.46	1.22	1.32	1.36	1.33	1.36	1.17
C4'(Liq.)	1.05	0.66	0.58	1.22	0.00	0.65	0.00	0.37
1,3-BD	0.02	0.03	0.03	0.02	0.03	0.04	0.04	0.04
total gases	19.37	21.30	18.52	20.96	17.32	17.43	18.02	16.19
Gasl.(C5+	46.64	46.22	41.18	50.06	48.01	49.33	41.63	41.13
LCO	15.60	15.07	17.05	14.08	18.44	17.49	17.53	17.32
HCO	13.91	13.21	20.79	9.14	13.87	13.50	19.99	23.24
Coke	4.55	4.19	2.54	5.82	2.35	2.26	2.83	2.13
Total	100.07	100.00	100.07	100.07	100.00	100.00	100.00	100.00

DF052	DF053	DF054	DF055	DF056	DF057	DF058	DF059	DF060
98/12/27	99/1/31	99/1//31	99/1/31	99/1/31	98/2/1	97/2/1	97/2/1	97/2/6
VGO3	VGO3	VGO3	VGO3	VGO3	VGO3	VGO3	VGO3	VGO3
NFC-97-7	NFC-97-7	NFC-97-7	NFC-97-7	NFC-97-7	NFC-97-7	NFC-97-7	NFC-97-7	NFC-97-7
1.10	1.26	1.11	0.98	1.55	1.10	0.91	0.70	1.27
550	600	600	600	600	600	600	600	601
64.5	60.9	61.8	62.3	62.1	107.3	111.3	112.7	105.5
69.4	69.3	74.8	73.3	75.0	72.9	77.7	78.9	74.3
100.0	100.0	100.0	100.0	100.0	100.0	100.0	100.0	100.0
0.04	0.06	0.07	0.06	0.07	0.07	0.07	0.06	0.08
0.64	1.13	1.52	1.31	1.37	1.39	1.39	1.26	1.48
0.49	0.82	1.13	0.98	1.02	0.99	0.95	0.86	1.03
0.76	1.48	1.93	1.70	1.73	1.79	1.82	1.72	1.85
0.44	0.50	0.66	0.56	0.60	0.65	0.62	0.53	0.70
5.15	6.13	7.78	6.79	6.78	8.23	9.25	9.09	8.49
2.09	1.47	1.75	1.47	1.56	1.97	2.02	1.77	2.12
0.33	0.30	0.38	0.33	0.34	0.39	0.17	0.36	0.42
1.91	2.05	2.57	2.23	2.22	2.54	2.97	3.04	2.63
1.53	1.68	2.14	1.96	1.87	2.15	2.50	2.55	2.23
2.59	2.70	3.45	3.10	3.01	3.43	4.07	4.29	3.53
1.41	1.53	1.93	1.71	1.67	1.90	2.23	2.28	1.97
0.71	0.00	0.00	0.00	0.45	0.00	0.33	0.39	0.00
0.04	0.05	0.08	0.11	0.07	0.07	0.08	0.08	0.07
18.15	19.90	25.39	22.32	22.75	25.57	28.46	28.29	26.60
49.07	46.72	46.41	48.21	49.30	43.54	45.58	47.35	43.53
16.35	17.74	14.95	15.30	15.04	15.23	13.43	12.75	14.61
14.21	12.92	10.27	11.45	9.92	11.82	8.82	8.39	11.10
2.22	2.79	2.92	2.72	2.93	3.84	3.70	3.28	4.10
100.00	100.07	99.94	100.00	99.94	100.00	100.00	100.06	99.94